QUERCETIN INHIBITS β-CATENIN IN RENAL DYSPLASIA

QUERCETIN INHIBITS β-CATENIN TRANSCRIPTIONAL ACTIVITY DURING KIDNEY DEVELOPMENT AND REDUCES THE SEVERITY OF RENAL DYSPLASIA

By **Joanna Cunanan, B.Sc. (Hons.)**

A Thesis Submitted to the School of Graduate Studies

in Partial Fulfillment of the Requirements

for the Degree Master of Science

TITLE: Quercetin inhibits β-catenin transcriptional activity during kidney development and reduces the severity of renal dysplasia

AUTHOR: Joanna Cunanan, B.Sc. (Hons.), McMaster University

PROGRAM: Medical Sciences Graduate Program, Division of Cancer and Genetics, McMaster University, Hamilton, Ontario Canada

SUPERVISOR: Darren Bridgewater, PhD

SUPERVISORY COMMITTEE: Bradley Doble, PhD and Nathan Magarvey, PhD

NUMBER OF PAGES: xv, 122

ABSTRACT

Renal dysplasia, defined as the abnormal development of kidney tissue, is the leading cause of kidney disease in children. While there are numerous causes of renal dysplasia (i.e. genetic, environmental and epigenetic factors), there is no cure to this abnormal defect. Kidney development occurs by two main processes: branching morphogenesis, which forms the collecting duct system, and nephrogenesis, which generates the nephrons, the functional units of the kidney. Our previous studies have demonstrated that β-catenin, a dual-function protein involved in cell adhesion and gene transcription, regulates branching morphogenesis and nephrogenesis. Furthermore, we discovered that nuclear β-catenin levels are increased in kidneys from patients with renal dysplasia, suggesting β-catenin can be a potential therapeutic target to modulate kidney development and renal dysplasia. Quercetin is a flavonoid that reduces β-catenin levels and inhibits its transcriptional activity, leading to improved outcomes in cancer and in kidney fibrosis. The role of quercetin in kidney development and in abnormal defects that arise during kidney development is yet to be examined. Using embryonic mouse kidney organ culture, I found that quercetin treatment resulted in a dose-dependent disruption in branching morphogenesis and nephrogenesis. In addition, quantitative reverse-transcriptase PCR revealed a decreased expression of β-catenin target genes essential for kidney development (i.e. *Pax2*, *Six2* and *GDNF*). Immunohistochemistry for β-catenin demonstrated that quercetin reduced nuclear β-catenin expression and increased cytoplasmic and membrane-bound expression in a dose-dependent manner. These results were confirmed by Western blot analysis. These novel findings demonstrate that quercetin treatment resulted in decreased levels of nuclear β-catenin, resulting in a decrease in its transcriptional activity which manifested in alterations in kidney developmental processes, suggesting quercetin is effective at reducing nuclear β-catenin in wild-type embryonic kidneys. Next, to determine

whether quercetin has any effects on renal dysplasia, I utilized transgenic mice models that overexpress β-catenin in select cells of the embryonic kidney. These models recapitulate the defects observed in human renal dysplasia, including disorganized branching morphogenesis and disrupted nephrogenesis. Quercetin treatment of embryonic dysplastic kidneys resulted in a partial rescue of renal dysplasia which was evident in marked improvements in branching morphogenesis and nephrogenesis, as well as an increase in the number of properly-developing nephrons in the kidney tissue. Analysis of β-catenin expression in quercetin-treated dysplastic kidneys revealed a decrease in nuclear levels and an increase in cytoplasmic and membrane-bound levels, resulting in a reduced expression of target genes (*Pax2*, *Six2*, and *GDNF*). Finally, this partial rescue of renal dysplasia was associated with an improved and organized E-cadherin expression in quercetin-treated dysplastic kidneys, suggesting a possible molecular mechanism of quercetin action in resolving abnormal kidney development. Overall, my findings demonstrate, for the first time, that quercetin reduces β-catenin transcriptional activity in normal and dysplastic kidneys and reduces the severity of defects in renal dysplasia.

ACKNOWLEDGEMENTS

First and foremost, I would like to give a big THANK YOU to my wonderful supervisor, Dr. Darren Bridgewater, who is hands down the best mentor any aspiring scientist can ever ask for. Thank you for taking a chance on me as a student and for providing me an amazing graduate research experience, despite having a limited research experience. Ever since, you have always been open to my ideas and I really appreciate the amount of enthusiasm and eagerness that you always give towards all aspects of this research, which really made the whole process an enjoyable learning experience. Thank you for always being patient and encouraging, for all of our discussions, the white-board sessions, the coffee chats, for writing my reference letters, for editing my written works, for helping me trouble-shoot experiments, and for all the exciting new opportunities you have given me. I learned a lot of things from you, both inside and outside of research. Thank you for all of your support, teaching, and mentoring and I am truly grateful for having the opportunity to work with you.

To my supervisory committee, Dr. Nathan Magarvey and Dr. Bradley Doble, I would like to thank them for their guidance and advice throughout this research, for kindly providing me with materials and reagents I needed for my experiments, and for giving me further insights and interesting ideas to further extend my research.

To Erin Deacon, I am so happy you picked our lab to work with for your undergrad research. I really enjoyed working with you and thank you for all of your assistance with my experiments. I am so grateful for all your help especially during the final stretch of my Master's. I enjoyed working with you in the lab and it made the process really fun. I really admire how you give everything your 150% towards your experiments, written work, your coursework, EFRT

(whether it's a patient needing resuscitation or a student with a broken nail), volunteering, etc. With all these, I know you're going to be an amazing doctor, and never give up on your dreams!!!

To our research assistant, Antje Ask, thank you for your guidance and support, not only to me but to the other students as well. Thank you for your kind assistance with the different aspects of my project and I really appreciate all the work you have contributed for this project to run successfully. You were an essential part of this project and I wish you all the best in your new role!

To Lily Morikawa, thank you for your assistance in histology! Your techniques are brilliant and I am really grateful for all the guidance and techniques you have shared with us.

To our previous student, Tony Yang, thank you for all of your insights and for helping me back when I was just starting in the lab. Thanks for helping me handle mice, for helping me dissect tiny kidneys, and for helping me with the Western blots. I know you're killing it in med school, you're an incredibly brilliant person and I know you will get really far in your career.

To Kate Todorova and Saakethiya Sriranjan, thank you both for your assistance with my experiments, for kindly providing me with materials and letting me use some of your equipment in the lab, for all our writing sessions (although we just casually hang out and write a total of five sentences after five hours of "working"), and for navigating grad school with me. I really appreciate you both taking the time out of your already busy schedules to help me with my work. And of course, outside of research, thanks for being amazing friends and a great support system!

Finally, to my parents and to my sister, thank you for all of your support with my studies. I really appreciate all your hardwork to make sure I can attend a good university and get a lot out of it. To my sister, Kristina, I'm really happy you got to work with us in the lab, and for helping me figure out the dreadful Western blots. You're an amazing and hardworking student and I know you will get really far in your studies. Thanks for baking a lot of cookies for our meetings.

TABLE OF CONTENTS

.

LIST OF SUPPLEMENTARY FIGURES

LIST OF FIGURES

DECLARATION OF ACADEMIC ACHIEVEMENT

I have personally accomplished all the research, laboratory experiments and procedures, and necessary tasks for Figure 1 through Figure 20. Our summer research student, Kristina Cunanan assisted with performing the Western blots for Figure 6. Our undergraduate thesis student, Erin Deacon, performed the quantifications for Figure 14 and the immunofluorescence staining for Figure 18.

BACKGROUND

1. MAMMALIAN KIDNEY ANATOMY AND FUNCTION

1.1 Gross anatomy of the kidneys

The kidneys are two bean-shaped organs, each located on the posterior abdominal wall on either side of the vertebral column (Supplementary Figure 1; *Preuss, 1993*). The right kidney is located below the liver, resulting in the right kidney being slightly lower than the left. Above each kidney is where the two adrenal glands are located. The kidneys are encapsulated by several layers of adipose and connective tissue *(Preuss, 1993)*. The **renal capsule** is a thin layer of fibrous connective tissue, comprised predominantly of collagen and elastin that covers the outermost surface of each kidney and helps counteracting high pressure within the kidney. A thick layer of adipose tissue surrounds the renal capsule, providing a cushioning layer protecting the kidneys against mechanical compression and injury. The **renal fascia** is another thin layer of connective tissue that surrounds the adipose tissue layer and anchors the kidneys and the surrounding adipose tissue onto the abdominal wall. The **renal hilum** is an indentation located towards the medial side of the kidney where the renal artery and nerves enter, and where the renal vein and ureter exit, the kidney. The renal hilum opens into the **renal sinus**, a cavity within the kidney occupied by the renal pelvis, renal calyces, vasculature, nervous and adipose tissue *(Preuss, 1993)*. Unfiltered blood enters the kidneys through the renal artery and blood that has been filtered returns to the main circulation through the renal vein. The urine then drains from the kidneys through the ureters and into the urinary bladder, and exits the body through the urethra *(Preuss, 1993)*.

Supplementary Figure 1: External anatomy of the kidneys

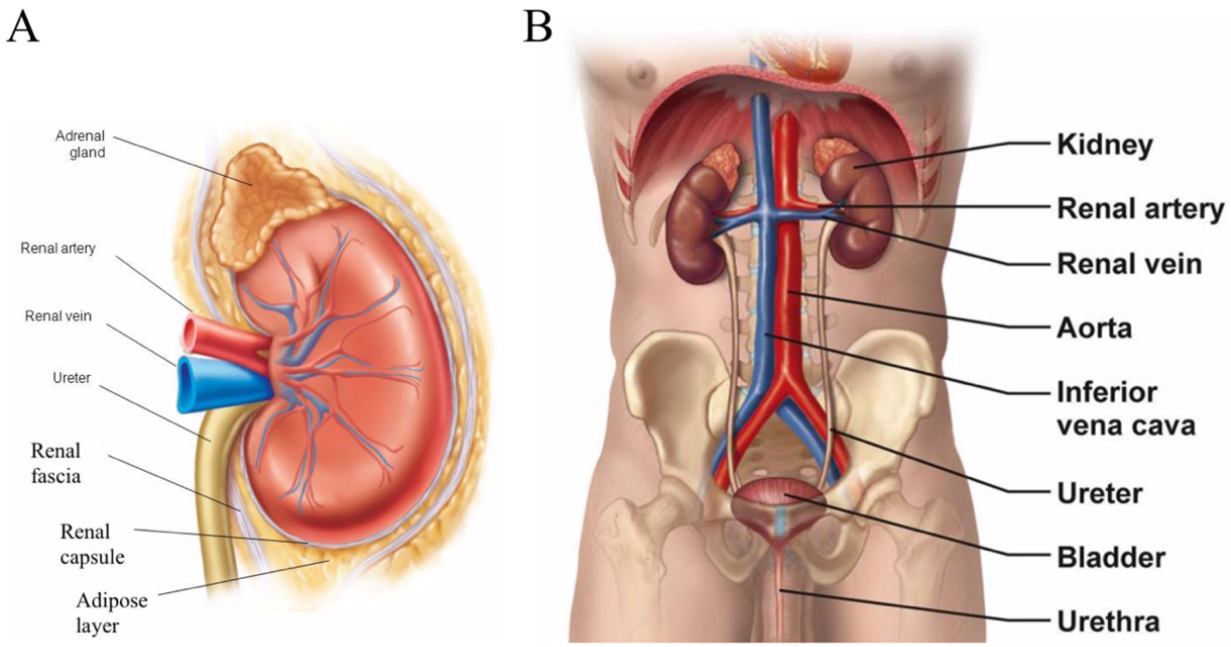

External anatomy of the kidneys. A) Protective layers of connective and adipose tissues around the kidney: renal capsule, adipose tissue layer around the capsule, and renal fascia. B) Anatomical position of the kidneys within the posterior abdominal wall, as well as the renal vasculature and the other major organs of the urinary system. *(Taken from Preuss, 1993)*.

1.2 Microanatomy of the kidneys

The kidney parenchyma (Supplementary Figure 2) is divided into two regions: the **renal cortex** on the outer surface of the kidney just under the renal capsule, and the **renal medulla** which forms the deeper region of the kidney *(Preuss, 1993)*. The renal medulla is comprised of **renal pyramids**, which are wedge-shaped tissues that have a striated appearance due to the presence of tubules. Between the renal pyramids are tissue projections from the cortex, called the **renal columns**. The tips of the renal pyramids towards the deeper region of the medulla are called **renal papilla**. Urine drains from the renal pyramids and collects into tubular structures called **minor calyces.** The minor calyces, in turn, converge to form the larger tubules called **major calyces**, at

which point the urine drains into the **renal pelvis**, a funnel-like tissue that directs the flow of urine towards the ureters *(Preuss, 1993)*.

Supplementary Figure 2: Microanatomy of the kidney

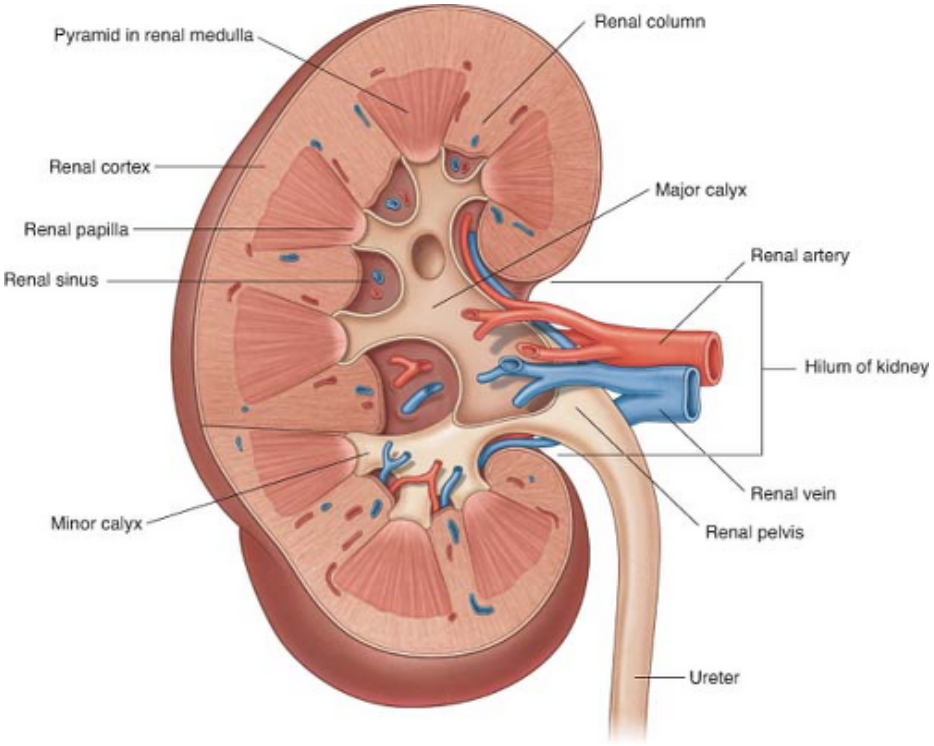

Microanatomy of the kidney. Frontal section of the kidney showing the renal cortex, and the renal medulla containing the renal pyramids, renal papilla, the minor and major calyces, renal pelvis, and ureter. *(Taken from Preuss, 1993).*

1.3 The nephron: basic structure and function

The nephron (Supplementary Figure 3) is the basic structural and functional unit of the kidneys *(Preuss, 1993)*. In a healthy adult, between 200,000 to 2 million nephrons are present in each kidney. The nephron is comprised of distinct functional segments *(Preuss, 1993)*. The **glomerulus** is a tuft of capillaries surrounded by **Bowman's capsule**. The lumen of Bowman's capsule is connected to the **proximal convoluted tubule**, which leads into the **loop of Henle**. The loop is divided into an **ascending limb** and a **descending limb**, and the descending portion is

continuous with the **distal convoluted tubule**. The distal convoluted tubule connects to the collecting duct *(Preuss, 1993)*.

The nephron plays a critical role in the homeostatic regulation of blood volume, blood pressure and blood plasma osmolarity by filtering the blood, reabsorbing essential molecules back into the bloodstream, and excreting the remaining product as urine *(Preuss, 1993)*. Urine formation begins when unfiltered blood enters the glomerulus *(Preuss, 1993)*. The glomerulus forms a selective barrier: the endothelial cells that comprise these capillaries are lined with several fenestrations and podocyte foot processes which together regulate the retention of important proteins and blood cells and the removal of small molecules and waste products from the blood. Essential blood components such as red blood cells and large proteins (i.e albumin) are not able to pass through the glomerular filtration barrier under normal conditions. Fluid, solutes, waste products and other small molecules are filtered from the blood plasma, forming a **filtrate** *(Preuss, 1993)*. The filtrate then collects into the Bowman's capsule. As the filtrate passes through the proximal convoluted tubule, this is the first site of water reabsorption back into the bloodstream, as well as where the bulk of water and sodium reabsorption takes place. Reabsorption in the proximal convoluted tubule occurs through both passive diffusion and active transport through ion pumps present throughout the basolateral membrane of the tubule *(Preuss, 1993)*. The filtrate then enters the loop of Henle. The descending portion of the loop is very permeable to water but impermeable to ions and small solutes, causing a large amount of water to passively diffuse out of the tubule and to be reabsorbed back into the bloodstream, and this causes a further increase in osmolarity of the filtrate. In contrast, the ascending portion of the loop is impermeable to water but highly permeable to ions, providing for more secretion of solutes from the blood plasma into the filtrate *(Preuss, 1993)*. As the filtrate enters the distal convoluted tubule, additional substances

such as drugs, toxins, and excess metabolites are removed from the blood and secreted into the filtrate *(Preuss, 1993)*. The filtrate then empties into the collecting duct, where water secretion and reabsorption is regulated by the hormone ADH (antidiuretic hormone). The filtrate from the collecting ducts drains into the minor and major calyces, collects in the renal pelvis and drains towards the urinary bladder through the ureters *(Preuss, 1993)*.

In summary, the highly complex and intricate structure of the nephron plays a critical role in important physiological functions. The filtration, reabsorption and secretion processes performed by the different segments of the nephron are necessary for maintaining acid-base balance, maintaining optimal osmolar concentrations of different ions, removing any excess solutes, metabolites and other waste products from the plasma, and regulating blood volume and blood pressure by accordingly removing or retaining water in the bloodstream.

Supplementary Figure 3: Basic structure and function of the nephron

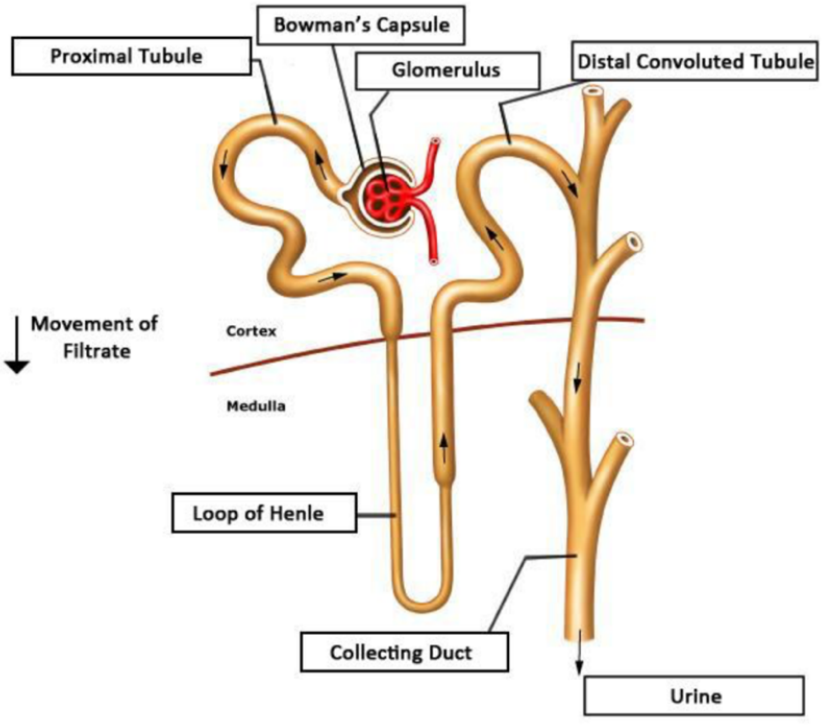

Basic structure and function of the nephron. Diagram representation of the different functional segments of the nephron: the glomerulus, Bowman's capsule, proximal convoluted tubule, loop of Henle, and the distal convoluted tubule. Black arrows demonstrate the flow of filtrate through the different nephron segments as it exits as urine through the collecting duct. *(Taken from Preuss, 1993)*.

2. STAGES OF KIDNEY DEVELOPMENT

2.1. Pronephric and mesonephric kidney development

In the developing fetus, the vertebrate kidney arises from the **intermediate mesoderm**, a narrow section of the mesoderm (one of the three main germ layers in embryonic development) located between the paraxial mesoderm and the lateral plate of the developing embryo *(Vize et al., 2003)*. The intermediate mesoderm generates the **urogenital system,** which is comprised of the kidneys, the gonads, and their respective ductal systems *(Vize et al., 2003)*. The urogenital ridge is a structure found along the posterior wall of the abdomen in the fetus (Supplementary Figure 4). It undergoes three successive stages of development of tubular nephric structures, referred to as the pronephros, the mesonephros, and the metanephros. In mammals, the pronephros and mesonephros are transient structures that do not further develop after the embryonic period, whereas the metanephros gives rise to the definitive and functional adult kidney *(Vize et al., 2003)*. The **pronephros** is made up of the pronephric duct (the precursor to the Wolffian duct) and several pronephric tubules that branch off perpendicularly from the pronephric duct *(Vize et al., 2003)*. The pronephros arises from the rostral-most region of the urogenital ridge at 22-days of gestation in humans and embryonic day (E) 8.5 in mice. The pronephros is functional during the larval stages in amphibians and fish, however this is a vestigial structure in mammals and completely disappears by the 4th week of embryonic development in humans *(Vize et al., 2003)*. The **mesonephros** develops caudal to the pronephros, along the mid-section of the urogenital ridge *(Vize et al., 2003)*. This structure is composed of the mesonephric duct (also referred to as the **Wolffian duct**), the caudal extension of the pronephric duct, and several mesonephric tubules branching off from the duct. The mesonephros develops into the functional excretory organ in many lower vertebrates and it may perform some filtering capacity during embryonic life in mammals between 4th-8th

weeks of development. However, the mesonephros also gradually degenerates before birth. Prior to its complete degeneration, parts of the ductal structures of the mesonephros become incorporated into the adjacent adrenogonadal primordia, the precursors of the adrenal glands and male and female gonads *(Vize et al., 2003)*.

Supplementary Figure 4: Stages of kidney development

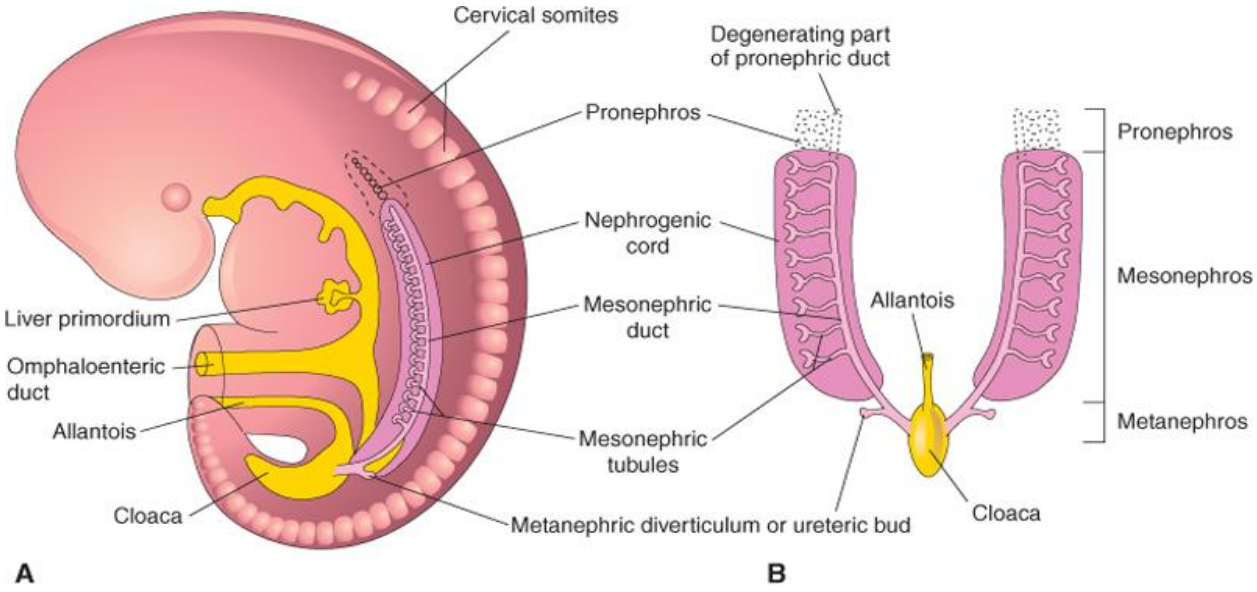

Stages of kidney development. A) Sagittal section of a 5-week old human embryo showing the anatomical location of the urogenital ridge. B) The three different stages of kidney development: pronephros, mesonephros and metanephros. *(Taken from Moore, Persaud, & Torchia, 2015).*

2.2. Mammalian metanephric kidney development

In mammals, the **metanephros** is the third and final developmental stage, giving rise to the formation of the functional adult kidney. The formation of the metanephric kidney involves the reciprocal inductive interaction among three cell lineages of the embryonic kidney: the **ureteric epithelium**, **metanephric mesenchyme**, and **renal stroma** *(Vize et al., 2003)*.

2.2.1. Branching morphogenesis

At embryonic day (E) 9.5 in mice (gestational day 22 in humans), a group of epithelial cells derived from the intermediate mesoderm of the embryo begin to form the **Wolffian duct**, a ductal structure that undergoes elongation towards the caudal end of the embryo *(Boivin et al., 2015a; Costantini & Kopan, 2010)*. The formation of the mammalian metanephric kidney begins at E10.5 in mice (gestational day 28 in human), where select epithelial cells near the caudal-most portion of the Wolffian duct begin to proliferate to form an outgrowth, termed the **ureteric bud**, the precursor for the ureter *(Boivin et al., 2015a; Costantini & Kopan, 2010)*. Adjacent to the ureteric bud is a population of mesenchymal cells called the metanephric mesenchyme derived from the ventral mesoderm. As the ureteric bud begins to invade the metanephric mesenchyme, the tip of the bud undergoes a burst of cell proliferation and swells to form an expanded tip. The tip will then begin to migrate at a 90-degree angle into the metanephric mesenchyme and at E11.5 in mice (E33.0 in human) will undergo the first bifurcation event to form a T-shaped structure *(Boivin et al., 2015a; Costantini & Kopan, 2010)*. This is followed by subsequent cycles of bifurcations of the ureteric epithelium where each newly formed tip continues to branch dichotomously. This process is called **branching morphogenesis** (Supplementary Figure 5), the process by which the ureteric epithelium develops and gives rise to the collecting ducts, major and minor calices, renal pelvis, and ureter, collectively referred to as the **renal collecting system**: the ductal structures into which the filtrate collects and exits the kidney for excretion *(Boivin et al., 2015a; Costantini & Kopan, 2010)*. Branching morphogenesis continues for a total of 10 cycles to form approximately 1500 collecting ducts in mice and 15 cycles to form around 60,000 collecting ducts in humans *(Saxén & Sariola, 1987)*. Branching morphogenesis is driven primarily by molecular inductive signals originating from the metanephric mesenchyme. These signals trigger the ureteric bud to

undergo the first round of bifurcation forming the T-shape and the subsequent branching of each newly-formed tip *(Boivin et al., 2015a; Costantini & Kopan, 2010)*. During the repeated cycles of branching events, the ureteric epithelium becomes organized into the tip and stalk regions *(Bridgewater & Rosenblum, 2009)*. The ureteric tip has high rates of cell proliferation whereas the stalk region has relatively lower rates of cell proliferation.

Supplementary Figure 5: The ureteric epithelium undergoes branching morphogenesis to form the renal collecting system

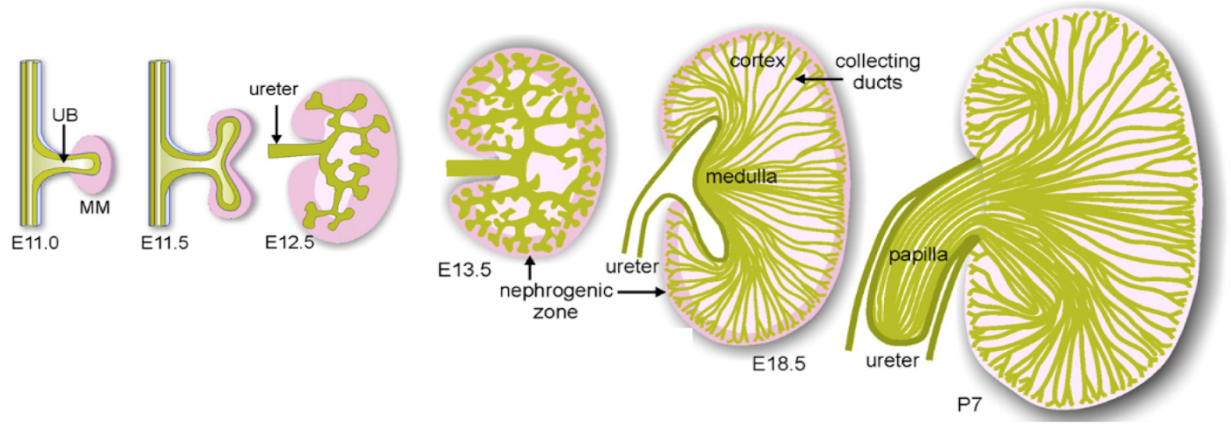

The ureteric epithelium undergoes branching morphogenesis, forming the renal collecting system. Diagram representation of branching morphogenesis, from the initial emergence and elongation of the ureteric bud (UB) and its invasion into the adjacent metanephric mesenchyme (MM) at E11.0, the first bifurcation event of the ureteric bud forming the T-shape at E11.5, the repeated rounds of branching of each ureteric tip at E12.5 onwards, and the resulting formation of the collecting duct system of the kidney. *(Taken from: Costantini & Kopan, 2010).*

2.2.1.1.Molecular basis of branching morphogenesis

GDNF/Ret (Glial Cell Derived Neurotrophic Factor/Ret Proto-oncogene) signaling plays a role in regulating branching morphogenesis of the ureteric epithelium (Supplementary Figure 6*)*. Before the ureteric bud begins to invade the adjacent metanephric mesenchyme, GDNF is expressed in the region of the mesenchyme that is adjacent to the caudal Wolffian duct where the ureteric bud will later develop *(Costantini & Shakya, 2006)*. After invasion of the ureteric bud, GDNF expression becomes restricted to the metanephric mesenchyme and this pattern of expression is maintained throughout renal development *(Costantini & Shakya, 2006)*. These observations suggest that GDNF is needed for both the initial ureteric bud induction and also for maintaining later branching generations. Ret, the cell membrane receptor for GDNF, is found along the length the Wolffian duct and has highest expression levels in the caudal portion of the duct *(Costantini & Shakya, 2006)*. After the outgrowth of ureteric bud at E10.5, Ret expression is decreased in the Wolffian duct and in the ureteric epithelium stalk regions. During the emergence of the T-shape at E11.5, Ret expression is restricted only to the ureteric bud tips and this is maintained until branching morphogenesis is completed *(Costantini & Shakya, 2006)*. Stimulation of Ret in the ureteric epithelium by GDNF signaling activates pathways that result to cellular processes such as proliferation, migration and survival, thus establishing the branching morphogenesis of the collecting system *(Bridgewater & Rosenblum, 2009)*.

Supplementary Figure 6: GDNF/Ret signaling in branching morphogenesis

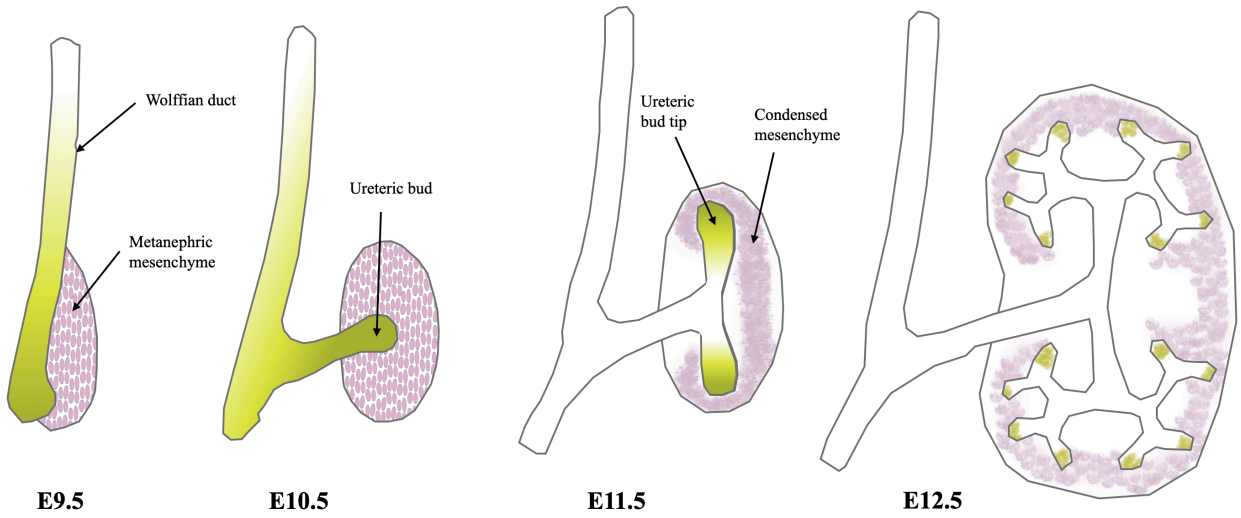

GDNF/Ret signaling in branching morphogenesis. Diagram representation of GDNF (pink) and Ret (yellow) spatiotemporal expression pattern during the different developmental stages of branching morphogenesis is critical in the proper formation of the renal collecting system. *(Adapted from Costantini and Shakya, 2006).*

2.2.2. Nephron formation

The functional unit of the kidney, termed the **nephron**, originates from the metanephric mesenchyme. As the ureteric epithelium undergoes branching morphogenesis, the metanephric mesenchyme simultaneously responds to inductive signals from the ureteric epithelium *(Boivin et al., 2015a; Costantini & Kopan, 2010)*. These signals trigger metanephric mesenchyme to condense and form aggregates around the surface of ureteric branch tips, forming the **condensed mesenchyme**. Depending on the nature of inductive signals from the ureteric epithelium, a subset of cells in the condensed mesenchyme either undergo **self-renewal** and repopulate the condensed mesenchyme niche or undergo differentiation through a process called **mesenchymal-to-epithelial transition** (Supplementary Figure 7; *Boivin et al., 2015a; Costantini & Kopan, 2010*). Mesenchymal-to-epithelial transition is a cellular process by which motile, multiplanar or spindle-shaped mesenchymal cells organize into planar arrays of polarized cells that form a continuous

tubule characterized by an apical-basolateral orientation and adherens junctions between adjacent epithelial cells *(Davies, 1996)*. This process is the basis of the proper development and formation of the renal epithelium. During mesenchymal-to-epithelial transition, a subset of the mesenchymal aggregates, termed **pretubular aggregates**, found adjacent and inferior to the tip of the ureteric bud begin the cell adhesion process to form a polarized **renal vesicle**, one end of which maintains contact with the UB epithelium *(Dressler, 2006)*. Inside the renal vesicle, a lumen forms to generate the **comma-shaped structure**, and the cleft of this structure is the site where endothelial cells will infiltrate and later on develop into the glomerular tuft *(Dressler, 2006)*. The comma-shaped structure continues to undergo tubular elongation and a second lumen forms to produce the **S-shaped structure** The S-shaped structure is oriented along the proximal-distal axis; the proximal end gets invaded with endothelial cells and different vascular and angiogenic factors, eventually forming the glomerular tuft and the filtration membrane, while the distal end fuses with the ureteric epithelium to produce a continuous epithelial tubule *(Dressler, 2006)*. The S-shaped structure continues to elongate and form the different segments of the nephron: Bowman's capsule, proximal convoluted tubule, loop of Henle, and distal convoluted tubule which is fused with the collecting duct *(Dressler, 2006)*. These processes involved in nephron formation are repeated between 600,000 to 1 million times in humans in each developing human kidney as new nephrons are repeatedly generated at the branch tips of the ureteric epithelium throughout fetal development *(Dressler, 2006)*. Nephron formation gives rise to approximately 10,000 nephrons in mice and between 200,000-1.8 million nephrons in humans *(Boivin et al., 2015a)*.

Supplementary Figure 7: The metanephric mesenchyme undergoes nephron formation to generate the functional units of the kidney

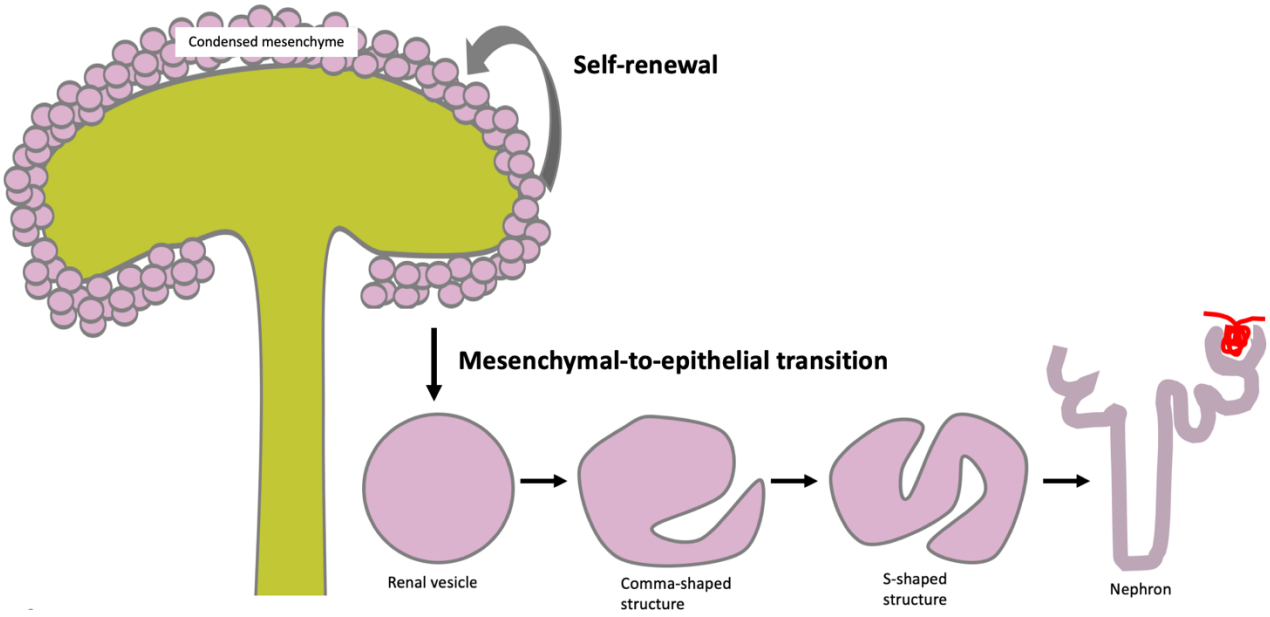

The metanephric mesenchyme undergoes nephron formation to generate the functional units of the kidney. Diagram representation of the different stages of nephron formation: condensed mesenchyme aggregation, comma-shape and S-shape formation, and tubular elongation, and the resulting formation of the different nephron segments.

2.2.2.1.Molecular basis of nephron formation

During nephrogenesis, a balance must be maintained between self-renewal of the progenitor cell population and differentiation of a subset of these cells that will develop into nephrons *(Karner et al., 2011)*. **Wnt9b** (Wnt Family Member 9B) and **Six2** (Sine Oculis Homeobox Homolog 2) have been shown to play a major role during progenitor self-renewal and induction of nephrogenesis (Supplementary Figure 8). At around E10.5-E11.0 in the metanephric kidney, Wnt9b is expressed in the epithelium of ureteric bud as it infiltrates the adjacent mesenchyme *(Carroll et al., 2005; Park et al., 2007)*. Six2 is a transcription factor that is highly expressed in self-renewing progenitor cells and expressed at lower levels in cells induced to undergo nephrogenesis through mesenchymal-to-epithelial transition *(Karner et al., 2011)*. Wnt9b

from the ureteric epithelium activates the expression of genes in the mesenchyme, such as **Wnt4** (Wnt Family Member 4), **Fgf8** (Fibroblast Growth Factor 8), **Pax8** (Paired Box 8), and **Lhx1** (LIM Homeobox 1). At E12.5, these markers are all expressed within the pretubular aggregates and renal vesicles; each of these markers are also expressed at later stages in tubular derivatives of the renal vesicles *(Park et al., 2007)*, demonstrating that these four genes play a role in regulating proper epithelialization of the nephrogenic structures and the sequential steps of nephron formation *(Stark et al., 1994; Park et al., 2007, Narlis et al., 2007)*. In self-renewing progenitor cells, Six2 inhibits the effect of Wnt9b on downstream targets in the mesenchyme, thereby maintaining the undifferentiated state of these cells *(Park et al., 2012)*.

Supplementary Figure 8: Wnt9b-mediated signaling in nephron formation

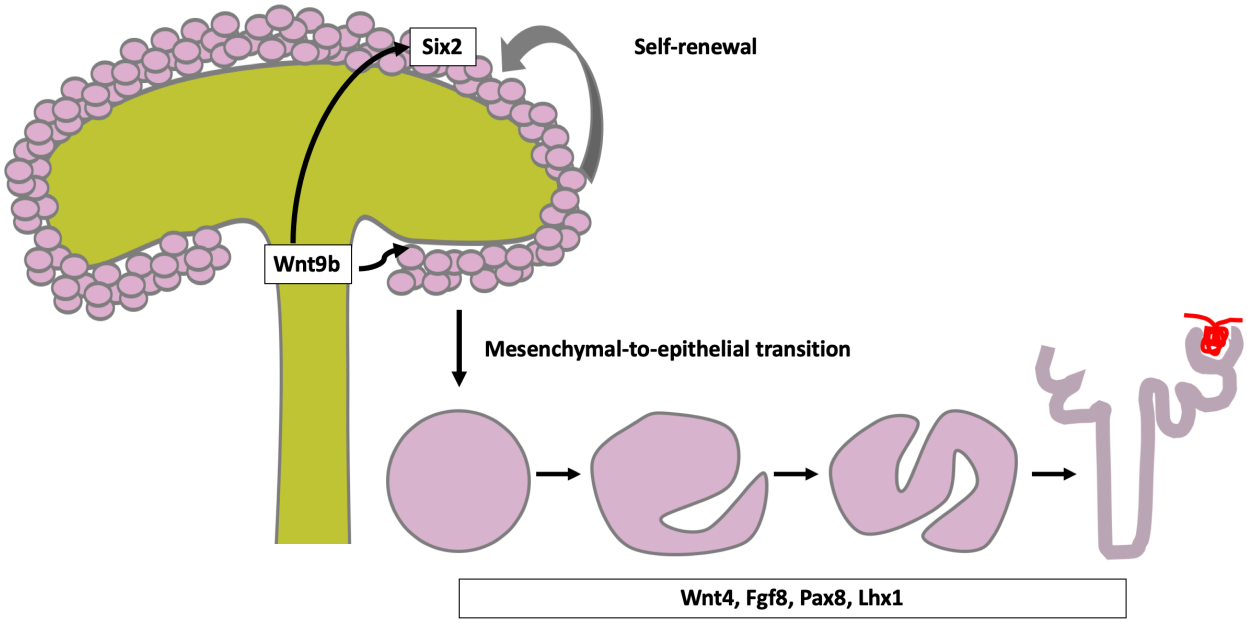

Wnt9b-mediated signaling in nephron formation. Wnt9b from the ureteric epithelium activates the expression of epithelialization factors (Wnt4, Fgf8, Pax8, Lhx1) in the subset of mesenchymal cells targeted to undergo differentiation. Six2 expressed in the self-renewing progenitors maintains the undifferentiated state of these cells.

2.2.3. Corticomedullar patterning

As the ureteric epithelium undergoes branching morphogenesis for the first few rounds, and the adjacent metanephric mesenchyme is concurrently induced to form nephrons, the kidney begins to become divided into two distinct regions: an **outer cortical region** where new nephrons are being induced, and an **inner medullary region** where older nephrons are maturing and where the collecting system will form (Supplementary Figure 9; *Combes et al., 2017; Schedl, 2007*). As the growth of the kidney continues, successive groups of nephrons are induced at the peripheral regions of the kidney, referred to as the **nephrogenic zone**. Therefore, within the developing kidney, the most mature nephrons are located in the medullary region and the most newly-formed nephrons are found in the most peripheral region *(Combes et al., 2017; Schedl, 2007)*.

Supplementary Figure 9: Corticomedullary patterning of the developing kidney

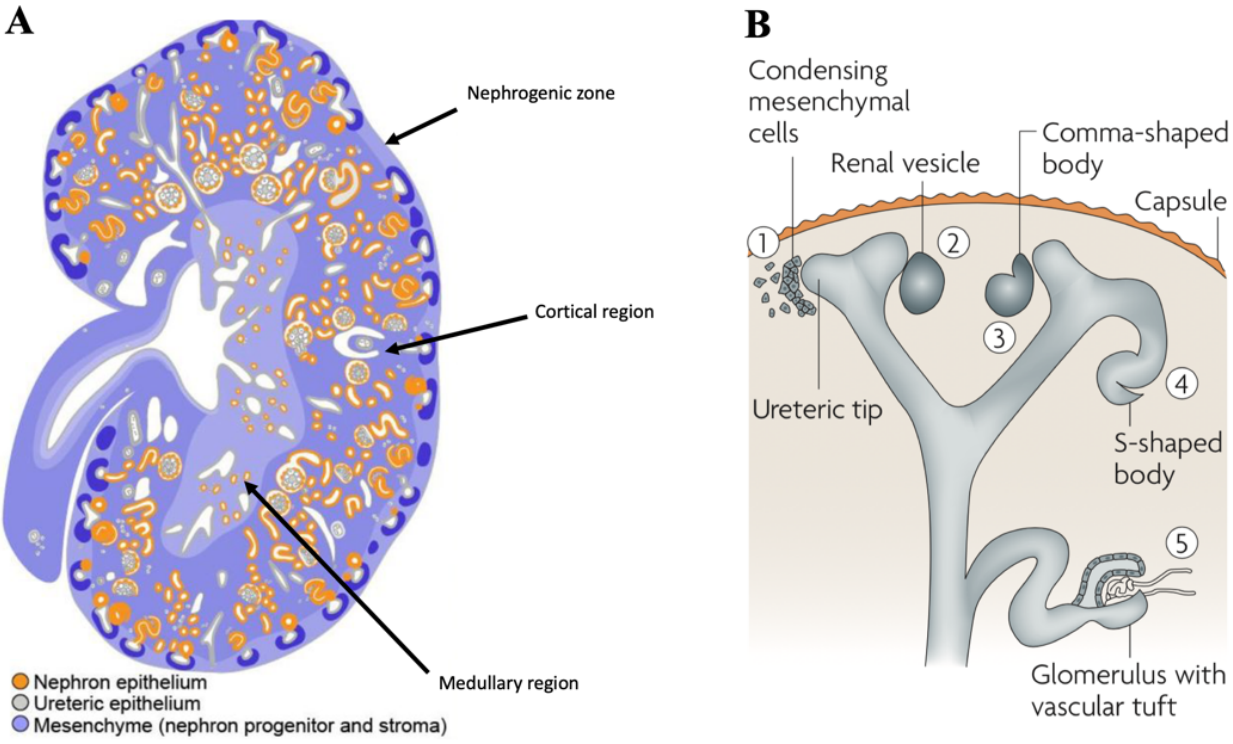

Corticomedullary patterning of the developing kidney. A) The kidney becomes stratified into an outer cortical region where newly-formed nephrons are found, and an inner medullary region where more mature nephrons and the collecting system are formed. The nephrogenic zone is the outermost layer of the kidney where new nephron progenitors are being induced. B) Section of a developing kidney showing condensed mesenchyme cells found in the nephrogenic zone, early-forming nephrons (renal vesicle, comma-shaped body and S-shaped body) found in the cortical region, and a maturing glomerulus found in the medullary region. *(Taken from Combes et al., 2017 and Schedl, 2007).*

2.2.4. Renal stroma formation

Shortly after the initial growth of the ureteric bud into the adjacent metanephric mesenchyme, a third cell population called the **renal stroma** is observed surrounding the condensed mesenchyme (Supplementary Figure 10; *Boivin et al., 2015a*). The renal stroma is a type of matrix-producing fibroblast cells that surround adjacent nephrogenic structures and early collecting ducts and provide structural support and framework to the developing kidney. These cells differentiate into the capsular, cortical and medullary stroma, therefore playing a role in the establishment of the corticomedullary patterning of the kidney. Studies have shown that the renal stroma cell population plays an important role in kidney development by modulating branching morphogenesis and nephrogenesis *(Boivin et al., 2015a)*. However, more studies are needed to provide a better understanding of the molecular mechanisms on how the renal stroma regulates kidney development.

Supplementary Figure 10: The renal stroma provides support to the developing kidney

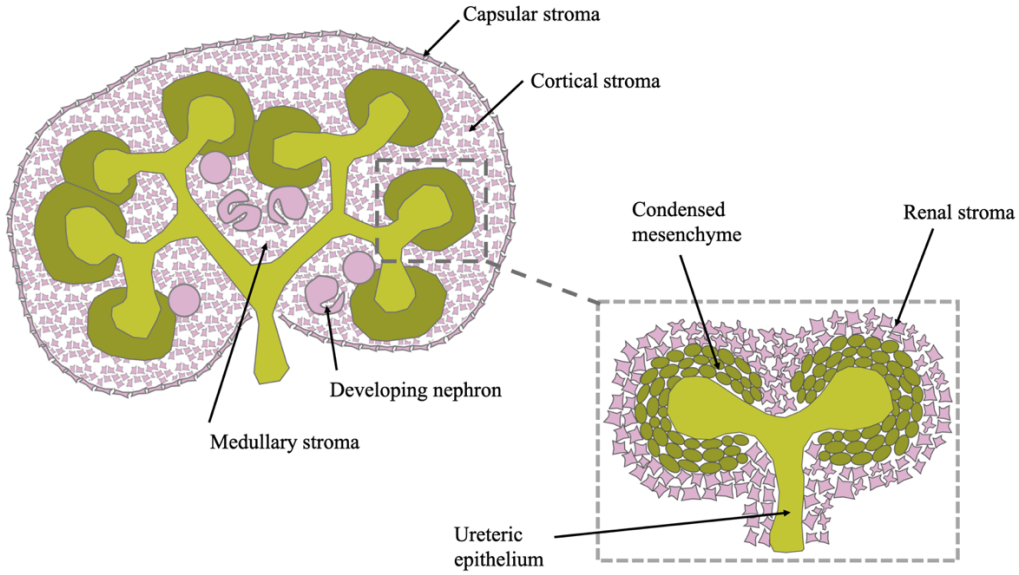

The renal stroma provides support to the developing kidney. The renal stroma cells surround the nephrogenic progenitors and ureteric epithelium, and differentiate to form the capsular, cortical, and medullary stroma.

3. Renal dysplasia

3.1. Epidemiology of human renal dysplasia

Congenital anomalies of the kidney and urinary tract (CAKUT) are the most common developmental defects diagnosed in the pediatric population, with an incidence of 1 in 250 live births *(Pohl et al., 2002)*. Among these defects, **renal dysplasia** is the most common developmental abnormality of the kidney, affecting up to **1 in 1000** of the general population *(Winyard & Chitty, 2008)*. Renal dysplasia is the leading cause of end-stage kidney disease in children *(Chen & Chang, 2015)*; dysplastic kidneys account for **40%** of all children on renal replacement therapy due to chronic kidney failure *(Kerecuk et al., 2008)*. Renal dysplasia is diagnosed during the perinatal period and in early childhood years, with a prevalence of **0.1%** in infants diagnosed by ultrasound screening and **4%** in fetuses and infants from autopsy findings *(Chen & Chang, 2015)*.

3.2. Characteristics of human renal dysplasia

Human renal dysplasia is a collection of disorders characterised by abnormalities in the development and formation of the kidneys *(Woolf et al., 2004)*. The phenotypic abnormalities of dysplastic kidneys can be observed at the gross and histopathological levels. At the **gross level** (Supplementary Figure 11), renal dysplasia has highly variable presentations that can include small kidney size and reduced number of nephrons (hypoplastic kidney), malformed kidney (dysplastic kidney), malformed kidney with the presence of cysts (cystic dysplastic kidney), malformed kidney with the presence of irregular cysts of varying sizes (multicystic dysplastic kidney), lack of formation of one or both kidneys (renal agenesis), formation of duplicate or multiple kidneys (multiplex kidneys) with duplicate or bifid ureters, and an immature, rudimentary kidney that remains in its underdeveloped state (severe renal hypodysplasia/aplasia) *(Kerecuk et al., 2008)*.

Supplementary Figure 11: Gross-level characteristics of renal dysplasia

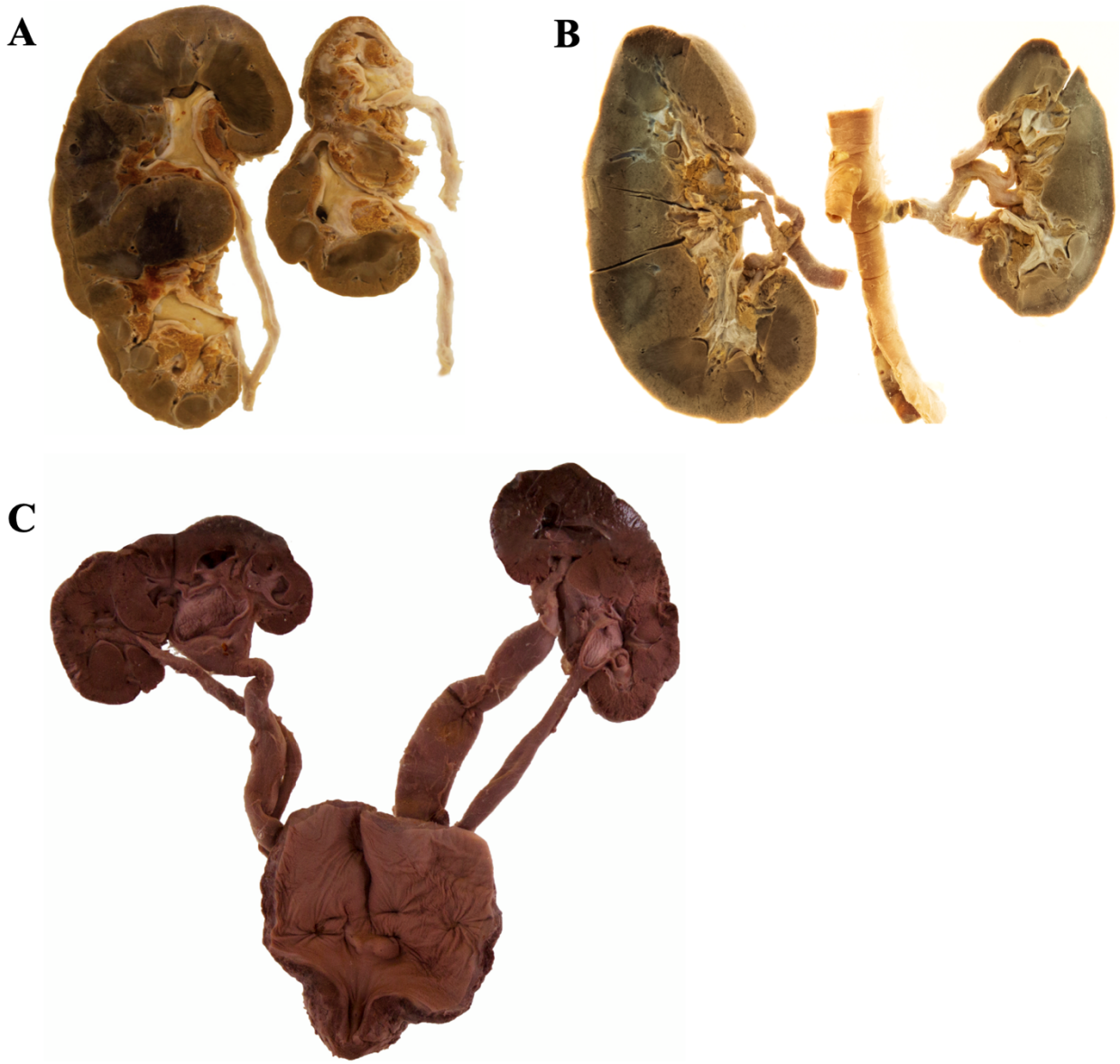

Gross-level characteristics of renal dysplasia. A) Multiplex dysplastic kidneys with bifid ureters. B) Unilateral hypoplastic kidney (affected right kidney is smaller in size compared to the unaffected left kidney). C) Multiplex dysplastic kidneys with bifid ureters, with hydroureter and hydropelvis (dilation of ureter and renal pelvis due to obstructed urine outflow).

At the **histopathological level** (Supplementary Figure 12), microscopic characteristics of renal dysplasia include: immature and poorly-differentiated nephrogenic and ductal structures, primitive dilated cystic tubules surrounded by a fibromuscular collar, disorganized corticomedullary patterning of the renal parenchyma, cyst formation, and presence of metaplastic cartilage (*Chen & Chang, 2015; Kakkar et al., 2006*).

Supplementary Figure 12: Histopathological abnormalities in renal dysplasia

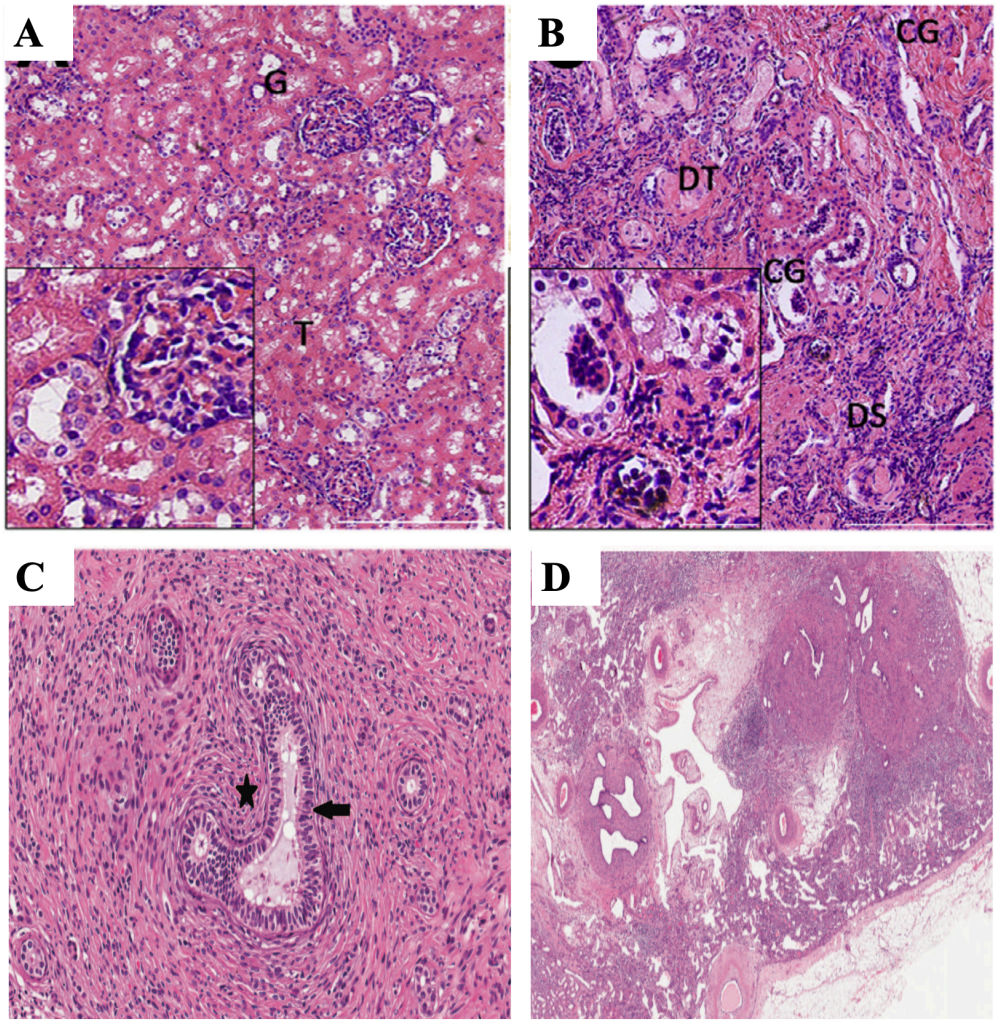

Histopathological abnormalities in renal dysplasia. A) Normal kidney tissue shows glomeruli (G) and tubular structures (T). B) Dysplastic kidneys have a disorganized renal parenchyma, dysplastic dilated cystic tubules (DT), cystic glomeruli (CG), and disorganized stroma (DS). *(Taken from: Sarin et al., 2014)*. C) Primitive ducts lined by cuboidal epithelium (arrow) and surrounded by a fibromuscular collar (star). D) Loss of normal formation of renal structures, showing a lobar disorganization *(Taken from: Chen & Chang, 2015)*.

3.3. Diagnosis and treatment

In clinical practice, renal dysplasia is diagnosed during the prenatal period by **ultrasound screening** (Supplementary Figure 13) and often manifests as large bright kidneys with or without cystic spaces and an absence of normal corticomedullary differentiation *(Winyard & Chitty, 2008)*.

Supplementary Figure 13: Renal dysplasia can be detected in the fetus by ultrasound

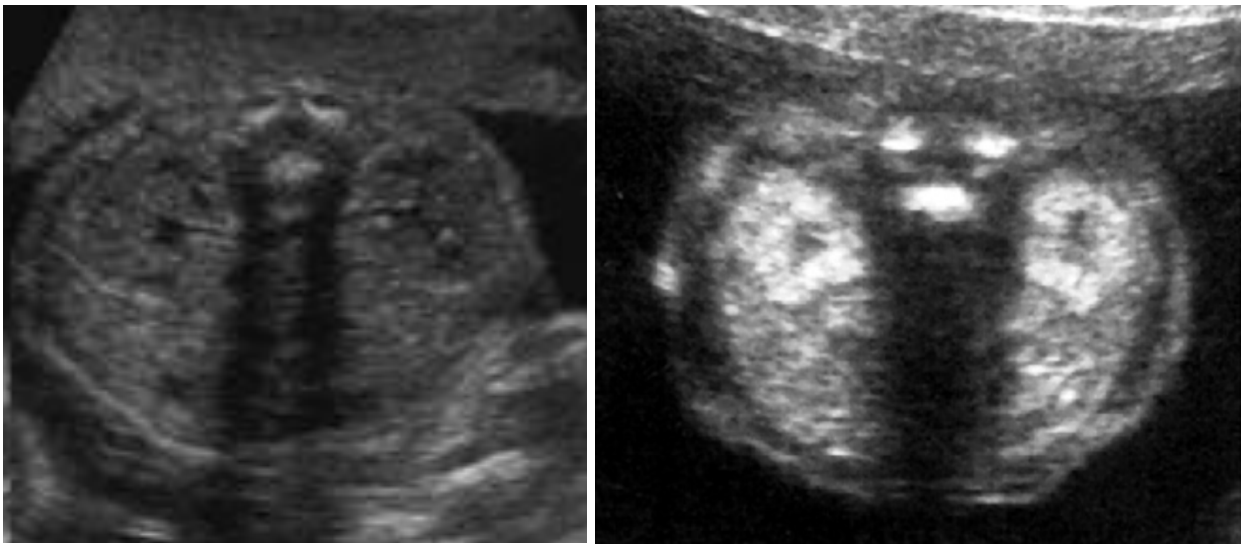

Renal dysplasia can be detected in the fetus by ultrasound. Ultrasound images of a normal human fetal kidney (left) and human dysplastic kidneys (right) taken on a transverse section. Dysplastic kidneys appear bright on ultrasound and have a notable lack of normal corticomedullary differentiation *(Taken from Winyard & Chitty, 2008).*

Other ultrasound findings include: abnormally low amniotic fluid levels in the mother (maternal oligohydramnios) and swelling of the kidneys due to urine buildup in the fetus (fetal hydronephrosis) *(Chen & Chang, 2015)*. Renal dysplasia also manifests postnatally during early childhood years with symptoms such as voiding dysfunction, urinary incontinence, repeated urinary tract infections, flank or abdominal pain, vaginal discharge, genital masses and chronic renal failure. Symptomatic renal dysplasia can be further analyzed and confirmed by renal ultrasound and magnetic resonance imaging, however a more definitive diagnosis can only be

made after the diseased kidney has been removed by nephrectomy or autopsy and analyzed by a pathologist *(Chen & Chang, 2015)*.

In terms of management and treatment for patients diagnosed with renal dysplasia, there are renal replacement therapies such as dialysis *(Kerecuk et al., 2008)*, as well as surgical procedures such as kidney transplants and nephrectomy *(Chen & Chang, 2015)*. However, these procedures are highly invasive and have significant limitations and adverse outcomes in patients. For instance, dialysis requires treatment 3-4 times a week for 4 hours per session *(Bonomini et al., 1972)* while transplants are limited due to organ availability and possibility of transplant rejection *(Huh et al., 2008)*. Nephrectomy involves risks and surgical complications such as intestinal obstruction, extensive hemorrhage, injuries to other visceral organs, vascular injury, and death *(Ritchey et al., 1992)*.

3.4. Etiology of human renal dysplasia

Abnormalities in kidney developmental processes leads to the various abnormalities observed in renal dysplasia. These abnormalities involve aberrations in molecular signaling between the ureteric epithelium and metanephric mesenchyme (and possibly the renal stroma), thereby affecting the branching of the collecting system and the formation of the nephrons *(Schedl, 2007)*. This can therefore result to the aforementioned gross and microscopic abnormalities observed in dysplastic kidneys. Lack of formation of one or both kidneys (renal agenesis) or the formation of an immature, rudimentary kidney that remains in its underdeveloped state (aplastic kidney) can arise from a defect in the initial outgrowth of the ureteric bud from the Wolffian duct, and/or from a lack of sufficient ureteric bud induction from the adjacent metanephric mesenchyme. Smaller kidney size and reduced number of nephrons (hypoplastic kidney) can arise from reduced

branching of the ureteric epithelium, and/or reduced induction and mesenchyme-to-epithelial transition of the nephron progenitors. In this case, formation of the structures in the innermost region of the kidney proceeded normally, however development of these structures towards the more peripheral areas of the kidney are disrupted. Malformed kidneys (i.e. in cystic/multicystic dysplastic kidney), can arise due to abnormalities in molecular signaling that trigger proper ureteric branching and proper nephron formation, resulting to the formation of immature and poorly-differentiated nephrogenic and ductal structures and the disorganized patterning of the renal parenchyma *(Schedl, 2007)*.

The broad variations of kidney abnormalities and phenotypes observed in renal dysplasia suggest that the underlying etiology can involve a complex interaction of a diverse array of environmental influences and genetic factors.

3.4.1. Environmental risk factors

Certain environmental factors before and during pregnancy can confer an increased risk for developing renal dysplasia in the fetus. Several case control studies conducted in North America have found a strong association between maternal pre-gestational diabetes mellitus and occurrence of renal dysplasia in the offspring (*Parikh et al., 2002; Dart et al., 2015*). Animal studies also support the role of maternal diabetes mellitus on renal dysplasia risk, indicating a strong association of increased calorie and protein intake and gestational hypoxia with decreased nephron endowment at birth (*Amri et al., 1999; Hoppe et al., 2007*). Other studies suggest that low levels of maternal vitamin A intake can result to a reduction in the number of nephrons in the fetal kidney (*Lelièvre-Pégorier & Merlet-Benichou, 2000; Merlet-Benichou, 2003)*.

3.4.2. Genetic risk factors

Linkage analysis, association studies and candidate gene approaches have been conducted to identify genetic factors that contribute to the etiology of renal dysplasia (*Renkema et al., 2011*). These resulted in the identification of several genes that play a role in renal dysplasia pathogenesis. For example, genetic mutations in *BMP4*, *EYA1*, *GDNF*, *GFRA1*, *HNF1β*, *PAX2*, *RET*, *ROBO2*, *SALL1*, *SIX1*, *SIX2*, *HOXA11*/*HOXD11*, *SOX17*, *UMOD*, and *UPK3A* have been associated with the various forms of renal dysplasia (*Renkema et al., 2011*). These analyses, however, have not revealed common candidate signaling networks that result in renal dysplasia, likely due to the complicated and multifactorial nature of the signaling pathways involved.

3.5. β-catenin in the pathogenesis of renal dysplasia

Despite the various causes of renal dysplasia, our studies have shown **elevated levels of β-catenin** in several cases of human renal dysplasia *(Sarin et al., 2014, Bridgewater et al., 2011; Boivin et al., 2016)*. Specifically, immunohistological analysis of human dysplastic kidney tissue shows increased levels of nuclear β-catenin in the mesenchyme-derived structures, ureteric epithelium, and renal stroma (Supplementary Figure 14). The use of mouse models with β-catenin overexpression only in specific cells in the embryonic kidney revealed hallmarks of human renal dysplasia, including abnormal kidney structure, irregular patterning of the renal parenchyma, disorganized formation of nephron progenitors, cystic dilated tubules, and immature or poorly-differentiated nephrogenic and early ductal structures *(Sarin et al., 2014)*. Therefore, our previous work has identified β-catenin, specifically its overexpression, as a key molecule in the pathogenesis of renal dysplasia.

Supplementary Figure 14: Elevated levels of nuclear β-catenin in renal dysplasia

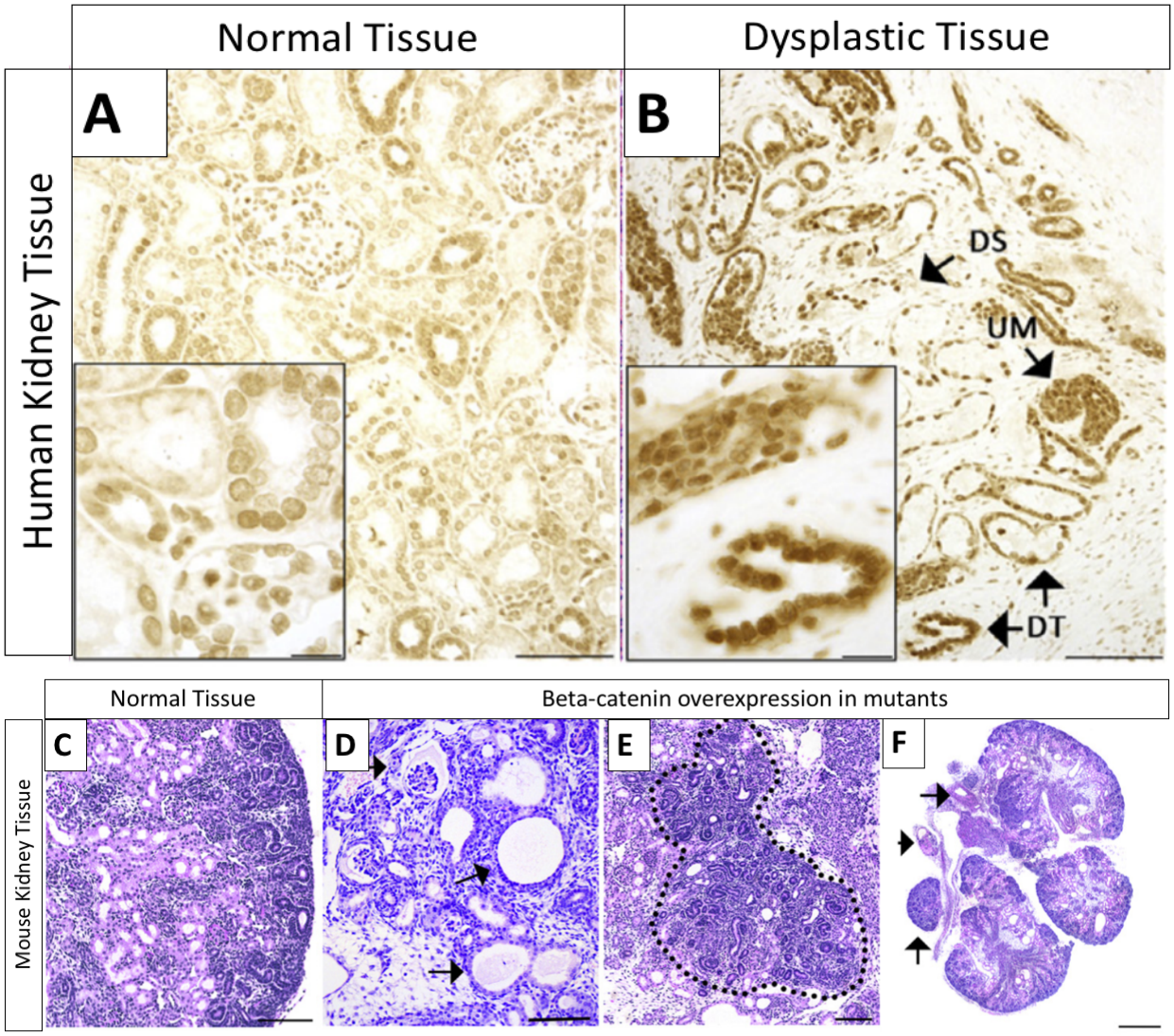

Elevated levels of nuclear β-catenin in renal dysplasia. A) and B) Histological findings from human renal dysplasia. Immunohistochemistry staining for activated β-catenin shows that compared to normal tissue (A), in renal dysplasia (B) there is increased expression of β-catenin (shown as higher staining intensity) in epithelial tubules, undifferentiated mesenchyme (UM) and stroma. C-F) Histological findings from mouse models of renal dysplasia where β-catenin is selectively overexpressed in the developing embryonic kidneys. In contrast to wild-types (C), mutant kidneys show characteristics consistent with human renal dysplasia, including multiple cystic glomeruli (D; black arrow: top), large cortical and medullar cysts (D; black arrow: bottom), undifferentiated dilated epithelial tubules (D; black arrow: middle), and disorganized nephrogenic zone with undifferentiated mesenchyme and tubules deep into the medulla (E; dotted black line), and abnormal kidney structure (F). *(Taken from Sarin et al., 2014).*

4. Wnt/β-catenin signaling in kidney development and renal dysplasia

4.1. Role of β-catenin in canonical Wnt signaling

The canonical Wnt/β-catenin signaling pathway is a signal transduction cascade that plays a central role in mammalian embryonic development and in the homeostatic control of cell turnover in a number of adult tissues (*Clevers, 2006*). β-catenin plays a key role in the canonical Wnt signaling pathway by acting as a signaling molecule and a transcriptional co-activator with T-cell-specific transctiption factor/lymphoid enhancer binding factor (Tcf/Lef) family of proteins (Supplementary Figure 15; *Boivin et al., 2015a; Nusse & Clevers*, *2017)*. The intracellular levels of β-catenin are tightly regulated by the Wnt signaling pathway as the cytosolic pool of β-catenin is constitutively targeted for enzymatic breakdown by a phosphorylation-based system (*Daugherty & Gottardi, 2007*). Wnt signaling is in its deactivated state in the absence of an extracellular Wnt ligand. Cytoplasmic β-catenin is bound by a destruction complex, which includes **Axin**, adenomatous polyposis coli (**APC**), and protein kinases casein kinase-1α (**CK1α**) and serine-threonine glycogen kinase-3 (**GSK3**). β-catenin is phosphorylated by a dual-kinase mechanism: CK1α first phosphorylates β-catenin at serine 45, and this primary phosphorylation leads to a subsequent phosphorylation by GSK3 at amino acid residues serine 33, serine 37 and threonine 41 (*Daugherty & Gottardi, 2007*). Axin is a scaffold protein that coordinates these phosphorylation events. APC is a tumour suppressor gene product that is a co-binding partner for axin and may play a role in separating phosphorylated β-catenin from the axin complex and promoting its transfer to the degradation machinery (*Daugherty & Gottardi, 2007*). β-catenin that is phosphorylated at serine residues 33 and 37 is recognized by the β-TrCP E3 ligase complex, targeting it for ubiquitination and proteaosomic degradation *(Daugherty & Gottardi, 2007)*. As a result, β-catenin is absent from the nucleus and the Tcf/Lef co-transcription factors are bound by

transcriptional corepressors such as the **Groucho/TLE** and histone deacetylase (**HDAC**) family of proteins, preventing the expression of Wnt target genes *(Boivin et al., 2015a; Nusse & Clevers, 2017)*. Wnt signaling is in its activated state when extracellular Wnt ligands bind to the receptors frizzled (**Fz**) and LDL receptor related protein 5/6 (**Lrp5/6**). This binding results in dishevelled (**Dsh**) sequestering the destruction complex proteins to the cell membrane, therefore preventing β-catenin degradation (*Boivin et al., 2015; Nusse & Clevers, 2017*). As a result, the non-phosphorylated β-catenin can accumulate in the cytoplasm and enter the nucleus. β-catenin then binds to Tcf/Lef co-transcription factors, displaces the transcriptional corepressors, and activates the expression of Wnt target genes. These target genes (i.e. *cyclin-D1*, *c-myc*, etc.) play a role in cell proliferation, cell fate determination, differentiation, and apoptosis (*Boivin et al., 2015a; Nusse & Clevers, 2017*).

Supplementary Figure 15: β-catenin is a transcriptional co-activator in the canonical Wnt signaling pathway

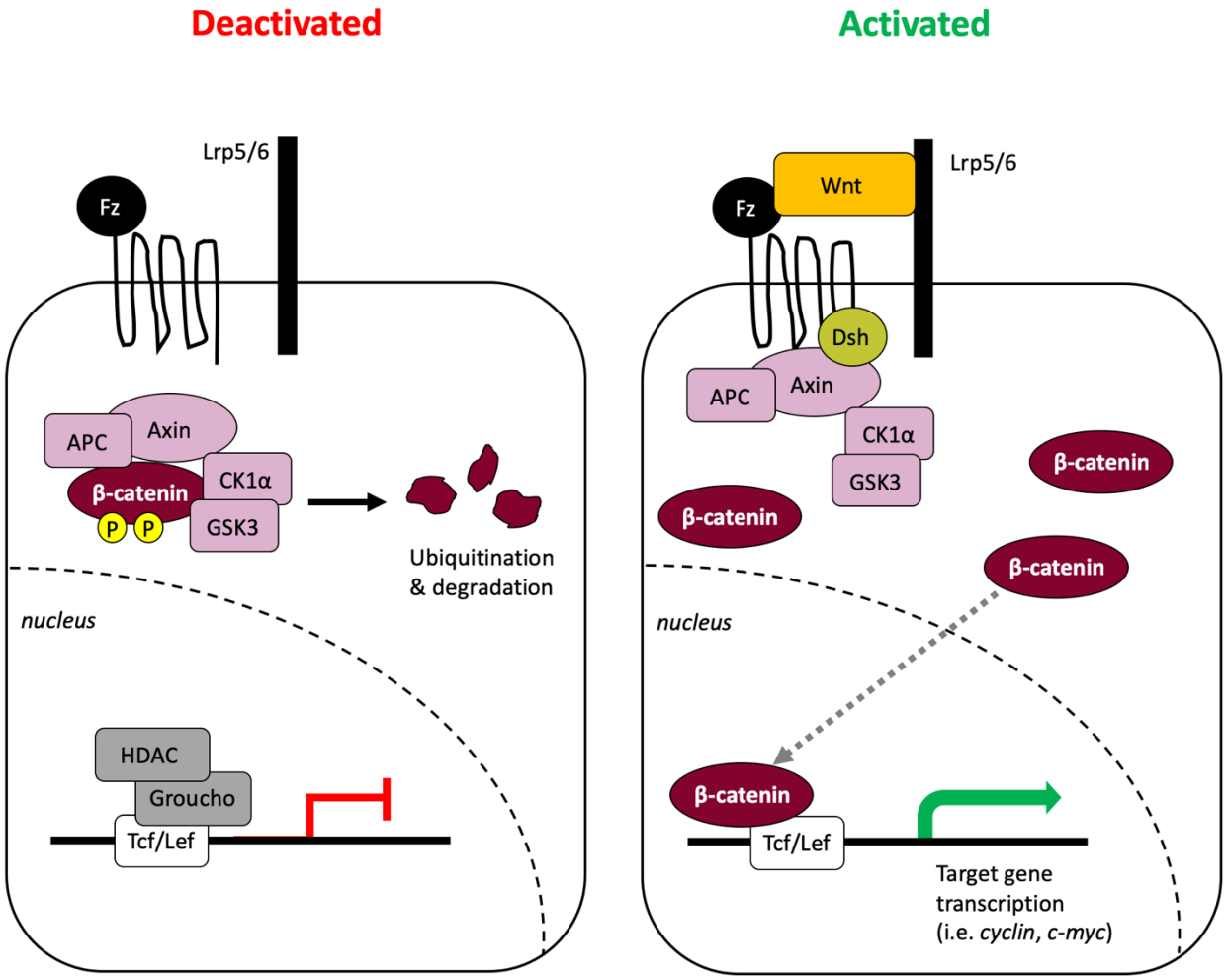

β-catenin is a transcriptional co-activator in the canonical Wnt signaling pathway. Left: In the deactivated state of the pathway, β-catenin is phosphorylated by the degradation complex (Axin, APC, GSK3 and CK1α) and undergoes degradation. Right: In the activated state of the pathway, non-phosphorylated β-catenin translocates into the nucleus and activates target gene expression.

4.2. Role of β-catenin in cell-cell adhesion

β-catenin also plays a critical role in regulating cell-cell adhesion as a central component of the cadherin/catenin adhesive complex (Supplementary Figure 16). Adherens junctions play a role in the creation and maintenance of epithelial cell layers by regulating cell growth and adhesion between adjacent epithelial cells *(Boivin et al., 2015a)*. Within these junctions, β-catenin binds to **α-catenin** and connects **E-cadherin** to actin microfilaments in the cell. Through this process, β-catenin regulates E-cadherin-mediated intercellular adhesion at the cell membrane and mitigates the dynamic interaction between the actin cytoskeleton and adherens junction proteins *(Brembeck et al., 2006)*. This process is critical for mediating cellular movements and migration involved in proper tissue morphogenesis and organ development *(Daugherty & Gottardi, 2007; Boivin et al., 2015a)*.

Supplementary Figure 16: Role of β-catenin in cell-cell adhesion

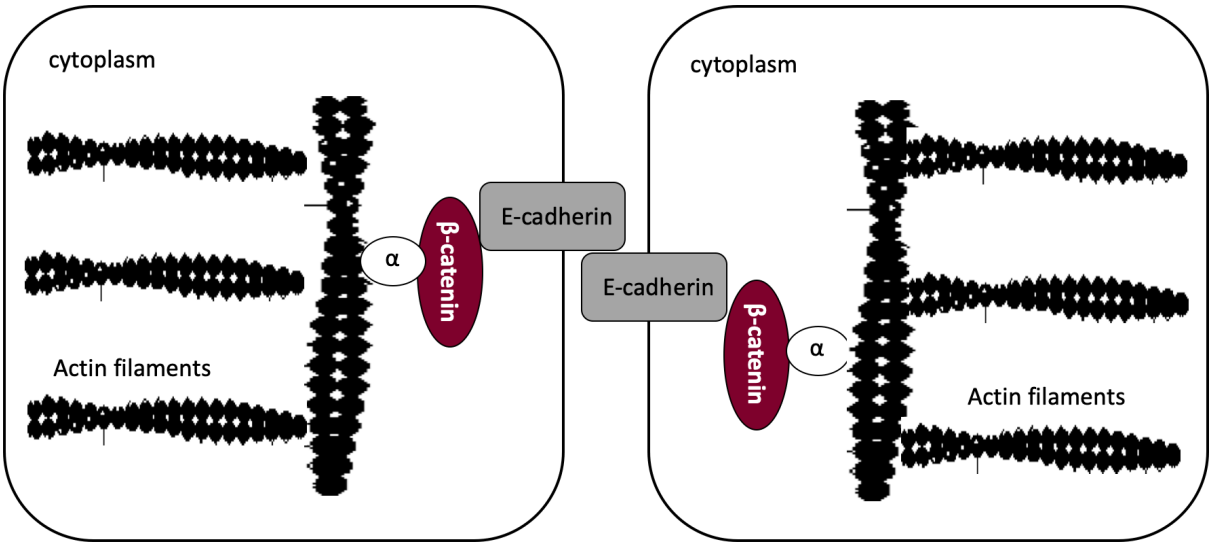

Role of β-catenin in cell-cell adhesion. β-catenin plays a role in adherens junctions linking adjacent epithelial cells; it mediates the connection between the actin cytoskeleton to α-catenin and to E-cadherin in the cell membrane.

4.3. β-catenin protein structure

β-catenin is a multifunctional protein that belongs to the armadillo family of proteins, which are characterized by a central region made up of a repetitive amino acid sequence called the 'armadillo repeats' *(Daugherty & Gottardi, 2007)*. β-catenin is a 92 kDa protein encoded by the *CTNNB1* gene *(Debuire et al., 2003)*. In humans, *CTNNB1* is located on the p-arm of chromosome 3 (genetic location: 3p22.1) and contains 14 protein-coding exons. The encoded protein (Supplementary Figure 17) has 781 amino acids which encompasses the following: phosphorylation sites for GSK3 and CK1α, 13 armadillo repeats which contains binding sites for α-catenin, APC, Axin/conductin, Tcf/Lef, and a transactivation domain *(Debuire et al., 2003)*.

Supplementary Figure 17: β-catenin protein structure

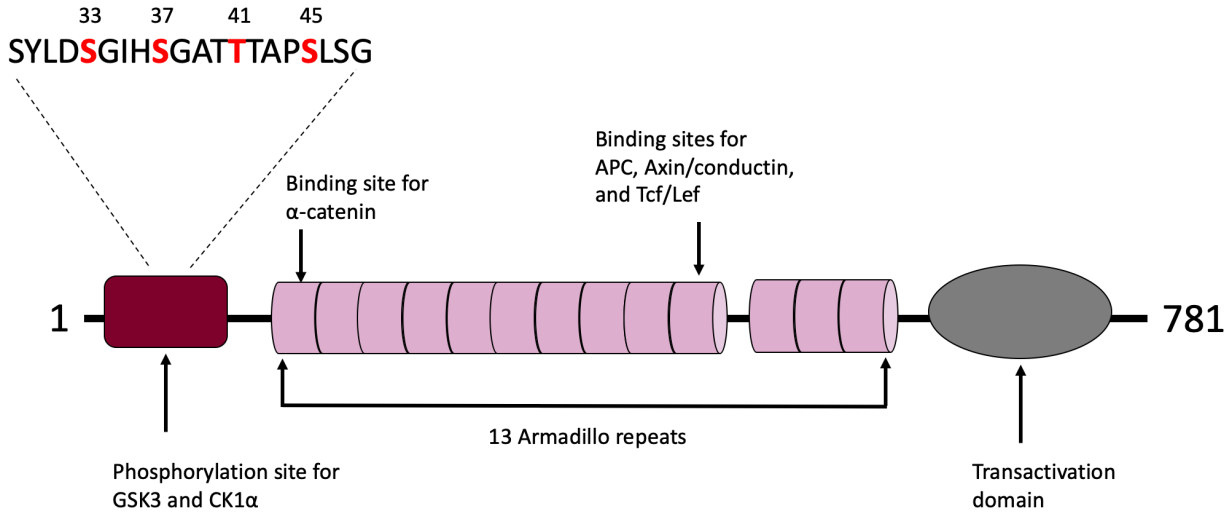

β-catenin protein structure. Representation of β-catenin protein structure with its protein-interacting domains, including (from N-terminus to C-terminus): phosphorylation sites for kinases GSK3 and CK1α including amino acid residues serine 33, serine 37, threonine 41 and serine 45; binding sites for APC, Axin/conductin and Tcf/Lef within the 13 armadillo repeats; and a transactivation domain. *(Adapted from: Debuire et al., 2003).*

4.4. β-catenin activity in kidney development

In the embryonic mouse and human kidney, β-catenin is expressed in all three cell lineages of the developing kidney: the ureteric epithelium, metanephric mesenchyme, and renal stroma (*Bridgewater et al., 2008; Sarin et al., 2014; Boivin et al., 2015b*). Within these cells, the cytoplasmic, nuclear and membrane-bound expression patterns of β-catenin demonstrate its important roles in mediating cell-cell adhesion and regulating gene transcription. During kidney development, β-catenin signaling regulates the transcriptional activation of genes that play roles in branching morphogenesis and nephron formation. For my Master's, I focused on three β-catenin transcriptional targets in the developing kidney: *Pax2*, *Six2*, and *GDNF*.

Pax2 (Paired Box 2) is a transcription factor that plays a role in nephrogenesis. Specifically, Pax2 is expressed in metanephric mesenchyme cells as these cells undergo mesenchymal-to-epithelial transition (*Torban et al., 2006*). Pax2 activates the expression of Wnt4 (one of the epithelialization markes), initiating the nephrogenic program (*Torban et al., 2006*).

Six2 (Sine Oculis Homeobox Homolog 2) is expressed in condensed mesenchyme cells in the nephrogenic zone. Throughout kidney development, Six2 tightly regulates the self-renewing nephron progenitor population by signaling in a cell-autonomous manner to maintain an undifferentiated nephron progenitor cell status (*Kobayashi et al., 2008*). In the condensed mesenchyme, Six2 binds to Tcf/Lef transcription factors and with Groucho/HDAC repressors, blocking binding sites for β-catenin and therefore preventing the β-catenin-driven activation of the nephrogenic initiation (*Park et al., 2012*).

GDNF (Glial Cell Derived Neurotrophic Factor) regulates branching morphogenesis of the ureteric epithelium. GDNF expressed in metanephric mesenchyme binds to Ret receptors on the branch tips of the ureteric epithelium. This binding initiates the formation and outgrowth of the

first ureteric bud and maintains the subsequent cycles of ureteric branching (*Sarin et al., 2014; Basson et al., 2006*).

4.5. Abnormal β-catenin levels and transcriptional activity in renal dysplasia

In renal dysplasia, elevated levels of nuclear β-catenin in the ureteric epithelium, metanephric mesenchyme and renal stroma, and consequently its increased transcriptional activity, contribute to the dysregulated activation of target genes involved in kidney development. This results to the aforementioned abnormalities in ureteric branching and disrupted nephron formation observed in dysplastic kidneys (*Sarin et al., 2014; Bridgewater et al., 2011; Boivin et al., 2015b*).

Increased levels of β-catenin in the developing kidney results to abnormalities in branching morphogenesis. In a mouse model of renal dysplasia where β-catenin is overexpressed in the metanephric mesenchyme, GDNF expression levels were increased, which resulted to the formation of several ectopic ureteric branches and a highly disorganized branching pattern (*Sarin et al., 2014*). Elevated GDNF expression in the mesenchyme resulted to increased Ret stimulation in the ureteric epithelium, which in turn led to an increase in nuclear β-catenin in the ureteric epithelium and resulted to altered expression of target genes involved in proper ureteric branching (*Sarin et al., 2014*). In another mouse model of renal dysplasia where β-catenin is overexpressed in the ureteric epithelium, abnormalities in ureteric branching and nephrogenesis were observed (*Bridgewater et al., 2011*). These mutants showed increased expression of Tgfβ2 and CK1α which inhibited ureteric branching, and also expanded the population of nephron progenitors undergoing differentiation. These mutants also exhibited increased expression of Wnt inhibitor Dkk1, which inhibited Wnt4 activity and led to a marked decrease in nephron structures. These findings

demonstrate that overexpression of β-catenin disrupts GDNF signaling and leads to the abnormal branching pattern.

Elevated levels of β-catenin in the developing kidney also results to disruptions in nephron formation. A mutant mouse model where β-catenin is selectively overexpressed in the metanephric mesenchyme showed disrupted expression patterns of Pax2 in the renal parenchyma and several sporadic regions of immature and improperly-developed Pax2-expressing nephrogenic structures deep in the medullary region (*Sarin et al., 2014*). These mutant mice also showed an abnormal expansion of the self-renewing mesenchymal cells deep into the medullary region (*Sarin et al., 2014*). This resulted to a marked decrease in the number of properly-forming nephrons in the renal parenchyma (*Sarin et al., 2014*). Further, these mutants revealed ectopic and disorganized expression patterns of Wnt4, Fgf8, Pax8, and Lhx1, demonstrating a lack of proper epithelialization of these nephrogenic structures (*Park et al., 2007*). Together, these observations demonstrate that β-catenin signaling is important in proper nephron formation. Consequently, overexpression of β-catenin results to disruptions in the cellular processes involved in proper mesenchymal-to-epithelial transition of the nephrogenic structures. In addition, maintenance of the progenitor cell population through Six2 binding with transcription factors may be necessary in order to ensure continued and proper nephron formation for the subsequent new waves of nephrogenesis until the progenitor cell population is exhausted at the end of nephrogenesis during early postnatal period (*Park et al., 2012*). Elevated β-catenin levels also disrupt normal Six2 expression levels and activity and can be a contributing factor to an early depletion of the progenitor pool and the resulting lack of proper nephron formation (*Park et al., 2012*).

5. Quercetin as a modulator of β-catenin activity

5.1. General overview of flavonoids

Flavonoids are natural phenols synthesized in plants. They are found in food sources such as parsley, blueberries, black tea, citrus fruits, wine, and cocoa. There are over 8,000 individual types known (*Pietta, 2000*) and they are widely investigated in biomedical research due to their pharmacological and therapeutic activities (*Amado et al., 2011, Selvaraj et al., 2014*). Abnormalities in the Wnt/β-catenin signaling pathway promote dysregulated cellular and physiological processes leading to the pathogenesis of various diseases. For this reason, it is not surprising that several studies have attempted to target this pathway. Flavonoids have demonstrated therapeutic potential in many human diseases through altering the Wnt/β-catenin signaling pathway (*Amado et al., 2011; Park & Choi, 2010*). For my Master's, I selected the flavonoid **quercetin** to test if it can mitigate abnormal β-catenin signaling in our mouse models of renal dysplasia. I selected quercetin because several *in-vitro* and *in-vivo* studies have demonstrated it is effective in reducing elevated β-catenin levels and transcriptional activity in different human cancer cell lines and in a mouse model of kidney fibrosis.

5.2. Quercetin: physicochemical properties, dietary sources and therapeutic effects

Quercetin (IUPAC name: 2-(3,4-dihydroxyphenyl)-3,5,7-trihydroxychromen-4-one) is a plant flavonoid categorized under the flavonol subclass *(Li et al., 2016)*. Supplementary Figure 18 shows the chemical structure of quercetin. Quercetin naturally occurs as an aglycone (i.e. lacking an attached sugar moiety). Physically, quercetin is a brilliant yellow needle-like crystal, has poor solubility in water but good solubility in alcohols, lipids and aprotic solvents like DMSO. Quercetin is one of the most abundant flavonoids found in the human diet and is found in a variety

of brightly coloured plant-based foods such as dark leafy vegetables, green tea, berries, capers, red onions, apples, citrus fruits, and red wine *(Li et al., 2016)*. Several *in-vitro* and *in-vivo* studies have demonstrated the biological effects of quercetin, such as having roles as an antioxidant, an antibacterial agent, an antineoplastic or antitumourigenic agent, a chelator, a free radical scavenger, and a protein kinase inhibitor. These observations provide insights on the protective and therapeutic benefits of quercetin against common human pathologies such as cancer, inflammation, cardiovascular and metabolic diseases, and neurodegenerative disorders *(D'Andrea, 2015)*.

Supplementary Figure 18: Chemical structure of quercetin

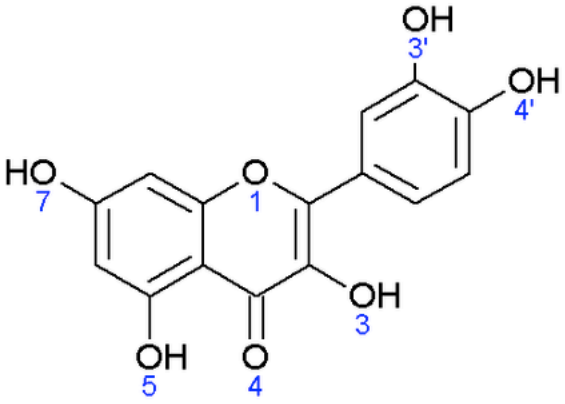

Chemical structure of quercetin. IUPAC nomenclature: 2-(3,4-dihydroxyphenyl)-3,5,7-trihydroxychromen-4-one). Quercetin contains the generic three-ringed fifteen-carbon skeleton (C6-C3-C6) structure of flavonoids, with five hydroxyl groups at positions 3, 5, 7, 3' and 4. *(Taken from: Li et al., 2016)*.

5.2. Quercetin mitigates abnormal β-catenin signaling in cancer

Several *in vitro* studies involving treatment of human cancer cell lines with quercetin have demonstrated reductions in β-catenin levels and transcriptional activity, which resulted in improved outcomes such as reduced tumour growth, decreased tumour cell proliferation and inhibition of metastasis and invasion. In a study by Srinivasan *et al.* (2016), increased levels of β-catenin expression and transcriptional activity is observed in triple-negative breast cancer (TNBC)

cells. Treatment of TNBC cells with quercetin significantly decreased β-catenin levels and activity, resulting in decreased cancer cell survival, migration and invasion (*Srinivasan et al., 2016*). Immunofluorescence analysis revealed nuclear localization of β-catenin in untreated controls, whereas cytoplasmic localization was observed in quercetin-treated cancer cells. These findings were further validated by Western blot analysis using lysates from nuclear and cytoplasmic fractions of the samples. Untreated cells show higher nuclear β-catenin expression levels compared to that of the quercetin-treated cells. Conversely, quercetin-treated cells show higher cytoplasmic β-catenin expression levels compared to that of the untreated controls (*Srinivasan et al., 2016*). Quantitative RT-PCR analysis showed a dose-dependent decrease in mRNA expression levels of *cyclin D1* and *c-myc* (*Srinivasan et al., 2016*). These findings demonstrate quercetin decreases nuclear β-catenin and consequently decreases target gene expression. *Cyclin D1* and *c-myc* are β-catenin target genes that play important roles in cell cycle regulation and their expression levels are deregulated in cancer cells. Quercetin treatment in TNBC cells, however, mitigated the expression levels of *cyclin-D1* and *c-myc* in a β-catenin-dependent manner, and this was correlated with decreased cancer cell survivability, migration and invasiveness (*Srinivasan et al., 2016*). Similarly, studies on pancreatic cancer cells (*Cao et al., 2015*) and colon cancer cells (*Park et al., 2005*) have also demonstrated a quercetin-induced decrease in nuclear β-catenin and reduction in the transcriptional activation of several factors involved in tumourigenesis, resulting to improved outcomes such as decreases in tumour cell viability, proliferation, self-renewal capacity, invasion, and drug resistance (*Cao et al., 2015; Park et al., 2005*).

5.3. Quercetin mitigates abnormal β-catenin signaling in kidney fibrosis

Another study in a mouse model of kidney fibrosis showed that in-vivo delivery of quercetin mitigates abnormal β-catenin signaling (*Ren et al., 2016*). In this study, mice were given unilateral obstructive uropathy (UUO) to simulate acute kidney fibrosis. Afterwards, mice were injected with either a control vehicle (no quercetin) or with quercetin. Normally, UUO triggers an abnormal increase in activated β-catenin in renal interstitial cells, triggering an increased expression of markers for fibroblast activity, ultimately leading to acute kidney fibrosis. However, treatment with quercetin reduced the amount of UUO-induced increase in activated β-catenin, resulting to decreased fibroblast activity and attenuating the progression of renal interstitial fibrosis *(Ren et al., 2016)*.

Combined, these studies on quercetin's therapeutic effects on cancer cells and on kidney fibrosis provide evidence that quercetin can decrease nuclear β-catenin levels in tissues and decrease the transcriptional activation of its targets, resulting to phenotypic outcomes that show decreased severity of the disease.

HYPOTHESIS AND OBJECTIVES

1. Rationale and general hypothesis

Previous studies from our laboratory have demonstrated elevated levels of β-catenin in fetal and perinatal human kidney tissue. Using mouse models of renal dysplasia, we have demonstrated that the overexpression of β-catenin leads to a disruption in genes essential for kidney development, resulting in renal dysplasia characterized by abnormal branching morphogenesis and disrupted nephrogenesis. Therefore, our previous work has identified that the β-catenin overexpression in dysplastic kidneys can be a potential therapeutic target. Quercetin modulates β-catenin signaling by decreasing nuclear β-catenin levels and reducing its transcriptional activity. Studies have demonstrated that quercetin treatment resulted in improved outcomes in a mouse model of renal fibrosis, as well as reduced tumour growth and migration in human cancer cell lines.

The goals of my Master's thesis are 1) to determine if quercetin treatment has any effects in the developing kidney and 2) to determine if quercetin treatment decreases β-catenin overexpression and rescue renal dysplasia. I hypothesize that **quercetin inhibits β-catenin transcriptional activity during kidney development and reduces the severity of renal dysplasia**.

2. Research questions:

1) Does quercetin treatment affect branching morphogenesis and nephron formation during normal kidney development?

Hypothesis: Quercetin decreases branching morphogenesis and nephron formation during kidney development in a β-catenin dependent manner.

2) Does quercetin reduce the severity of renal dysplasia in a β-catenin-dependent manner?

Hypothesis: Quercetin reduces β-catenin activity and reduces the severity of renal dysplasia.

MATERIALS AND METHODS

Mouse models

All animal studies were performed in accordance with institutional animal care guidelines as set by McMaster University (Animal Utilization Protocol #180312). During the course of my Master's, I used 6 different mouse strains (listed below). All mice have a CD1 genetic background. For all strains, 12:00 PM on the day of vaginal plug was considered embryonic day (E) 0.5. Pregnant females were euthanized via cervical dislocation at E13.5.

- Wild-type CD1 male and female mice, crossed to generate wild-type embryos
- Male FoxD1-Cre male mice were used to drive Cre expression specifically in the renal stroma (*Boivin et al., 2016*)
- Male RarB2-Cre mice were used to drive Cre expression specifically in the metanephric mesenchyme (*Sarin et al., 2014*)
- Female $\beta cat^{fx/fxGOF}$ mice that have LoxP sites flanking exon 3 of the β-catenin allele. Exon 3 codes for a phosphorylation site of β-catenin, therefore its excision through Cre-recombinase activity creates an isoform of β-catenin that cannot be degraded and β-catenin accumulates in the cell
- Male FoxD1-Cre mice crossed with female $\beta cat^{fx/fxGOF}$ to generate embryos with β-catenin overexpression in the renal stroma (termed $\beta cat\text{-}GOF^{RS}$)
- Male RarB2-Cre mice crossed with female $\beta cat^{fx/fxGOF}$ to generate embryos β-catenin overexpression in the metanephric mesenchyme (termed $\beta cat\text{-}GOF^{MM}$)

PCR genotyping

Embryo heads, tail, or adult male ear notch were used to isolate DNA. The DNA Fast Extract Kit (Wisent Inc.) was utilized as per manufacturer's instructions. Lysates were centrifuged at 12,500 rpm for 2 minutes. Genotyping was performed for *Cre* using the following primer sequences: forward strand: 5'-gcggcatggtgcaagttgaat-3' and reverse strand: 5'-cgttcaccggcatcaacgttt-3'. The PCR conditions for *Cre* amplification were set at 94˚C for 45 seconds, 58˚C for 40 seconds, and 72˚C for 40 seconds, for 35 cycles. PCR products were run on a 1% agarose gel with 5 µL RedSafe (Sigma Aldrich) in a 1X Tris-acetate-EDTA (TAE) buffer at 135V for 50 minutes.

Embryonic mouse kidney microdissection and organ culture

Wild-type, βcat-GOF^{MM} and βcat-GOF^{RS} kidneys were resected from E13.5 mouse embryos using Dumont #5 INOX surgical forceps in cold phosphate-buffered saline (PBS), pH 7.4, under an Olympus SZ61 microscope. Resected kidneys were grown on 3 µm polyethylene terephthalate transwell filters (Millipore Sigma) in a 6-well culture plate containing Dulbecco's minimal essential medium (DMEM; Life Technologies) with 1% penicillin/streptomycin (ThermoFisher Scientific) and supplemented with 0 µM (untreated control), 40 µM, 80 µM, and 160 µM of quercetin (Sigma Aldrich, Catalog # Q4951) for 48 hours in 37˚C and 5% CO_2. Quercetin was first prepared as a 50 mM stock concentration in 100% dimethyl sulfoxide.

Tissue preparation and histological staining

After culture, kidneys were fixed in 4% paraformaldehyde at 4˚C for 48 hours. Kidneys were then processed through serial ethanol and xylene washes, followed by paraffin infiltration

and embedding as described. Paraffin-embedded kidneys were sectioned on a microtome (Leica) into 5 μm-thick sections, mounted onto Superfrost microscope slides (VWR), and dried at room temperature for 24 hours. Sectioned kidneys were heated at 60°C in an oven, deparaffinized using xylene washes and rehydrated using graded ethanol washes (100%, 95%, 75%, 50%), followed by staining with Hematoxylin and Eosin (Sigma Aldrich). Slides were fixed using non-aqueous Vectamount mounting medium (Vector Labs) and imaged using Olympus brightfield microscope.

Whole-mount immunofluorescence

After culture, kidneys were collected and fixed in 100% methanol at -20°C for 24 hours. Kidneys were washed 3 times in sterile PBS (pH 7.4) with gentle agitation, blocked in 10% normal goat serum, then incubated with primary antibodies to cytokeratin (Sigma Aldrich; host species: mouse; diluted at 1:200) and Pax2 (Abcam/BioLegend; host species: rabbit; diluted at 1:400) at 37°C for 1.5 hours. Primary antibodies were diluted in an incubation buffer containing 1% PBS, 3% bovine serum albumin, 5% normal goat serum and 0.3% Tween20. Kidneys were washed 3 times in sterile PBS, then incubated with secondary antibodies Alexa Fluor 488 anti-rabbit (Life Technologies; host species: goat; diluted at 1:300) and Alexa Fluor 594 anti-mouse (Invitrogen; host species: goat; diluted at 1:300) at 37°C for 1.5 hours. Secondary antibodies were also diluted in an incubation buffer containing 1% PBS, 3% bovine serum albumin, 5% normal goat serum and 0.3% Tween20. Kidneys were washed 3 times in PBS and imaged on Olympus fluorescence microscope.

Immunofluorescence and immunohistochemistry

Deparaffinization and rehydration of samples were performed by immersing slides in xylene and graded ethanol washes (100%, 95%, 70% and 50%). Slides were washed in PBS, then heat-induced epitope retrieval was performed for 5 minutes in 11.4 mM/L sodium citrate buffer solution (pH 6.0) in a pressure cooker. For immunofluorescence, samples were blocked with 7.5% normal goat serum and 4.5% bovine serum albumin at room temperature for 1 hour, followed by incubation with primary antibodies to cytokeratin (Sigma Aldrich; host species: mouse; diluted at 1:200), Pax2 (Abcam/Biolegend; host species: rabbit; diluted at 1:200), Six2 (Abcam; host species: rabbit; diluted at 1:200), and E-cadherin (Abcam, host species: mouse; diluted at 1:100) at 4°C in a humidified chamber overnight. Primary antibodies were diluted in an incubation buffer containing 1% PBS, 3% bovine serum albumin, 5% normal goat serum and 0.3% Tween20. Samples were washed 3 times in PBS, then incubated with secondary antibodies Alexa Fluor 488 anti-rabbit (Life Technologies; host species: goat; diluted at 1:1000) and Alexa Fluor 594 anti-mouse (ThermoFisher Scientific; host species: goat; diluted at 1:1000) at room temperature for 1 hour. Samples were then counterstained with DAPI (Sigma Aldrich; diluted at 1:1000) for 5 minutes. Slides were washed in PBS then fixed using Fluoromount mounting medium (Sigma Aldrich).

Immunohistochemistry was performed using the Vectastain Elite avidin-biotin complex kit (Vector Labs). After antigen retrieval, slides were immersed in 3% hydrogen peroxide at room temperature for 30 minutes to block endogenous peroxidase activity, followed by 5% normal goat serum in phosphate-buffered saline with Tween20 (PBST) at room temperature for 30 minutes to block any non-specific secondary antibody binding. Avidin and biotin blocking reagents (Vector Labs) were then applied on the samples, as per manufacturer protocols, to block endogenous

biotin-blocking activity. Mouse-on-mouse blocking reagents (Vector Labs) were applied on the samples, as per manufacturer protocols, to block any non-specific binding of the primary antibody. Incubation with primary antibodies to active β-catenin clone 8E7 (Millipore; host species: mouse; diluted at 1:200 in PBST) and total β-catenin (BD Biosciences; host species: mouse; diluted at 1:200 in PBST) was performed overnight at 4˚C. Samples were washed with PBS then incubated with HRP-conjugated/biotinylated secondary antibody anti-mouse (Abcam; host species: goat; diluted at 1:500 in PBST) at room temperature for 45 minutes. Avidin-Biotin Complex (ABC) reagent (Vector labs) was applied on the samples followed by colorimetric visualization using diaminobenzidine (Vector labs) as per manufacturer protocols. Slides were dehydrated using graded ethanol washes (50%, 75%, 95%, and 100%) and xylene washes, followed by non-aqueous mounting using Vectamount mounting medium (Vector Labs). Samples were imaged using Olympus brightfield microscope.

Western blot

After culture, kidneys were snap-frozen at -80˚C. Kidneys were lysed by homogenizing samples in RIPA lysis solution (Millipore) containing 0.05 M Tris-HCl (pH 7.4), 0.15 M NaCl, 0.25% deoxycholic acid, 1% NP-40, 1 mM EDTA, and supplemented with 1% protease inhibitor cocktail and 1% phosphatase inhibitor cocktail (ThermoFisher Scientific). Supernatants were collected after centrifugation at 13,000 rcf at room temperature for 10 minutes. Protein concentration was determined by Bradford protein assay (BioRad). Thirteen μg of total protein was added to loading buffer containing 2.5% SDS, 62.5 mM Tris-HCl (pH 6.8), 0.02% Bromophenol Blue, 0.7135 M 2-mercaptoethanol, and 10% glycerol, and heated at 100˚C for 5 minutes. Samples were loaded into 10% Mini-PROTEAN TGX precast polyacrylamide gels

(BioRad) and SDS-PAGE was run using running buffer containing 2.5 mM Tris, 19.2 mM glycine and 0.1% SDS, at 120V, at room temperature for 1 hour. Samples were electrotransferred onto nitrocellulose blotting membrane with a 0.2 μM pore size (GE Healthcare) using transfer buffer containing 2.5 mM Tris and 19.2 mM glycine at 100V, on ice at 4°C for 50 minutes. Nitrocellulose membranes were blocked in 5% skimmed milk in tris-buffered saline with Tween20 (TBST) at room temperature with gentle agitation, followed by primary antibody incubation at 4°C overnight. The following primary antibodies were used: non-phosphorylated β-catenin Ser33/Ser37/Thr41 (Cell Signalling; host species: rabbit; diluted at 1:1000) and total β-catenin (BD Biosciences; host species: mouse; diluted at 1:2000). Primary antibodies were diluted in an incubation buffer containing 5% bovine serum albumin (BSA) in TBST. Nitrocellulose membranes were washed in TBST, followed by secondary antibody incubation for 1 hour at room temperature. The following secondary antibodies were used: HRP-conjugated anti-rabbit (Abcam; host species: goat; diluted at 1:2000) and HRP-conjugated anti-mouse (Abcam; host species: goat; diluted at 1:2000). Secondary antibodies were diluted in blocking buffer containing 5% skimmed milk in TBST. Chemiluminescent detection was performed using Pierce ECL Western Blotting Substrate (ThermoFisher Scientific), as per manufacturer instructions, and blots were imaged using GeneSys chemiluminescence imaging software. Total protein was used as loading control, by staining blots with Red Ponceau (Sigma Aldrich). Quantification of Western blots was performed using densitometry analysis on ImageJ (version 1.52). A rectangular selection tool with fixed dimensions was used to measure the density values of each individual band, and 'raw integrated density' values from each band were taken as expression levels. Comparisons in protein levels were made using a two-tailed Student's t-test on independent samples (p-values of <0.05 were considered statistically significant). Statistical analyses were performed using GraphPad Prism software (version 8.1.2).

Quantitative reverse-transcriptase real-time PCR (qRT-PCR)

After culture, kidneys were collected and snap-frozen at -80˚C for 24 hours. Total RNA was isolated from each kidney explant using the RNeasy Micro kit (QIAGEN), and reverse transcribed to cDNA using the RT^2 First Strand kit (QIAGEN) as per manufacturer recommendations. Real-time PCR reaction mix contained 3 ng of each cDNA sample, 300 nM of each primer, 1X SYBR Green ROX PCR Master Mix (QIAGEN) and RNAse-free H_2O for a total volume of 25 µL per reaction of a 96-well qRT-PCR plate. Real-time PCR amplification was performed using the Applied Biosystems StepOne standard RT-PCR system. Relative mRNA levels were quantitated using the $2^{\Delta\Delta Ct}$ quantitation method, using cDNA from the untreated kidneys as reference sample and *B2M* as endogenous control. Comparisons were made using a two-tailed Student's t-test (p-values of <0.05 were considered statistically significant). Statistical analyses were performed using GraphPad Prism software (version 8.1.2). Primers for *Pax2*, *Six2*, *GDNF* and *B2M* were designed using the NCBI Primer-BLAST designing tool (https://www.ncbi.nlm.nih.gov/tools/primer-blast/) and verified using the UCSC genome bioinformatics website (https://genome.ucsc.edu). The following primer sequences were used:

Pax2 (forward: 5'-taggaaggacgctcaaagactc-3'; reverse 5'-taatggagactcccagagtggt-3')

Six2 (forward 5'-cttctcatcctcggaactgc-3'; reverse: 5'-ggagaacagcgagaactcca-3')

GDNF (forward: 5'- agccctgaacatattgtcacct-3'; reverse: 5'-tcccctatgttctcctgtctgt-3')

B2M (forward: 5'-ccgaacatactgaactgctacg-3'; reverse: 5'- cacatgtctcgatccagtaga-3')

Quantifying ureteric branch tips

Whole-mount cytokeratin-stained ureteric branch tips were counted in the outer surface of the kidney explants, with at least five individual kidney explants per treatment group. The number

of branch tips in each treatment group was analyzed using two-tailed Student's t-test on independent samples and p-values of <0.05 are considered statistically significant. Statistical analyses were conducted using GraphPad Prism software (version 8.1.2).

Quantifying nephrogenic structures

Formalin-fixed, paraffin-embedded tissue sections from wild-type, untreated βcat-GOF^{MM} and quercetin-treated βcat-GOF^{MM} were used to count nephrogenic structures. Two sections, each 10 μm apart, were collected per kidney for analysis. For each kidney, one section was stained with hematoxylin and eosin, and the other section was immuno-stained with cytokeratin and Pax2 (with a DAPI counterstain). Using an Olympus microscope, images were taken at 10X magnification in one randomly selected area of the renal parenchyma per tissue section For each image taken, area of the tissue (in mm^2) was measured using ImageJ (version 1.52). The fixed measurement scale was calibrated and set prior to measuring the area of the tissue, and using the polygon selection tool, the outermost aspects of the tissue was manually traced. Nephrogenic structures were counted per image by counting the following structures: comma-shaped structures, S-shaped structures, late-S-shaped structures, early glomeruli and maturing glomeruli. The following structures were not included in the counts: cap mesenchyme cells, pretubular aggregates, renal vesicles, collapsed or apoptotic glomeruli, and abnormally-formed nephrogenic structures (i.e. mesenchymal cells that lack proper apical-basolateral orientation and tubular formation). Comparisons in the number of nephrogenic structures per mm^2 for each treatment group, with at least five individual kidneys per treatment group, were analyzed using two-tailed Student's t-test on independent samples and p-values of <0.05 are considered statistically significant. Statistical analyses were conducted using GraphPad Prism software (version 8.1.2).

RESULTS

1. Quercetin treatment causes a dose-dependent decrease in normal branching morphogenesis

β-catenin plays a critical role during the development of the embryonic kidney *(Boivin et al., 2015a)*. Therefore, prior to determining if quercetin is an effective treatment for renal dysplasia, I first determined whether quercetin has any effects on β-catenin activity in the normally-developing kidney. β-catenin regulates branching morphogenesis during normal kidney development *(Bridgewater & Rosenblum, 2009)*. Therefore, if quercetin affects β-catenin activity during normal kidney development, then alterations in branching morphogenesis should be observed.

Whole kidney explants treated with increasing doses of quercetin (40 μM, 80 μM, and 160 μM) or without quercetin (untreated control) were used for whole-mount immunofluorescence for cytokeratin, a protein expressed exclusively in the ureteric epithelium, to visualize branching morphogenesis. Kidneys grown without quercetin treatment (**Figure 1A**) showed seven branching generations and 93.57±8.641 branch tips (n=7). In comparison to untreated controls, a dose-dependent reduction in branching morphogenesis was observed in quercetin-treated kidneys. Kidneys grown in media supplemented with 40 μM quercetin (**Figure 1B**) had about six branching generations and 64.83±8.072 branch tips (n=6, p=0.0352). Kidneys treated with 80 μM quercetin (**Figure 1C**) had about five branching generations and 50.22±5.096 branch tips (n=9, p=0.0005). Kidneys treated with 160 μM quercetin (**Figure 1D**) showed the greatest decrease in ureteric branching, with only four branching generations and 23.88±3.507 branch tips (n=8, p<0.0001).

Figure 1E shows the dose-dependent reduction in branching morphogenesis as a result of quercetin treatment.

In kidneys treated with quercetin, the ureteric epithelium tended to elongate but failed to bifurcate at the branch tips. A closer analysis of the morphology of individual ureteric epithelial cells in untreated controls revealed a short columnar epithelium with a normal pattern of cell-cell adhesion and with the nucleus located at the basal side of the cell, indicating proper apical-basolateral organization (**Figures 2A and 2A'**). Kidneys grown with 40 μM quercetin showed abnormally-elongating branches on the outer surface of the kidney, and a slightly disorganized arrangement and organization of epithelial cells that make up the tubule (**Figures 2B and 2B'**). Kidneys grown with 80 μM and 160 μM quercetin also have abnormally-elongating branches on the outer surface of the kidney with a more severe disorganization of the epithelial cells and with a marked lack of cell-cell adhesion and apical-basolateral orientation of the cells that make up the ureteric epithelium. Interestingly, the disorganization of epithelial cells observed in kidneys treated with 160 μM quercetin (**Figures 2D and 2D'**) was not as severe as that observed in kidneys grown in 80 μM quercetin (**Figures 2C and 2C'**).

Together, these findings demonstrate that quercetin disrupts branching morphogenesis in a dose-dependent manner in wild-type embryonic kidneys.

Figure 1: Quercetin treatment results in a dose-dependent decrease to branching morphogenesis in wild-type embryonic kidneys

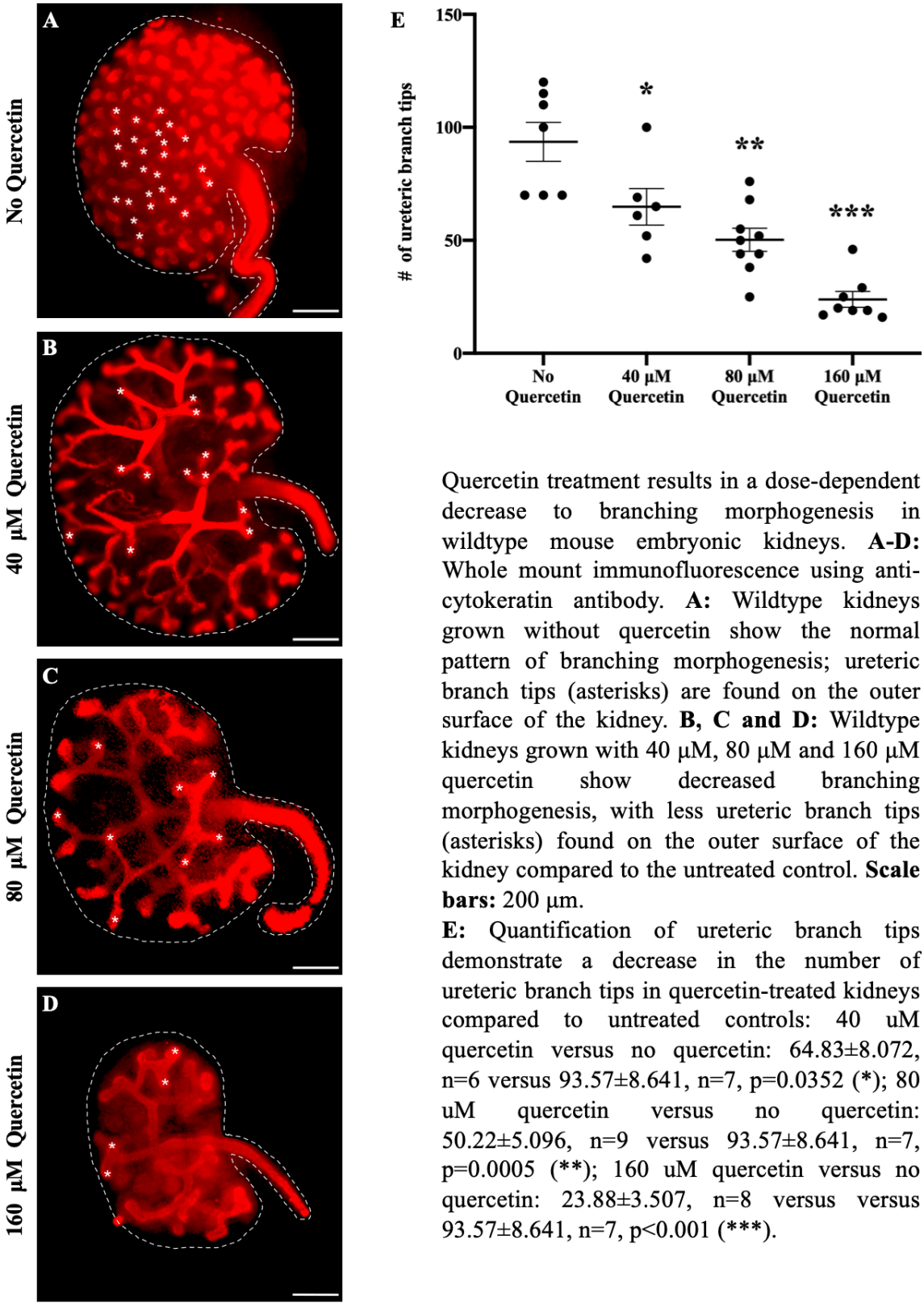

Quercetin treatment results in a dose-dependent decrease to branching morphogenesis in wildtype mouse embryonic kidneys. **A-D:** Whole mount immunofluorescence using anti-cytokeratin antibody. **A:** Wildtype kidneys grown without quercetin show the normal pattern of branching morphogenesis; ureteric branch tips (asterisks) are found on the outer surface of the kidney. **B, C and D:** Wildtype kidneys grown with 40 µM, 80 µM and 160 µM quercetin show decreased branching morphogenesis, with less ureteric branch tips (asterisks) found on the outer surface of the kidney compared to the untreated control. **Scale bars:** 200 µm.

E: Quantification of ureteric branch tips demonstrate a decrease in the number of ureteric branch tips in quercetin-treated kidneys compared to untreated controls: 40 uM quercetin versus no quercetin: 64.83±8.072, n=6 versus 93.57±8.641, n=7, p=0.0352 (*); 80 uM quercetin versus no quercetin: 50.22±5.096, n=9 versus 93.57±8.641, n=7, p=0.0005 (**); 160 uM quercetin versus no quercetin: 23.88±3.507, n=8 versus versus 93.57±8.641, n=7, p<0.001 (***).

Figure 2: Quercetin treatment prevents ureteric branch tip bifurcation in wild-type embryonic kidneys

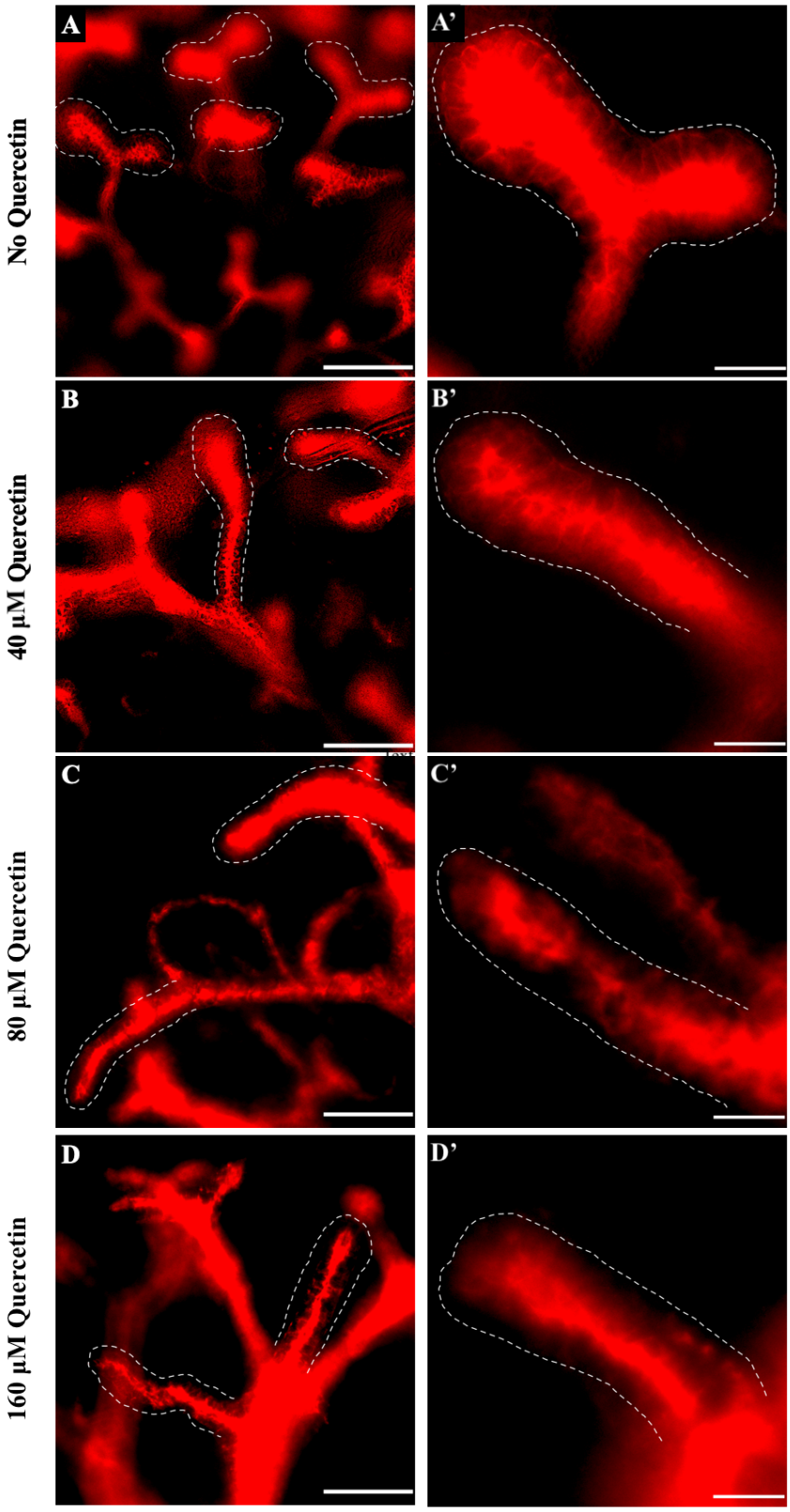

Quercetin treatment prevents ureteric branch tip bifurcation in wild-type embryonic kidneys. **A-D:** 10X magnification showing ureteric branch tips on the outer surface of the kidney. **A'-D':** 40X magnification focusing on individual ureteric branch tips. **A and A'**: Wild-type kidneys grown without quercetin show bifurcating ureteric branch tips (dotted lines) on the outer surface of the kidney, with proper cell-cell adhesion and apical-basolateral orientation of epithelial cells that make up the structure. **B and B'; C and C'; D and D':** Wild-type kidneys grown with 40 µM, 80 µM and 160 µM quercetin, respectively, show ureteric branch tips (dotted lines) that have a lack of proper bifurcation and are abnormally elongating on the outer surface of the kidney. These abnormal branch tips have a disorganized arrangement of the epithelial cells, showing a lack of proper cell-cell adhesion and disrupted apical-basolateral polarity. **Scale bars:** 100 µm (**A-D**); 20 µm (**A'-D'**).
Note: These images are representative examples of multiple independent experimental trials.

2. Quercetin treatment causes disrupted nephron formation in normal kidneys

β-catenin also plays a role in regulating nephron formation during normal kidney development (*Park et al., 2007*). Therefore, if quercetin affects β-catenin activity during normal kidney development, then disruptions in nephron formation should also be observed.

First, whole kidney explants treated with increasing doses of quercetin (40 μM, 80 μM, and 160 μM) or without quercetin (untreated control) were used for whole-mount immunofluorescence for Pax2, a protein that plays a role in the development of nephrogenic structures (*Dressler & Woolf, 2003*). Kidneys grown without quercetin treatment showed distinct tightly-clustered nephron progenitors that are consistently uniform in size and have a uniform spatial distribution throughout the tissue (**Figure 3A**). In contrast, kidneys grown in medium supplemented with 40 μM quercetin showed irregularly-sized clusters of nephron progenitors that have an abnormal pattern and sporadic distribution in the tissue (**Figure 3B**). Kidneys treated with 80 μM and 160 μM quercetin showed a more severely disrupted spatial arrangement and irregular patterning of nephron progenitors, with larger zones of abnormally-formed clusters of nephron progenitors (**Figures 3C and 3D**).

Next, I performed immunofluorescence for Pax2 on formalin-fixed, paraffin-embedded embryonic kidney tissue to better analyze the effects of quercetin on nephrogenesis. Kidneys grown without quercetin treatment showed a distinct nephrogenic zone containing nephron progenitors that are tightly aggregating around the ureteric bud tips (**Figure 4A**). Early nephrogenic structures that are undergoing epithelial transition and tubularization (such as the comma-shaped and S-shaped bodies) are also found throughout the cortex (**Figure 4A'**). Within the medullary region of these kidneys, I observed the formation of maturing nephron segments, including developing glomeruli (**Figure 4A''**). In contrast, kidneys treated with 40 μM quercetin

have several regions of uninduced mesenchyme cells along the nephrogenic zone of the outer cortex (**Figure 4B**); these cells are loosely packed along the surface of the ureteric epithelium (**Figure 4B'**). In addition, there are no early nephron progenitors (renal vesicles, comma-shaped bodies, S-shaped bodies) found on the cortex of these kidneys, and there are several ectopic and stalled nephrogenic structures in the medulla (**Figure 4B''**). These disruptions in the nephrogenic program are further exacerbated in kidneys treated with 80 μM and 160 μM quercetin. Kidneys treated with 80 μM quercetin showed a markedly fewer self-renewing mesenchymal cells found in the nephrogenic zone (**Figure 4C**); again, these cells are loosely packed and are not tightly aggregated along the surface of the ureteric bud tips (**Figure 4C'**). Kidneys treated with 160 μM quercetin have sparse regions of self-renewing mesenchymal cells in the cortex (**Figure 4D**), and these cells are also uninduced by the ureteric epithelium (**Figure 4D'**). In both kidneys treated with 80 μM and 160 μM quercetin, there are no early nephrogenic structures found in the cortex, and there are several ectopic and immature nephron segments found in the medullary area (**Figures 4C'' and 4D''**).

I also performed immunofluorescence for Six2, a protein expressed in cells in the condensed mesenchyme (*Park et al., 2012*), to further demonstrated the dose-dependent decrease in the self-renewing cells in the condensed mesenchyme. Kidneys grown without quercetin treatment showed clusters of Six2-positive cells within the nephrogenic zone that are tightly-aggregated along the ureteric bud tips (**Figures 5A and 5A'**). In contrast, kidneys treated with 40 μM quercetin showed a gap between the ureteric bud tip and the Six2-positive progenitor cells (**Figures 5B and 5B'**). Kidneys treated with 80 μM quercetin (**Figure 5C**) and 160 μM quercetin (**Figures 5D**) reveal sporadic regions of Six2-positive cells along the nephrogenic zone that are not induced by the ureteric epithelium. Compared to kidneys treated with 40 μM quercetin, kidneys

treated with 80 μM and 160 μM quercetin have a markedly wider gap between the ureteric bud tips and the Six2-positive cells (**Figures 5C' and 5D'**).

Taken together, these observations demonstrate that quercetin disrupts nephron formation in a dose-dependent manner in wild-type embryonic kidneys.

Figure 3: Quercetin treatment results in a dose-dependent decrease to nephron formation in wild-type embryonic kidneys

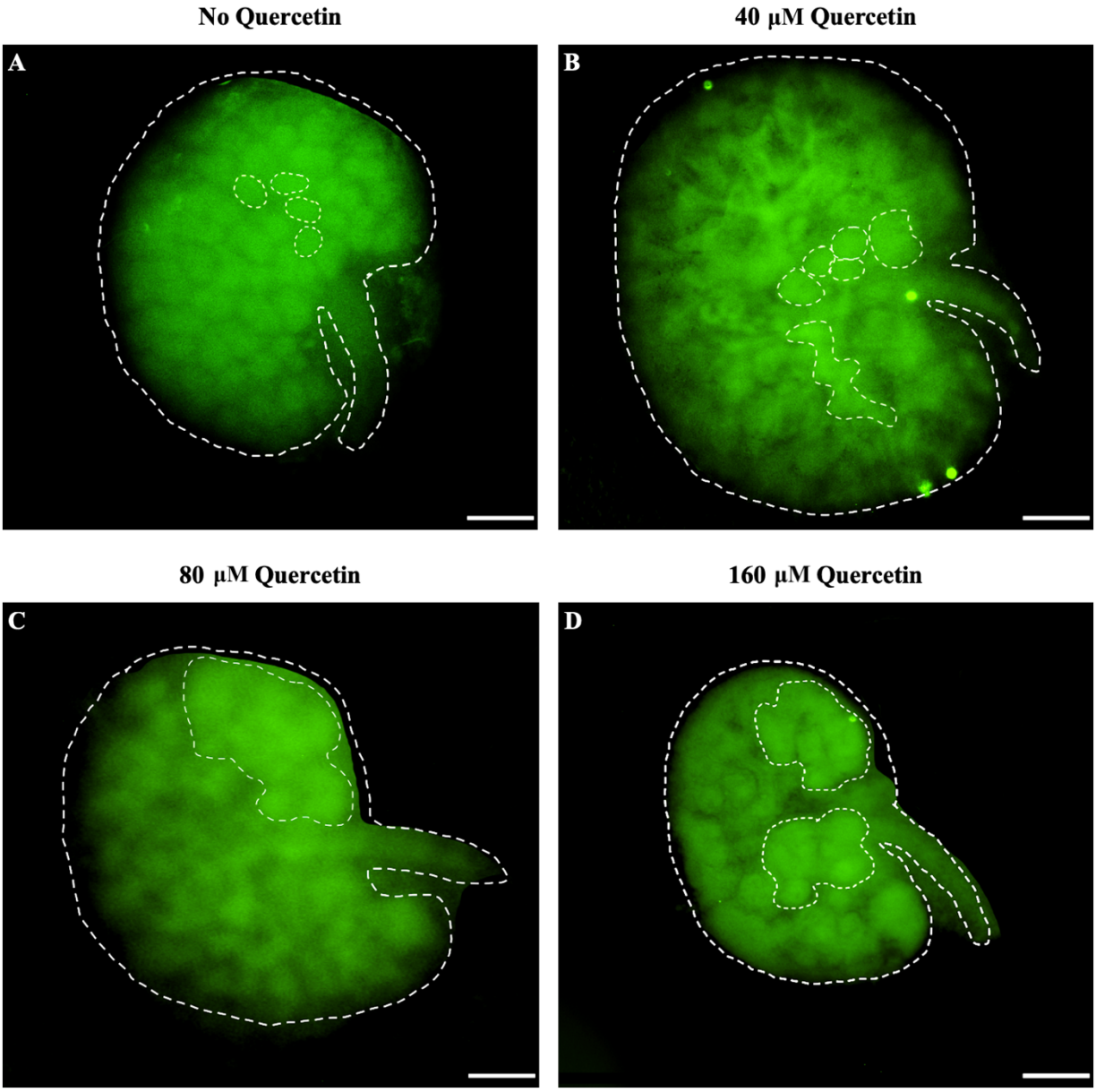

Quercetin treatment results in a dose-dependent decrease to nephron formation in wild-type embryonic kidneys. **A-D**: Whole-mount immunofluorescence using anti-Pax2 antibody. **A**: Wild-type kidneys grown without quercetin show the normal pattern of nephron formation, including clusters of nephron progenitors (inner dotted lines) that are uniform in size and evenly-distributed in the kidney tissue. **B, C and D**: Wild-type kidneys grown with 40 µM, 80 µM and 160 µM quercetin, respectively, show a dose-dependent decrease in nephron formation, as shown in the progressive disruptions observed in irregularly-sized clusters of nephron progenitors (inner dotted lines) that have an abnormal pattern and sporadic distribution in the tissue. **Scale bars:** 200 µm. **Note:** These images are representative examples of multiple independent experimental trials.

Figure 4: Quercetin treatment results in disruptions to nephron formation in wild-type embryonic kidneys

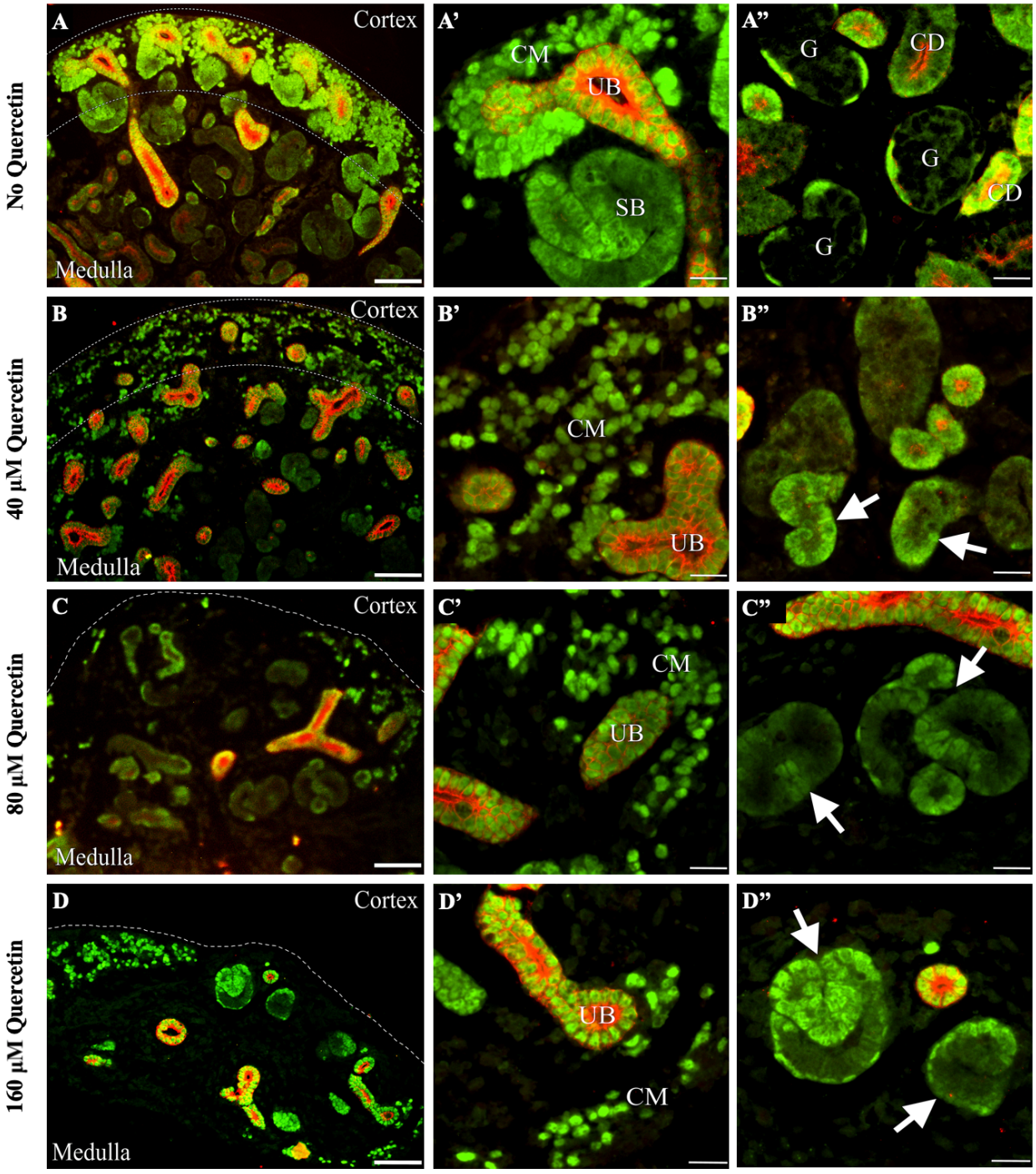

Quercetin treatment results in disruptions to nephron formation in wild-type embryonic kidneys. **A-D'':** Immunofluorescence using anti-Pax2 (green) and anti-cytokeratin (red) antibodies. **A-D:** Low magnification images showing the renal parenchyma. **A'-D':** Insets focusing on regions of

the cortex. **A''-D'':** Insets focusing on regions of the medulla. **A, A' and A'':** Wild-type kidneys grown without quercetin demonstrate the normal pattern of nephron formation: an organized nephrogenic zone on the outer cortex of the kidney where condensed mesenchyme cells (CM) form tight aggregates along the surface of the ureteric bud epithelium (UB), early nephrogenic structures such as the s-shaped body (SB) forming along the cortex, and maturing glomeruli (G) and early collecting ducts (CD) found in the medulla. **B, B' and B''; C, C' and C''; D, D' and D'':** Wild-type kidneys grown with 40 μM, 80 μM and 160 μM quercetin, respectively, reveal a progressive disruption in the pattern of nephron formation, including loosely packed condensed mesenchyme cells (CM) along the nephrogenic zone, a lack of early nephrogenic structures (renal vesicles, comma- and s-shaped bodies) on the cortex, and several immature and stalled nephrogenic structures (arrows) found deep in the medulla. **Scale bars:** 100 μm (**A-D**); 20 μm (**A'-D'**); 20 μm (**A''-D''**). **Note:** These images are representative examples of multiple independent experimental trials.

Figure 5: Quercetin treatment results in disruptions to nephron progenitor self-renewal in wild-type embryonic kidneys

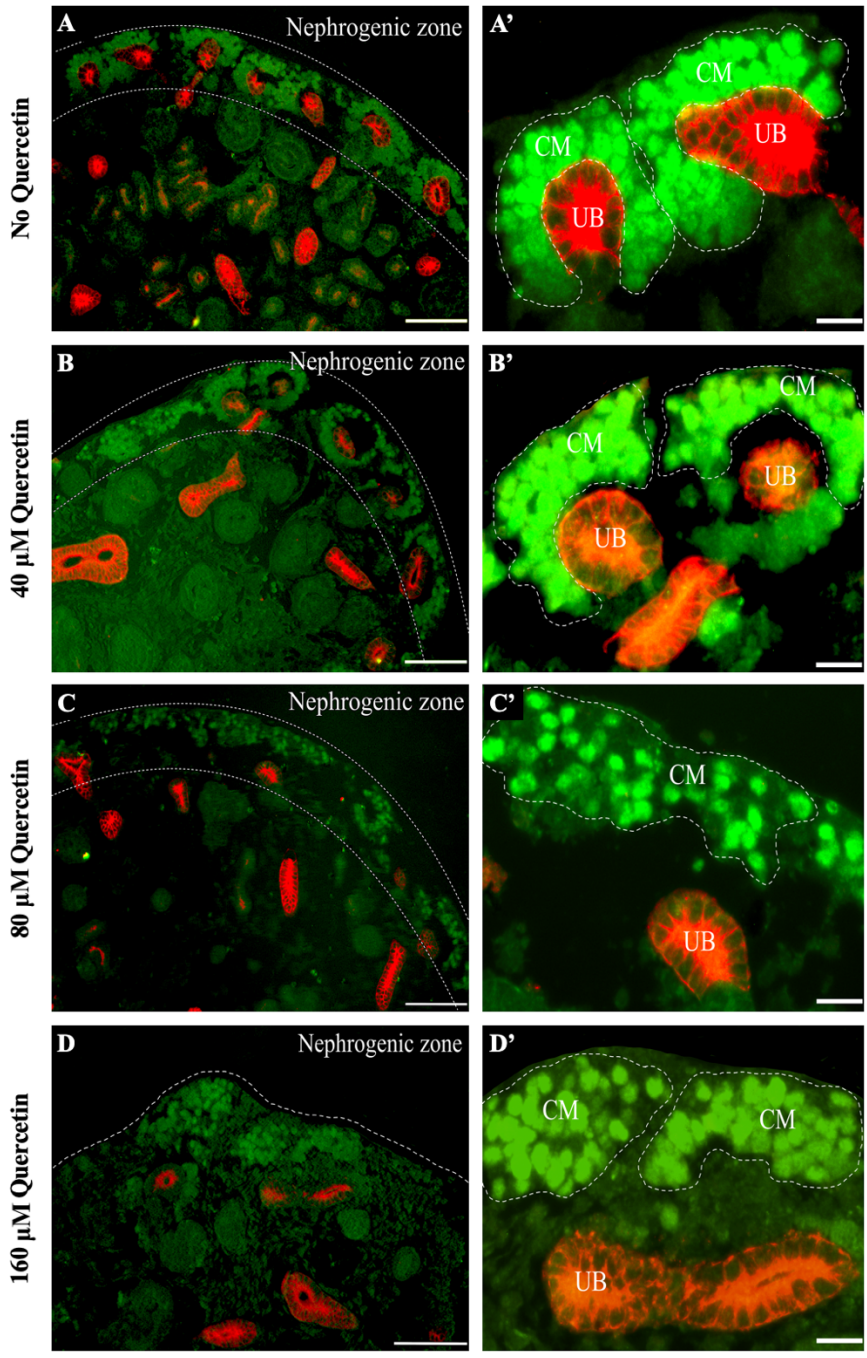

Quercetin treatment results in disruptions to nephron progenitor self-renewal in wild-type embryonic kidneys. **A-D':** Immunofluorescence using anti-Six2 (green) and anti-cytokeratin (red) antibodies. **A-D:** Low-magnification images of the kidney tissue. **A'-D':** Insets focusing on regions of the nephrogenic zone. **A and A'**: Wild-type kidneys grown without quercetin show clusters of condensed mesenchyme cells (CM) within the nephrogenic zone that are tightly aggregated along the ureteric bud epithelium (UB). **B and B'; C and C'; D and D':** Wild-type kidneys treated with 40 µM, 80 µM and 160 µM quercetin, respectively, reveal several regions of loosely packed condensed mesenchyme cells (CM) that are not tightly aggregated along the ureteric bud epithelium (UB). **Scale bars:** 100 µm (**A-D**); 20 µm (**A'-D'**). **Note:** These images are representative examples of multiple independent experimental trials.

3. Quercetin treatment causes a dose-dependent decrease in β-catenin levels

Since β-catenin regulates branching morphogenesis (*Bridgewater & Rosenblum, 2009*) and nephrogenesis (*Park et al., 2007*) and these processes are disrupted with quercetin treatment, I next determined whether quercetin has effects on β-catenin.

Western blot was performed on kidney lysates using antibodies against active β-catenin (non-phosphorylated on amino acid residues serine 33, serine 37 and threonine 41) and total β-catenin. Total protein was used as loading control. In comparison to untreated controls, increasing doses of quercetin treatment resulted in a dose-dependent decrease in the levels of non-phosphorylated β-catenin (**Figures 6A and 6B**): 40 μM quercetin versus no quercetin: 0.7185±0.07013, n=3 versus 0.9445±0.03720, n=3, p= 0.0465; 80 μM quercetin versus no quercetin: 0.5725±0.08279, n=3 versus versus 0.9445±0.03720, n=3, p= 0.0149; 160 μM quercetin versus no quercetin: 0.2545±0.05300, n=3 versus 0.9445±0.03720, n=3, p= 0.0004). I also observed that quercetin treatment resulted in modest reductions in the levels of total β-catenin, but these changes were not significant (**Figures 6A and 6C**).

Taken together, these data support my hypothesis that quercetin affects β-catenin levels in the developing kidney.

Figure 6: Quercetin treatment causes a dose-dependent decrease in β-catenin levels

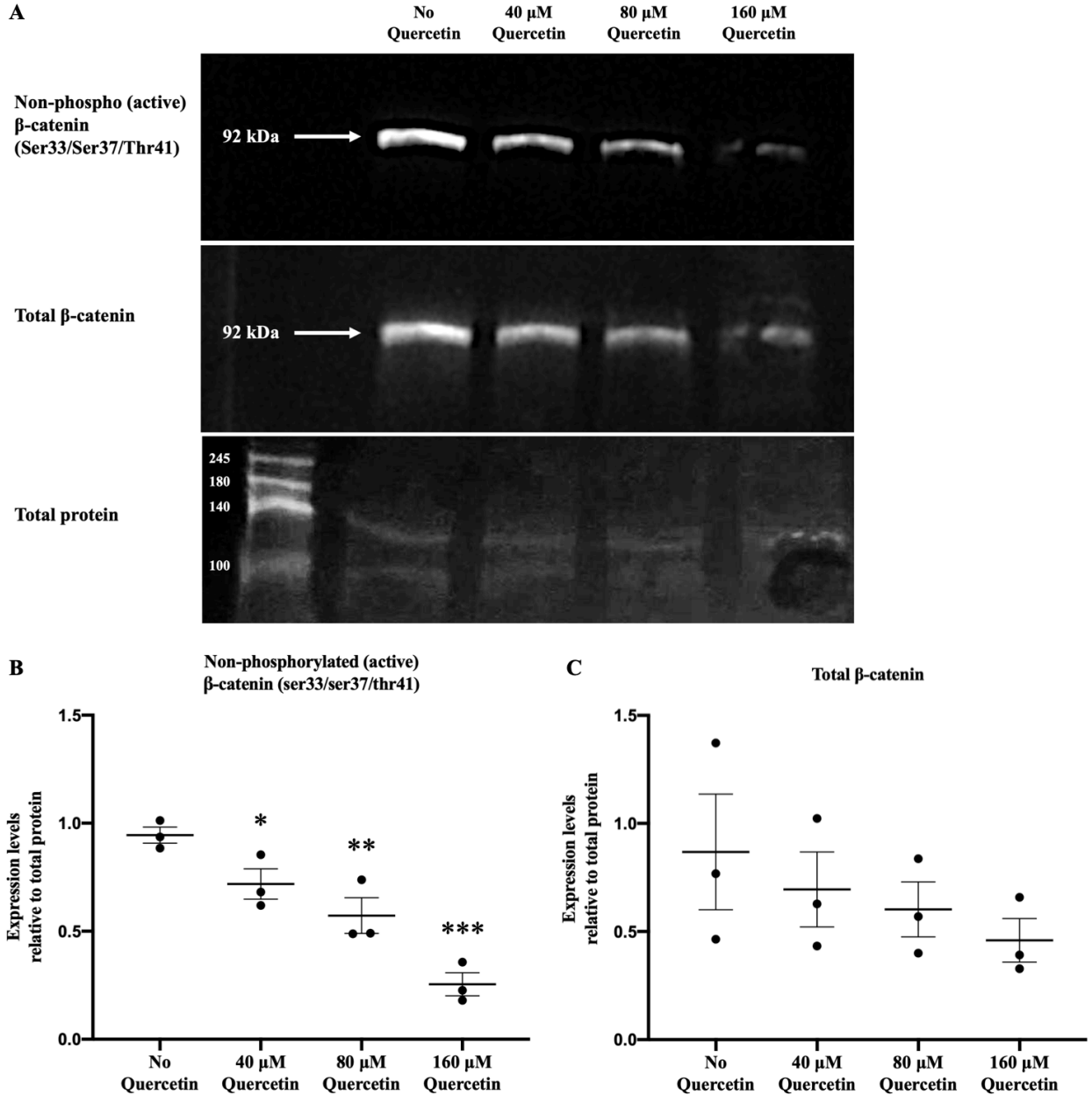

Quercetin treatment decreases expression levels of β-catenin. **A:** Western blot for non-phosphorylated β-catenin (top panel) and total β-catenin (middle panel); Total protein (bottom panel) was used to demonstrate equal protein loading. **B and C:** Measurement of expression levels using densitometry analysis of western blot bands. **B:** Quercetin treatment causes a dose-dependent decrease in levels of non-phosphorylated β-catenin: 40 µM quercetin versus no quercetin: 0.7185±0.07013, n=3 versus 0.9445±0.03720, n=3, p= 0.0465 (*); 80 µM quercetin versus no quercetin: 0.5725±0.08279, n=3 versus 0.9445±0.03720, n=3, p= 0.0149 (**); 160 µM quercetin versus no quercetin: 0.2545±0.05300, n=3 versus 0.9445±0.03720, n=3, p= 0.0004 (***). **C:** Quercetin treatment does not cause a significant decrease in levels of total β-catenin.

4. Quercetin treatment alters the cellular distribution of β-catenin

I observed that quercetin causes a dose-dependent decrease in the levels of non-phosphorylated (active) β-catenin and modest changes in levels of total β-catenin. I next analyzed the cellular distribution of β-catenin. Immunohistochemistry using an antibody against active β-catenin (non-phosphorylated on amino acid residues Serine 37 and Threonine 41) was performed on formalin-fixed, paraffin-embedded kidney explants. In kidneys cultured without quercetin, β-catenin expression was detected in the nuclei of the cells and in the cytoplasmic and membrane-bound compartments (**Figures 7A and 7A'**). Compared to untreated controls, kidneys treated with 40 μM quercetin showed a decreased staining intensity of active β-catenin in the nuclei of cells, and active β-catenin was found predominantly in the cytoplasmic compartments (**Figures 7B and 7B'**). Kidneys treated with 80 μM quercetin (**Figures 7C and 7C'**) and 160 μM quercetin (**Figures 7D and 7D'**) have the lowest staining intensity of active β-catenin in the nuclei of cells and staining is found mostly in the cytoplasmic and membrane-bound components. In addition, kidneys treated with 80uM and 160μM quercetin showed increased staining intensity of active β-catenin in the adherens junctions between adjacent epithelial cells in the ureteric epithelium and in the early nephron progenitors.

Taken together, these results demonstrated that quercetin treatment is associated with reductions of the transcriptionally active form of β-catenin in the nucleus of cells and β-catenin is redistributed to the cytoplasmic and membrane-bound compartments of these cells.

Figure 7: Quercetin treatment alters the cellular expression pattern of non-phosphorylated (active) β-catenin

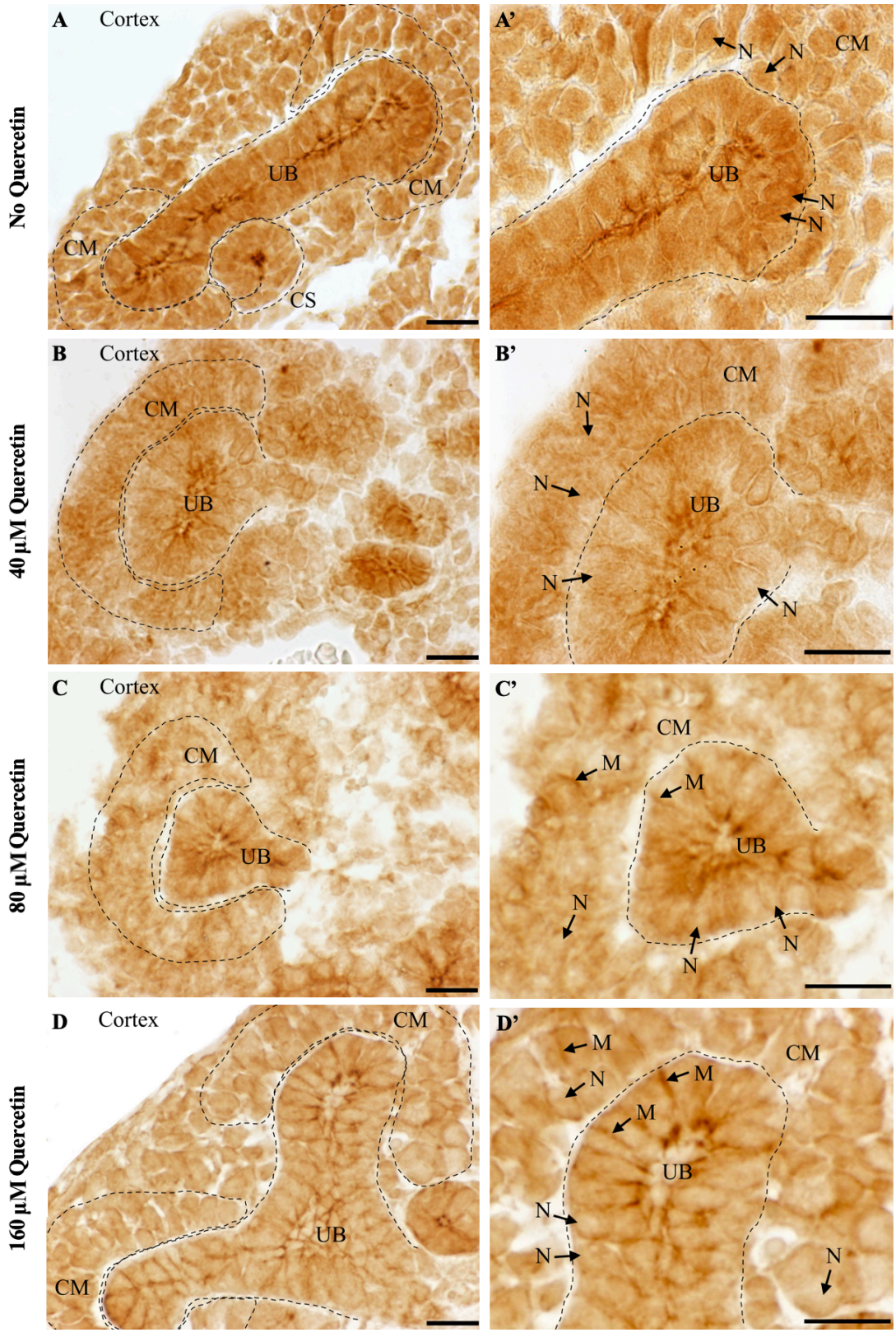

Quercetin treatment alters the cellular expression pattern of non-phosphorylated (active) β-catenin. **A-D'**: Immunohistochemistry using anti-non-phosphorylated (active) β-catenin antibody. **A-D:** High magnification images focusing on regions of the cortex. **A'-D':** Oil immersion insets focusing on individual cells within the cortical structures. **A and A'**: Wild-type kidneys grown without quercetin show a higher staining intensity of active β-catenin in the nuclei of cells (arrows, N) compared to that of the cytoplasmic and membrane-bound compartments. CM: condensed mesenchyme cells, CS: comma-shaped structure, UB: ureteric bud epithelium. **B and B'**: Wild-type kidneys grown with 40 μM quercetin show a decreased staining intensity of active β-catenin in the nuclei of cells (arrows, N) in comparison to untreated controls. CM: condensed mesenchyme cells, UB: ureteric bud epithelium. **C and C'; D and D'**: Wild-type kidneys grown with 80 μM and 160 μM quercetin show a further decrease in the staining intensity of active β-catenin in the nuclei of cells (arrows, N) and a subsequent increase in staining intensity in the membrane-bound compartments (arrows, M), where the adherens junctions between adjacent cells are located. CM: condensed mesenchyme cells, UB: ureteric bud epithelium. **Scale bars:** 20 μm (**A-D**), 10 μm (**A'-D'**). **Note:** These images are representative examples of multiple independent experimental trials.

5. Quercetin treatment decreases β-catenin transcriptional activity

The decrease in the expression levels of active β-catenin in the nuclei of the quercetin-treated kidney explants should result in a decrease in its transcriptional activity. To test this, I performed quantitative RT-PCR on known β-catenin target genes that have been showed to play important roles in kidney development: *Pax2*, *Six2* and *GDNF*. *Beta-2-Microglobin* (*B2M*) was used as an endogenous control. Quantitation of changes in mRNA expression using the $2^{\Delta\Delta Ct}$ method showed that compared to kidneys grown without quercetin treatment, increasing doses of quercetin treatment resulted in a dose-dependent decrease in *Pax2* expression levels (**Figure 8A**): 40 μM quercetin versus no quercetin: 0.6207±0.09948, n=3 versus 1.00, n=3, p=0.0189; 80 μM quercetin versus no quercetin: 0.5071±0.05380, n=3 versus 1.00, n=3, p=0.0008; 160 μM quercetin versus no quercetin: 0.3261±0.06756, n=3 versus 1.00, n=3, p=0.0006. Quercetin treatment causes a significant decrease in the expression levels of *Six2* only at the 40 μM and 160 uM doses: 40 μM quercetin versus no quercetin: 0.7139±0.08498, n=3 versus 1.00, n=3, p=0.0281; 160 μM quercetin versus no quercetin: 0.4030±0.06763, n=3 versus 1.00, n=3, p=0.0009; there is a modest but non-significant decrease in *Six2* expression at the 80 μM dose compared to untreated controls. Quercetin treatment causes a significant decrease in the expression levels of *GDNF* only at the 160 uM dose: 0.3074±0.05334, n=3 versus 1.00, n=3, p=0.0002; there is a moderate but non-significant decrease in *GDNF* expression at the 40 μM and 80 μM doses in comparison to untreated controls. This indicates there are likely off-target or confounding effects of the quercetin treatments; for instance, a decrease in *Six2* or *GDNF* expression may activate a negative feedback mechanism involving another signaling pathway that increases the expression levels of these developmental factors back to steady-state conditions.

Taken together, these results demonstrated that quercetin treatment reduces the transcriptional activity of β-catenin on *Pax2* in a dose-dependent manner. Quercetin also decreases *Six2* and *GDNF* levels, however these reductions do not show a dose-dependent response.

Figure 8: Quercetin treatment decreases β-catenin transcriptional activity

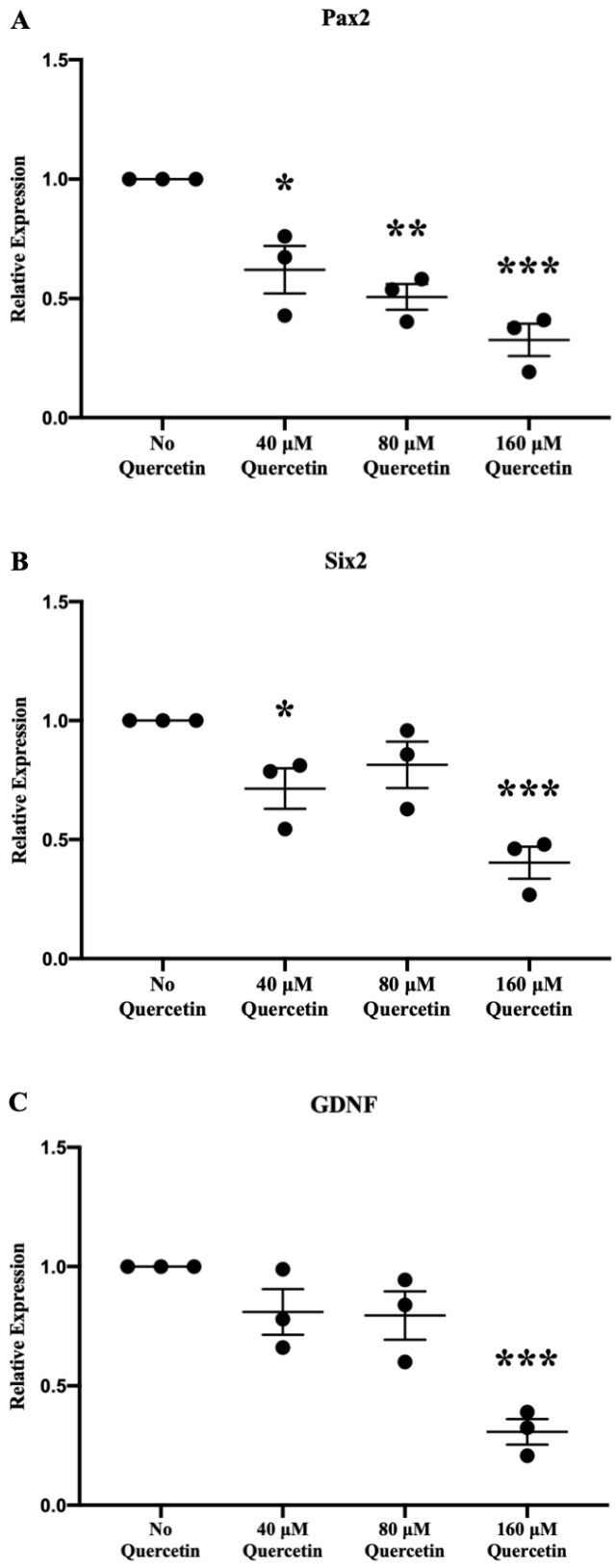

Quercetin treatment decreases β-catenin transcriptional activity. **A-C:** Quantitative reverse-transcriptase PCR for β-catenin transcriptional targets: *Pax2*, *Six2* and *GDNF*. Relative expression levels are determined using the $2^{\Delta\Delta Ct}$ quantitation method, using No Quercetin as reference control and *Beta-2-Microglobin* (*B2M*) as endogenous control. **A:** Quercetin treatment causes a dose-dependent decrease in the expression levels of *Pax2*: 40 µM quercetin versus no quercetin: 0.6207±0.09948, n=3 versus 1.00, n=3, p=0.0189 (*); 80 µM quercetin versus no quercetin: 0.5071±0.05380, n=3 versus 1.00, n=3, p=0.0008 (**); 160 µM quercetin versus no quercetin: 0.3261±0.06756, n=3 versus 1.00, n=3, p=0.0006 (***). **B:** Quercetin treatment causes a decrease in the expression levels of *Six2* at the 40 µM and 160 uM doses: 40 µM quercetin versus no quercetin: 0.7139±0.08498, n=3 versus 1.00, n=3, p=0.0281 (*); 160 µM quercetin versus no quercetin: 0.4030±0.06763, n=3 versus 1.00, n=3, p=0.0009 (***). **C:** Quercetin treatment causes a decrease in the expression levels of *GDNF* at the 160 uM dose: 0.3074±0.05334, n=3 versus 1.00, n=3, p=0.0002 (***).

6. βcat-GOF^{MM} mutants demonstrate renal dysplasia

So far, I have demonstrated that increasing doses of quercetin inhibits β-catenin transcriptional activity by preventing the transcriptionally active form of β-catenin from entering and accumulating in the nuclei of cells, therefore decreasing the transcription of target genes involved in kidney development. Consequently, this resulted in a dose-dependent reduction in branching morphogenesis and a dose-dependent decrease in nephron formation during normal kidney development. With these findings, I have demonstrated that quercetin affects branching morphogenesis and nephron formation during the developmental stages through a β-catenin dependent mechanism.

Next, I utilized my mouse models of renal dysplasia to test whether quercetin can reduce abnormally-elevated β-catenin levels and determine if this rescues or lessens the severity of the developmental defect in my mouse models. Our laboratory generated a mouse model in which β-catenin is specifically overexpressed in the metanephric mesenchyme of the embryonic kidney, termed βcat-GOF^{MM} (β-catenin gain-of-function in the metanephric mesenchyme). Briefly, the RarB2 promoter drives Cre expression exclusively in the metanephric mesenchyme of the embryonic kidney, and male RarB2-Cre mice were crossed with female mice that contain LoxP sites flanking exon 3 of the *β-catenin* gene (*Sarin et al., 2014*). Therefore, progeny of this cross will have a genetic deletion of exon 3, generating a mutated form of the β-catenin protein that lacks a phosphorylation site required for enzymatic degradation, resulting in the accumulation of β-catenin in the mesenchyme cells (**Figure 9A**; *Sarin et al., 2014*). Wild-type and βcat-GOF^{MM} mutant embryos were identified by PCR genotyping for the Cre transgene (**Figure 9B**).

The wild-type mouse embryonic kidneys display a highly organized architecture of the kidney tissue, normal corticomedullary patterning of the renal parenchyma, and proper

development of the nephrogenic and early ductal structures (**Figure 9C**). In contrast, dysplastic kidneys from βcat-GOF^{MM} mutants reveal hallmarks of human renal dysplasia including an abnormal overall architecture of the tissue, a highly disorganized patterning of the renal parenchyma which lacks distinct cortical and medullary regions, an abnormal kidney shape with the formation of several ectopic kidney-like tissues that fused together, and several dilated tubules and disorganized formation of nephrogenic structures (**Figure 9D**). βcat-GOF^{MM} mutants also demonstrated bilateral renal dysplasia, with both the left and right kidneys of the mouse embryo displaying equal levels of severity of the developmental defect.

Figure 9: βcat-GOF^{MM} mutants demonstrate renal dysplasia

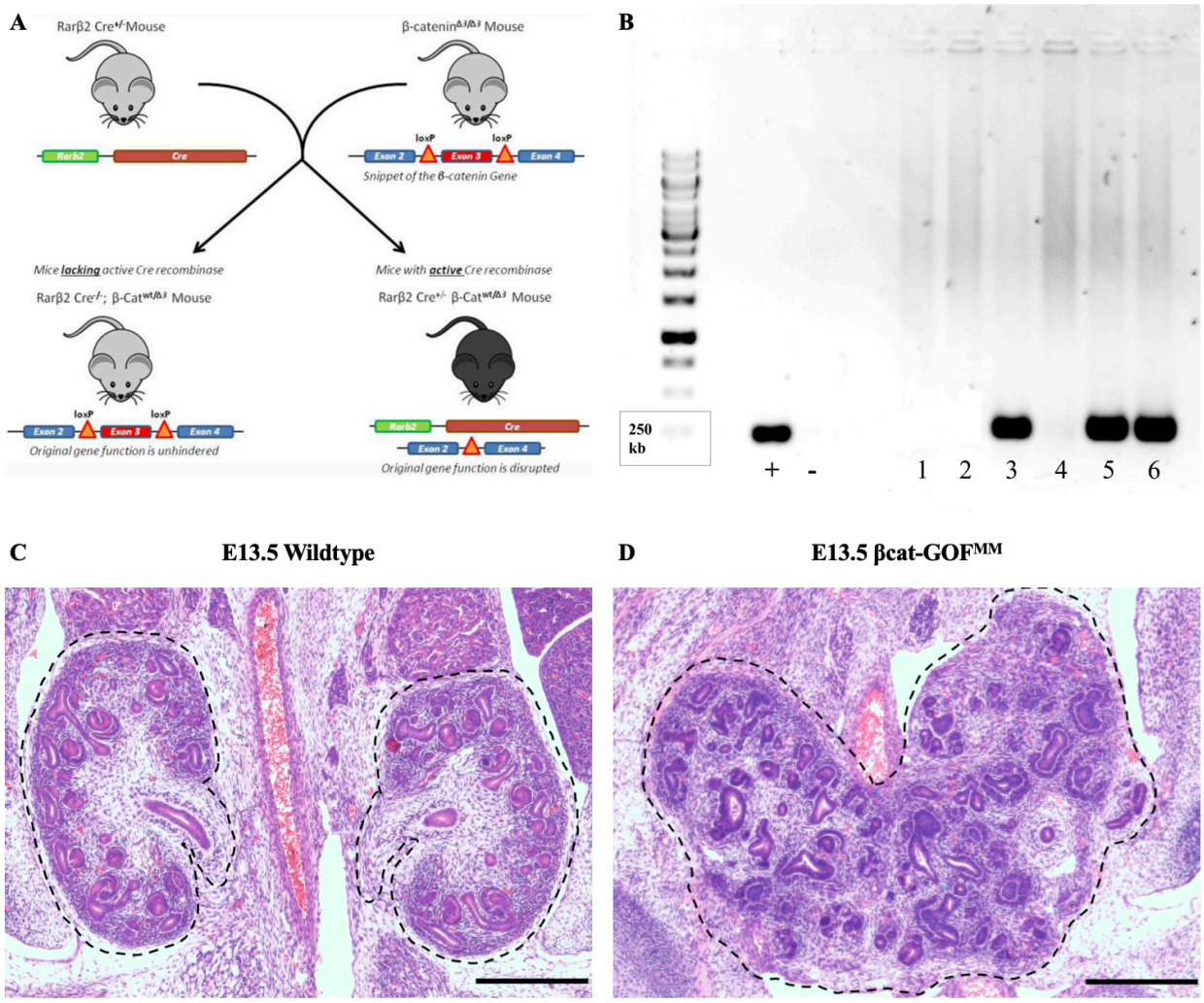

βcat-GOF^{MM} mutants demonstrate renal dysplasia. **A:** Diagram outlining the mouse cross breeding scheme used to generate βcat-GOF^{MM} embryos. Cre-Lox gene editing technique removes exon 3 (a phosphorylation site) of β-catenin, generating a constitutively activated form of the β-catenin protein. **B:** PCR genotyping of embryo heads using primers for the Cre transgene to identify βcat-GOF^{MM} mutant embryos. Mutants are identified by the presence of a 200 bp amplicon band. A known mutant (+ve) was used to determine if the PCR reaction was successful and as a comparison for detecting positive bands in the samples, and a negative control (-ve) was used to show that there is no contamination in the PCR reaction. **C:** Histological analysis of E13.5 wild-type mouse embryonic kidneys show normal kidney structure, including proper corticomedullary patterning of the renal parenchyma, bean-shaped structure of the kidney, and normally-developing nephrogenic and ductal structures. **D:** Histological analysis of E13.5 βcat-GOF^{MM} mutant kidneys reveal an abnormal kidney structure, including highly disorganized patterning of the renal parenchyma which lacks distinct cortical and medullary regions, abnormal kidney shape with the formation of several ectopic kidney-like tissues that fused together, and several dilated tubules and disorganized formation of nephrogenic structures. **Scale bars:** 200 μm.

7. Quercetin treatment reduces the severity of renal dysplasia in βcat-GOF^{MM}

Previous studies have demonstrated the therapeutic properties of quercetin. These studies have showed that quercetin mitigates abnormally-elevated β-catenin levels and activity in breast (*Srinivasan et al., 2016*), colon (*Park et al., 2005*) and pancreatic (*Cao et al., 2015*) human cancer cell lines and in a mouse model of renal fibrosis (*Ren et al., 2016*), resulting in significant reductions to tumourigenic properties of the cells and improved outcomes such as decreased cancer cell growth, proliferation and metastasis, and reduced activation of pro-fibrotic pathways. I hypothesize that quercetin can rescue or reduce the severity of the developmental abnormalities in my mouse model of renal dysplasia where β-catenin is overexpressed specifically in the metanephric mesenchyme of the developing kidneys (βcat-GOF^{MM}).

To test if quercetin had effects on the dysplastic kidney, I cultured βcat-GOF^{MM} kidneys either without quercetin or with 40 μM quercetin. Dysplastic kidneys grown without quercetin treatment demonstrated overt renal dysplasia, including a highly disorganized renal parenchyma, lack of a distinct nephrogenic zone and lack of early nephrogenic structures in the cortex, several sporadic regions of uninduced mesenchyme cells, disorganized distribution of renal stroma cells, collapsed or abnormally-developed glomeruli, and immature or poorly-differentiated nephrogenic structures (**Figure 10A**). Compared to untreated controls, quercetin-treated dysplastic kidneys reveal a more organized renal parenchyma, a more distinct corticomedullary patterning with self-renewing nephron progenitors and early nephrogenic structures found along the nephrogenic zone of the outer cortex, several maturing nephrons found in the medulla, and medullary stromal cells surrounding the developing nephrons (**Figure 10B**). Overall, the quercetin-treated dysplastic kidneys demonstrated corticomedullary patterning that is more similar

to that of a wild-type mouse embryonic kidney (**Figure 1°C**) compared to the disorganized renal parenchyma observed in untreated dysplastic kidneys (**Figure 10A**).

Taken together, this analysis showed that quercetin mitigates the severity of the phenotypic abnormalities in this mouse model of renal dysplasia, resulting to a phenotype that more closely resembles that of normal kidney development.

Figure 10: Quercetin reduces the severity of renal dysplasia in βcat-GOF^{MM}

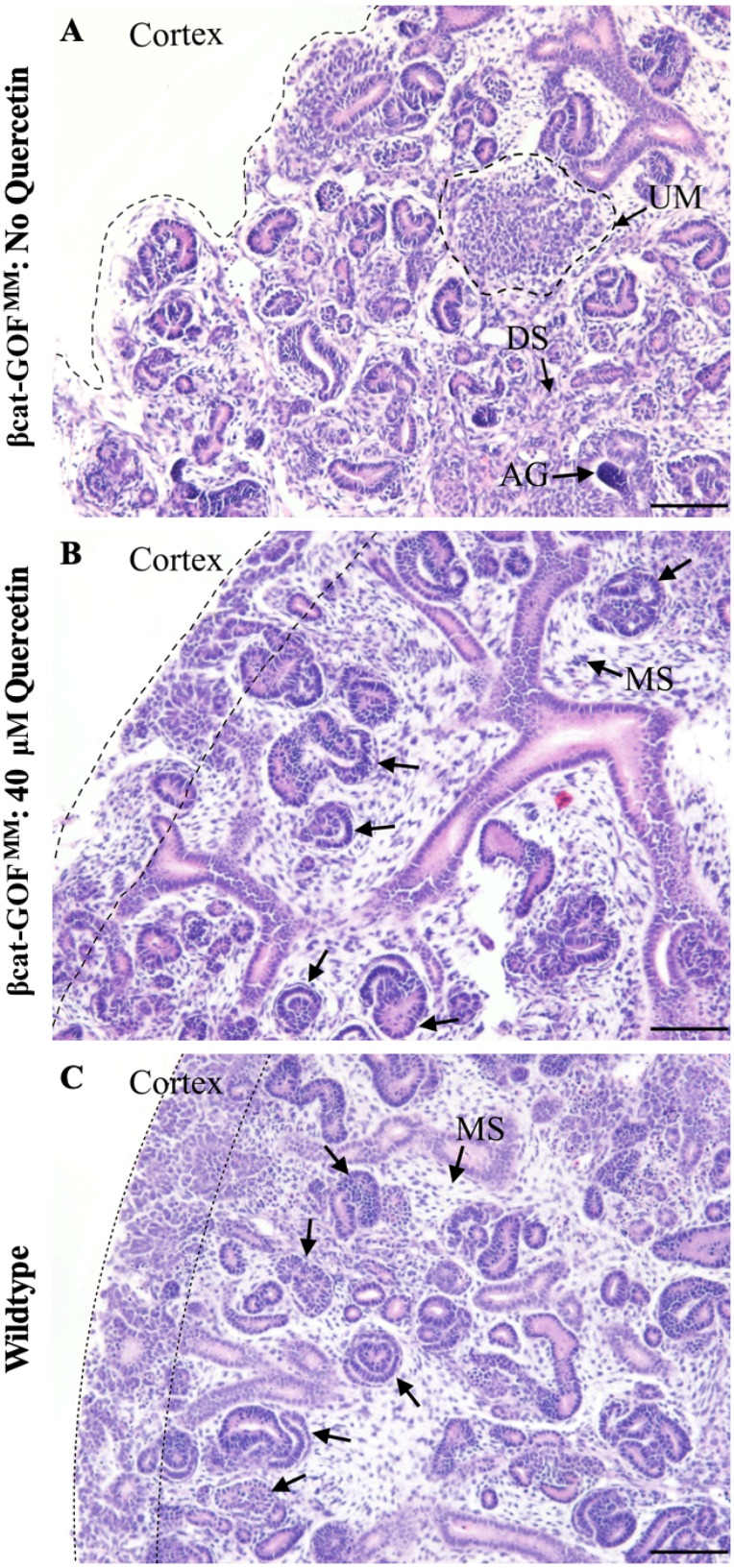

Quercetin reduces the severity of renal dysplasia in βcat-GOF^{MM}. **A-C:** Hematoxylin and eosin staining. **A:** Dysplastic kidneys grown without quercetin treatment demonstrate histological abnormalities of renal dysplasia, including irregular patterning of the renal parenchyma, lack of a distinct nephrogenic zone, sporadic clusters of uninduced mesenchyme cells (arrow, UM), disorganized stroma (arrow, DS), abnormally developed glomeruli (arrow, AG) and immature or poorly-differentiated nephrogenic structures. **B:** Dysplastic kidneys treated with 40 µM quercetin show a less severe phenotype compared to that of untreated dysplastic kidneys: a more distinct corticomedullary patterning of the renal parenchyma with self-renewing nephron progenitors and early nephrogenic structures found along the nephrogenic zone (dotted lines) of the outer cortex and several maturing nephrons found in the medullary area (arrows), and medullary stromal cells (MS) surrounding the developing nephrons. Dysplastic kidneys treated with 40 µM quercetin demonstrate corticomedullary patterning that is more similar to that of an age-matched wild-type mouse embryonic kidney (**C**) compared to the disorganized renal parenchyma observed in untreated dysplastic kidneys. **Scale bars:** 100 µm. **Note:** These images are representative examples of multiple independent experimental trials.

8. Quercetin treatment rescues abnormal branching morphogenesis in βcat-GOF^{MM}

I observed that quercetin treatment resulted in a partial rescue of βcat-GOF^{MM} dysplastic kidneys at a histological level. Next, I further analyzed whether quercetin can reduce the severity of abnormal branching morphogenesis in this mouse model of renal dysplasia.

In βcat-GOF^{MM} mutants, β-catenin overexpression in the metanephric mesenchyme results to abnormal GDNF/Ret signaling in the developing kidney, which leads to ectopic and disrupted branching pattern of the ureteric epithelium *(Sarin et al., 2014)*. These previous findings show that increased β-catenin activity disrupts key cellular processes that drive ureteric branching, ultimately leading to an abnormal branching pattern of the ureteric epithelium.

I resected E13.5 embryonic kidneys from βcat-GOF^{MM} mutants. The kidneys were cultured either in the presence or absence of 40 μM quercetin and whole-mount immunofluorescence staining for cytokeratin was performed to visualize the branching pattern of the ureteric epithelium. As expected in this mouse model, I observed that dysplastic kidneys grown without quercetin display several abnormally-elongating branches and the formation of an ectopic kidney with highly disorganized cytokeratin-positive structures (**Figure 11A**). In contrast, dysplastic kidneys cultured in 40 μM quercetin have resolving ectopic kidneys, few abnormally-elongating branches and ectopic branches (**Figure 11B**). These quercetin-treated kidneys were more comparable in terms of branching pattern and overall structure to wild-type mouse embryonic kidneys (**Figure 11C**). A closer analysis of the anti-cytokeratin labelled kidney explants demonstrated that dysplastic kidneys grown without quercetin have ureteric branch tips that failed to bifurcate and continue elongating (**Figures 11A' and 11A''**). On the other hand, dysplastic kidneys cultured with quercetin treatment have fewer abnormally-elongating branches and have ureteric branch tips that display the proper pattern of bifid branch bifurcation (**Figures 11B' and 11B''**), a pattern that is

more comparable to that of wild-type kidneys (**Figures 11C' and 11C''**). In the quercetin-treated dysplastic kidneys, the proper bifid branching pattern of the ureteric epithelium is re-established in the nephrogenic zone of the kidney.

Taken together, this analysis demonstrated that quercetin treatment partially rescues or reduces the severity of abnormal branching morphogenesis in this mouse model of renal dysplasia, resulting in a ureteric branching pattern that more closely resembles that of normal kidney development.

Figure 11: Quercetin treatment rescues abnormal branching morphogenesis in βcat-GOF^{MM}

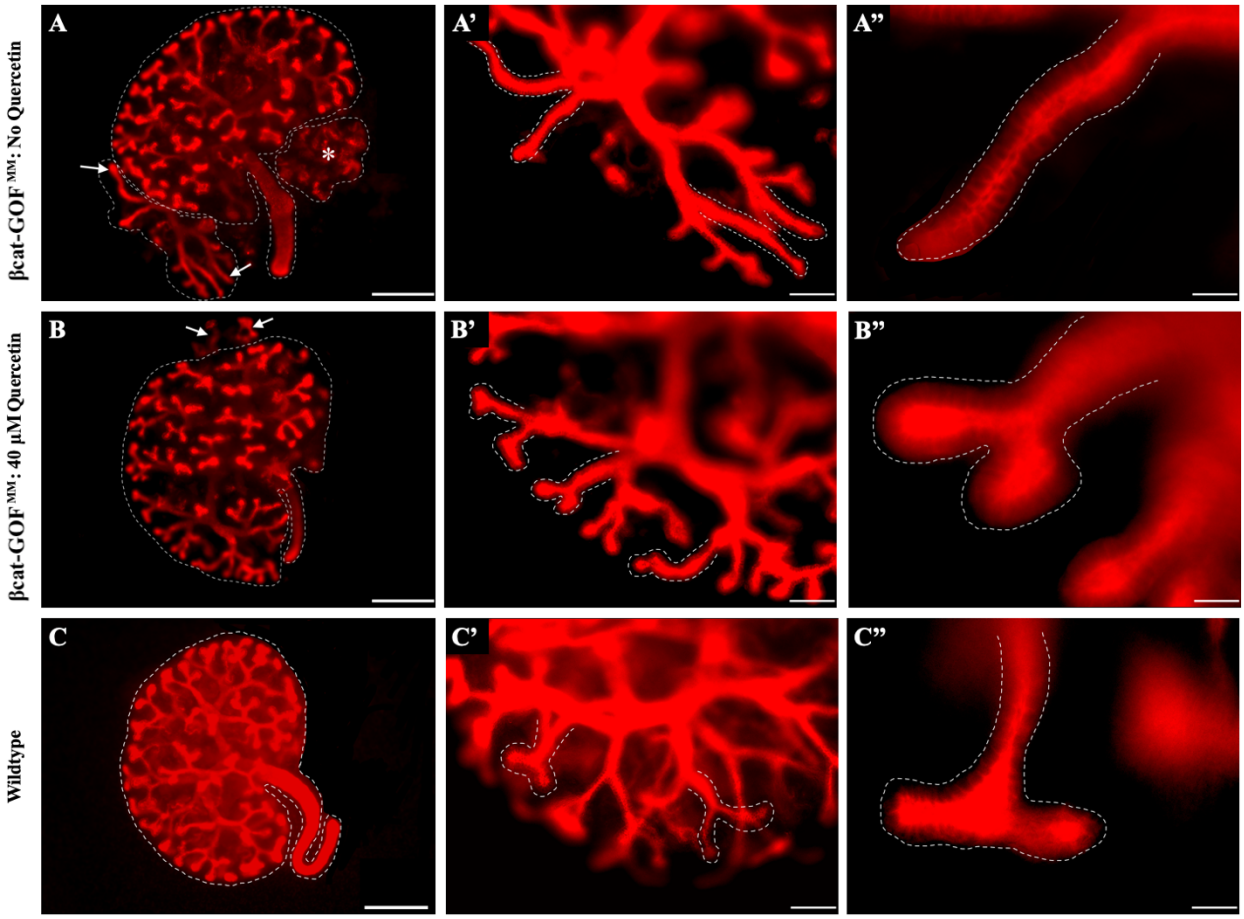

Quercetin treatment rescues abnormal branching morphogenesis in βcat-GOF^{MM}. **A-C'':** Whole-mount immunofluorescence using anti-cytokeratin antibody. **A-C:** 4X magnification showing the whole kidney. **A:** Dysplastic kidneys grown without quercetin treatment demonstrate abnormal branching morphogenesis, the formation of multiplex kidneys (dotted lines), an ectopic kidney with cytokeratin-positive structures that failed to branch properly (asterisk), and several ectopic and abnormally elongating branches (arrow). **B:** Dysplastic kidneys treated with 40 μM quercetin show a less severe branching pattern compared to that of untreated dysplastic kidneys: no multiplex kidneys and fewer ectopic branches (arrows); quercetin-treated dysplastic kidneys have a branching pattern that is more similar to that of an age-matched wild-type mouse embryonic kidney (**C**) compared to that of untreated dysplastic kidneys. **A'-C':** 10X magnification showing ureteric branch tips on the outer surface of the kidney. **A''-C'':** 40X magnification focusing on individual ureteric branch tips. **A' and A'':** Untreated dysplastic kidneys have abnormally-elongating ureteric branch tips (dotted lines). **B' and B''**: Dysplastic kidneys treated with 40 μM quercetin have bifurcating ureteric bud tips (dotted lines) on the outer surface of the kidney, similar to the bifurcation pattern of ureteric bud tips observed in age-matched wild-type mouse embryonic kidneys (**C' and C''**). **Scale bars:** 200 μm (**A-C**); 100 μm (**A'-C'**); 20 μm (**A''-C''**). **Note:** These images are representative examples of multiple independent experimental trials.

9. Quercetin treatment rescues abnormal nephron formation in βcat-GOF^{MM}

My results demonstrating a rescue in disorganized branching morphogenesis in quercetin-treated βcat-GOF^{MM} dysplastic kidney explants led us to investigate whether there is also a rescue in disrupted nephrogenesis in these diseased kidneys. I next analyzed whether quercetin can also reduce the severity of abnormal nephron formation in this mouse model of renal dysplasia.

In βcat-GOF^{MM} mutants, β-catenin overexpression in the mesenchymal cells resulted in a disorganization of the nephrogenic structures, a lack of proper mesenchymal-to-epithelial transition of developing nephrons, focal areas of stalled and immature nephrogenic structures found deep in the medullary region, and an abnormal expansion of the self-renewing mesenchymal cell populations deep into the medulla *(Sarin et al., 2014).* These previous findings showed that elevated levels of β-catenin in the metanephric mesenchyme disrupts the cellular and morphological processes that drive the nephrogenic program, leading to abnormally-formed nephrons in the renal parenchyma.

I resected embryonic kidneys from βcat-GOF^{MM} mutants. These kidneys were cultured either with or without 40 μM quercetin and I performed Pax2 immunofluorescence on formalin-fixed, paraffin-embedded kidney explants. As expected in this model, dysplastic kidneys grown without quercetin display several sporadic clusters of stalled and poorly-differentiated nephrogenic structures throughout the tissue, a lack of properly-developed and maturing nephrons in the medulla, and a lack of self-renewing nephrogenic progenitors in the nephrogenic zone of the cortex (**Figure 12A**). In contrast, dysplastic kidneys grown in 40 μM quercetin have a more organized pattern of nephron formation, with properly-developing and maturing nephrons found in the medullary area and self-renewing nephron progenitors and early nephrogenic structures forming at the cortical region of the kidney (**Figure 12B**). The pattern of nephron formation observed in

dysplastic kidneys treated with 40 μM quercetin is similar to the nephrogenic program observed in wild-type mouse embryonic kidneys (**Figure 12C**).

I also performed immunofluorescence staining for Six2 in order to detect changes in nephron progenitor self-renewal as a result of the quercetin treatment. As expected in this mouse model, I observed that dysplastic kidneys grown without quercetin have an abnormal pattern of nephron progenitor self-renewal. In contrast to age-matched wild type kidneys where Six2-positive nephron progenitor cells are highly organized and evenly distributed along the nephrogenic zone of the cortex (**Figure 13C**), dysplastic kidneys grown without quercetin have Six2-positive cells that are sparsely distributed along the cortex of the kidney and ectopic regions of Six2-positive cells found in the medulla (**Figure 13A**) . On the other hand, dysplastic kidneys cultured in 40 μM quercetin showed a more organized spatial arrangement and a more even distribution of the Six2-positive cells along the nephrogenic zone (**Figure 13B**), and this organization is markedly similar to that of the wild-type kidneys (**Figure 13C**). The quercetin-treated dysplastic kidneys also do not have any ectopic regions of Six2-positive progenitor cells in the medulla.

Taken together, this analysis showed that quercetin treatment partially rescues or reduces the severity of abnormal nephron formation in this mouse model of renal dysplasia, resulting in a nephrogenic program that more closely resembles that of normal kidney development.

Figure 12: Quercetin treatment rescues abnormal nephron formation in βcat-GOF^{MM}

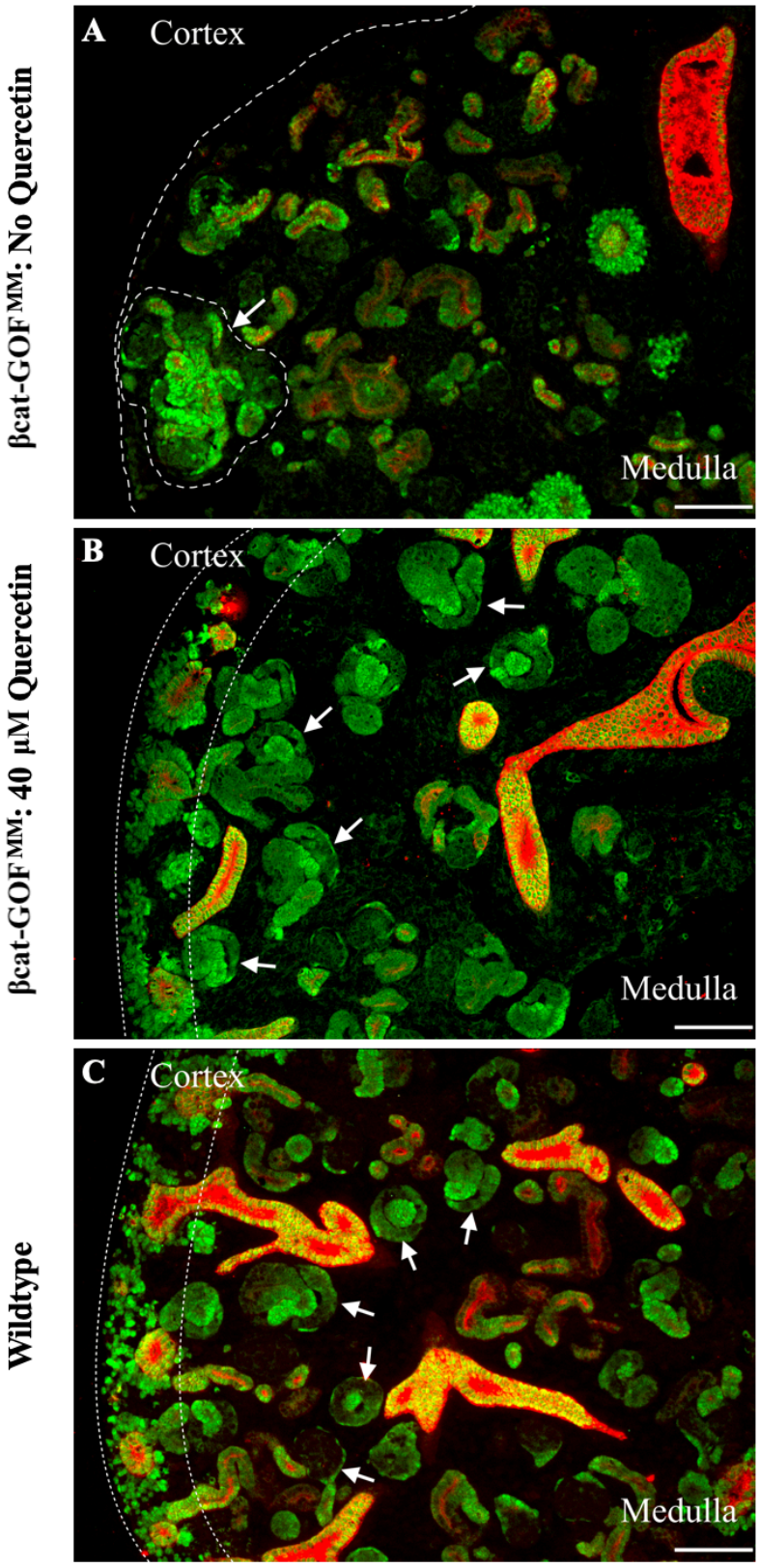

Quercetin treatment rescues abnormal nephron formation in βcat-GOF^{MM}.
A-C: Immunofluorescence using anti-Pax2 and anti-cytokeratin antibodies. **A:** Dysplastic kidneys grown without quercetin show a lack of self-renewing nephron progenitors in the nephrogenic zone and regions of stalled or abnormally-developing nephrons (arrow). **B:** Dysplastic kidneys treated with 40 µM quercetin show a more defined pattern of nephron formation, with self-renewing cells and early nephrons forming along the nephrogenic zone (dotted lines) and maturing nephrons within the medulla (arrows), and this pattern is similar to that of a wild-type mouse embryonic kidney (**C**). **Scale bars:** 100 µm. **Note:** These images are representative examples of multiple independent experimental trials.

Figure 13: Quercetin treatment rescues abnormal nephron progenitor self-renewal in βcat-GOF^{MM}

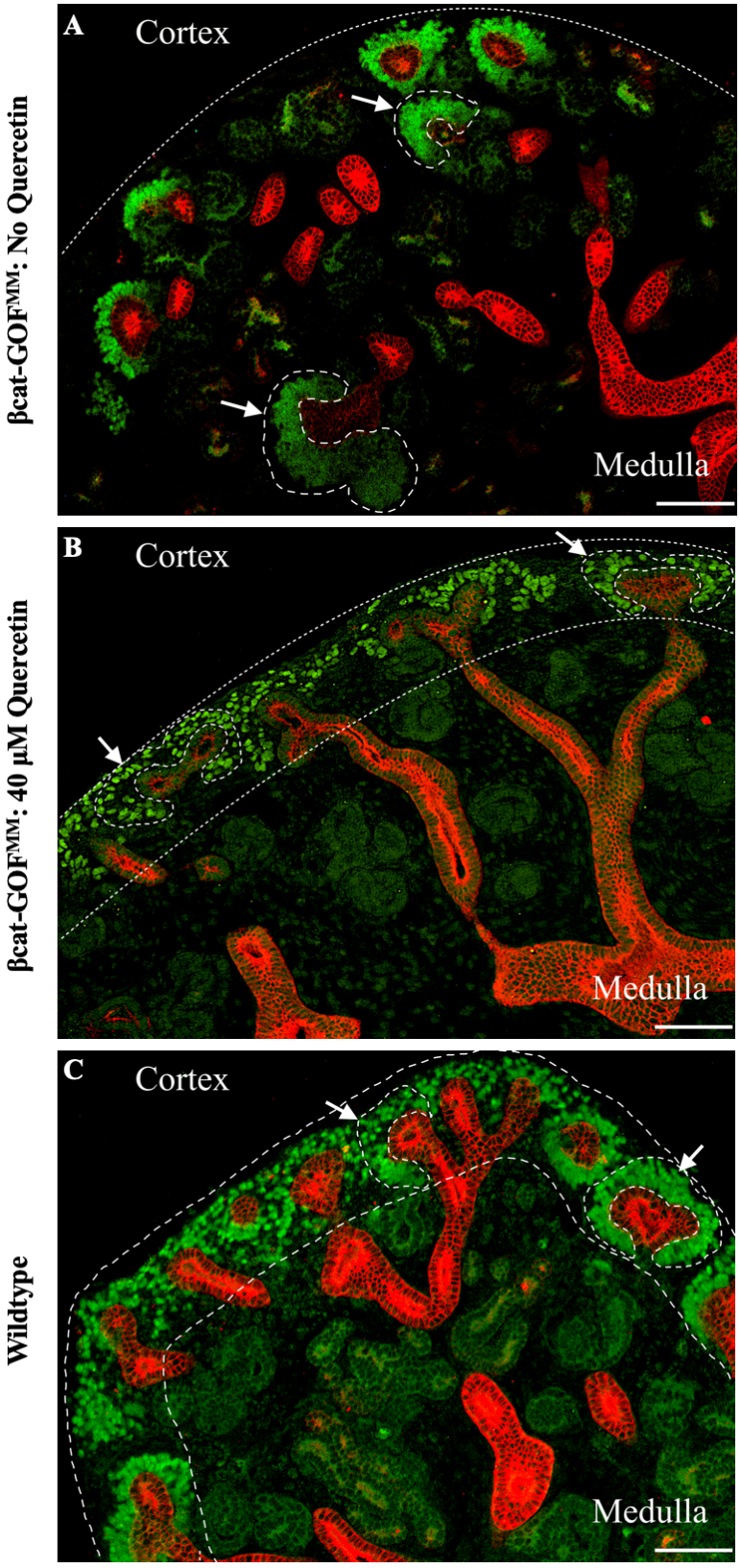

Quercetin treatment rescues abnormal nephron progenitor self-renewal in βcat-GOF^{MM}.
A-C: Immunofluorescence using anti-Six2 and anti-cytokeratin antibodies. **A:** Dysplastic kidneys grown without quercetin show an abnormal expansion of self-renewing nephron progenitor cells beyond the nephrogenic zone (dotted line) and deep in the medulla (arrows). **B:** Dysplastic kidneys treated with 40 µM quercetin show self-renewing nephron progenitors properly organized along the nephrogenic zone (dotted lines) of the outer cortex, and this pattern is similar to that of a wild-type mouse embryonic kidney (**C**). **Scale bars:** 100 µm. **Note:** These images are representative examples of multiple independent experimental trials.

10. Quercetin treatment increases the number of nephrogenic structures in βcat-GOF^{MM}

I observed that the abnormal nephrogenic program in βcat-GOF^{MM} mutants can be rescued with quercetin treatment. In βcat-GOF^{MM} mutants, abnormalities in the cellular changes involved in nephron formation leads to a marked reduction in properly-developing nephrons in the renal parenchyma *(Sarin et al., 2014)*. This led us to quantify changes in the number of properly-developing nephrogenic structures in untreated versus quercetin-treated kidneys, in order to demonstrate whether quercetin treatment can mitigate the decrease in numbers of nephrogenic structures in these dysplastic kidneys.

Using histological sections, I performed a quantitation of the number of properly-developing nephrogenic structures in untreated βcat-GOF^{MM} kidneys, quercetin-treated βcat-GOF^{MM} kidneys, and wild-type kidneys. As expected in this model, there is a marked decrease in the number of nephrogenic structures per mm^2 of tissue in untreated βcat-GOF^{MM} dysplastic kidneys (**Figure 14A**) compared to wild-type kidneys (**Figure 14C**): 13.25±1.309, n=7, versus 23.71±1.757, n=5, p=0.0006 (**Figure 14D**). In contrast, treatment of βcat-GOF^{MM} dysplastic kidneys with 40 μM quercetin (**Figure 14B**) resulted in a 44.45% increase in the number of nephrogenic structures per mm^2 of tissue, compared to untreated dysplastic kidneys: 19.14±2.009, n=8, versus 13.25±1.309, n=7, p=0.0335 (**Figure 14D**).

These findings demonstrated that quercetin treatment rescues abnormal nephron formation and consequently results to an improvement in the number of nephrogenic structures in βcat-GOF^{MM} dysplastic kidneys.

Figure 14: Quercetin treatment increases the number of nephrogenic structures in βcat-GOF^{MM}

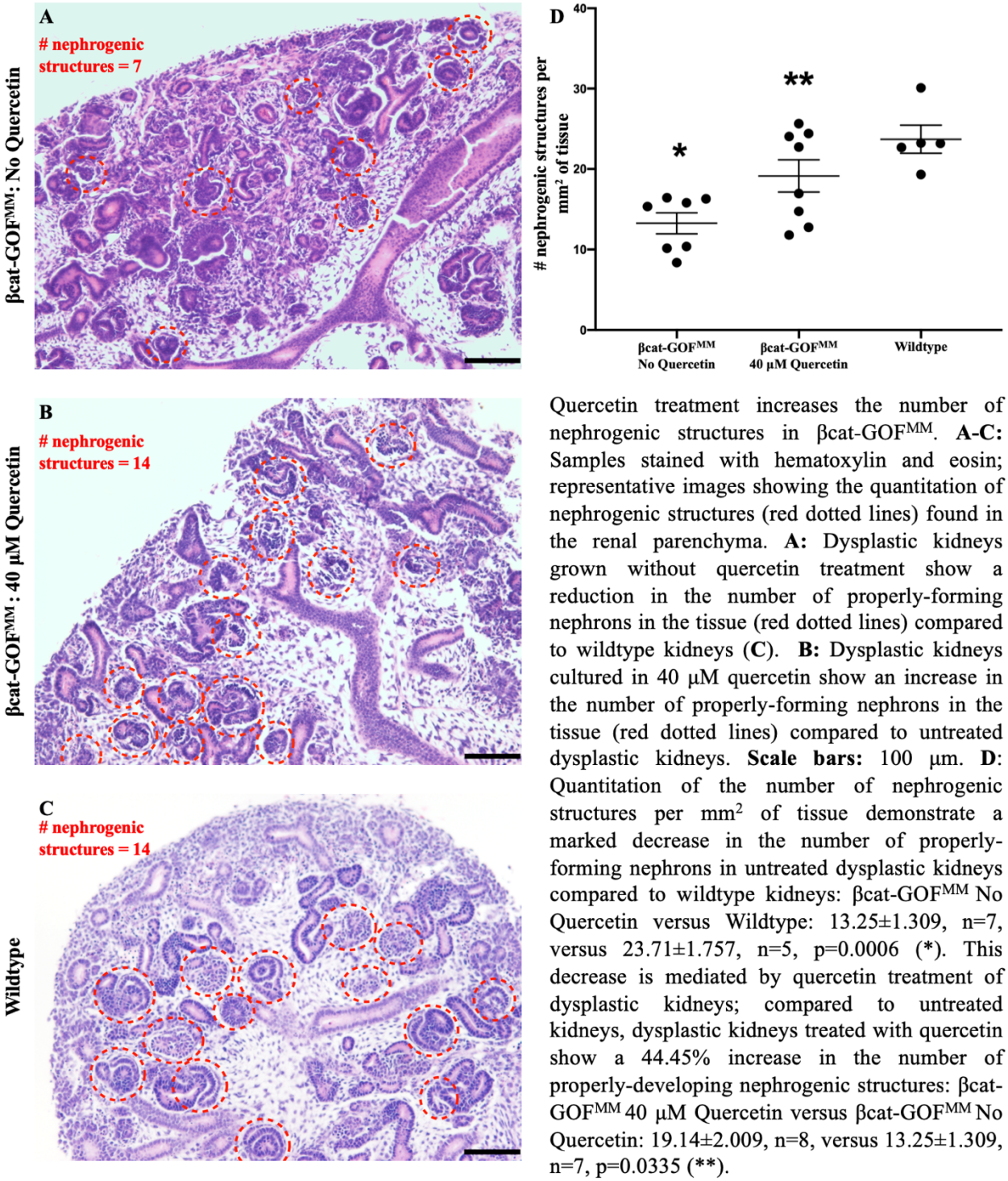

Quercetin treatment increases the number of nephrogenic structures in βcat-GOF^{MM}. **A-C:** Samples stained with hematoxylin and eosin; representative images showing the quantitation of nephrogenic structures (red dotted lines) found in the renal parenchyma. **A:** Dysplastic kidneys grown without quercetin treatment show a reduction in the number of properly-forming nephrons in the tissue (red dotted lines) compared to wildtype kidneys (**C**). **B:** Dysplastic kidneys cultured in 40 μM quercetin show an increase in the number of properly-forming nephrons in the tissue (red dotted lines) compared to untreated dysplastic kidneys. **Scale bars:** 100 μm. **D**: Quantitation of the number of nephrogenic structures per mm^2 of tissue demonstrate a marked decrease in the number of properly-forming nephrons in untreated dysplastic kidneys compared to wildtype kidneys: βcat-GOF^{MM} No Quercetin versus Wildtype: 13.25±1.309, n=7, versus 23.71±1.757, n=5, p=0.0006 (*). This decrease is mediated by quercetin treatment of dysplastic kidneys; compared to untreated kidneys, dysplastic kidneys treated with quercetin show a 44.45% increase in the number of properly-developing nephrogenic structures: βcat-GOF^{MM} 40 μM Quercetin versus βcat-GOF^{MM} No Quercetin: 19.14±2.009, n=8, versus 13.25±1.309, n=7, p=0.0335 (**).

11. Quercetin treatment reduces the nuclear levels of β-catenin in βcat-GOF^{MM}

Our previous work has demonstrated that the elevated levels of β-catenin in the developing kidney is a contributing factor to the pathogenesis of human renal dysplasia (*Sarin et al., 2014; Bridgewater et al., 2011; Boivin et al., 2016*). Therefore, I hypothesize that quercetin reduces the severity of renal dysplasia in βcat-GOF^{MM} mutants and this is associated with reductions in nuclear β-catenin in the mesenchymal cells of these dysplastic kidneys.

To test this, I analyzed β-catenin expression in untreated and treated dysplastic kidneys. Immunohistochemistry using an antibody against β-catenin was performed on formalin-fixed, paraffin-embedded kidney explants cultured either without quercetin or with 40 μM quercetin. As expected, dysplastic kidney explants grown without quercetin showed elevated levels of β-catenin in the nuclei of sporadic clusters of uninduced mesenchyme cells found in the cortex (**Figures 15A and 15A'**). In contrast, dysplastic kidneys treated with 40 μM quercetin do not have these sporadic regions of uninduced mesenchyme and showed decreased levels of β-catenin in the nuclei of condensed mesenchyme cells (**Figures 15B and 15B'**). The majority of β-catenin in the quercetin-treated kidneys is localized in the cytoplasmic compartment of the cells. Some of these mesenchyme cells also showed β-catenin expression at the cell membrane (**Figures 15B and 15B'**). This pattern of β-catenin expression in condensed mesenchyme cells is more similar to wild-type mouse embryonic kidneys (**Figures 15C and 15C'**). I next analyzed the cellular expression pattern of β-catenin in the maturing nephrons found in the medullary region of the kidneys. Dysplastic kidneys cultured without quercetin treatment showed high levels of β-catenin in the nuclei of sporadic clusters of uninduced mesenchyme cells found in the medulla (**Figures 16A and 16A'**). In contrast, dysplastic kidneys cultured with 40 μM quercetin do not have these abnormal clusters of uninduced mesenchyme in the medullary area and showed decreased β-

catenin levels in the nuclei of developing glomeruli found in the medulla, and β-catenin is mostly detected within the cytoplasmic pool of these cells (**Figures 16B and 16B'**). Some of these cells also showed β-catenin expression at the membrane-bound compartment of cells. This pattern of β-catenin expression in developing glomeruli is similar to that observed in a wild-type mouse embryonic kidney (**Figures 16C and 16C'**).

These findings demonstrated that in this model of renal dysplasia, quercetin treatment prevents β-catenin from accumulating in the nuclei of mesenchymal cells. These results are consistent with my hypothesis that quercetin rescues dysplastic kidneys by decreasing the abnormally-elevated levels of nuclear β-catenin.

Figure 15: Quercetin treatment reduces nuclear β-catenin levels in cortical structures in βcat-GOF^{MM}

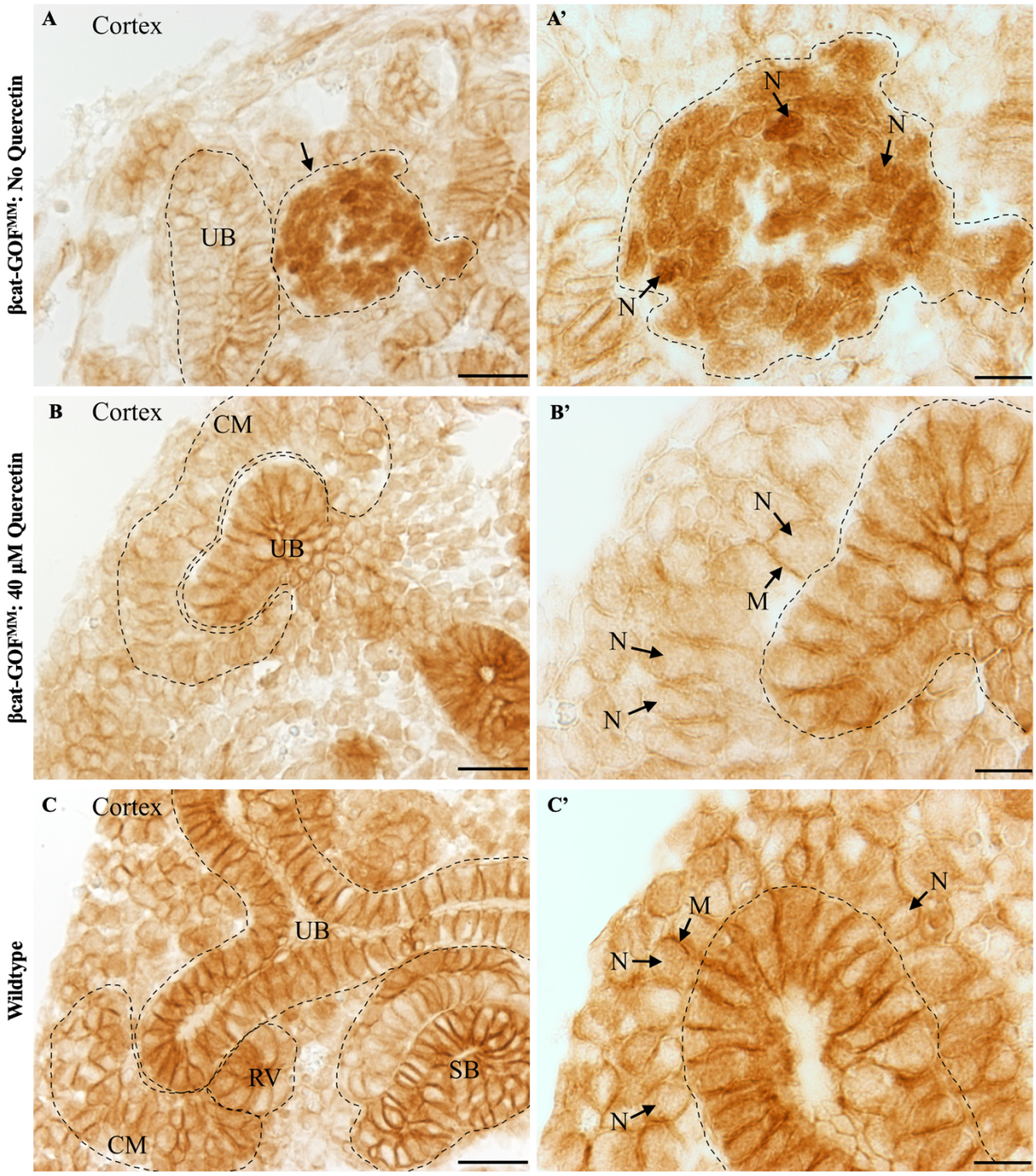

Quercetin treatment reduces nuclear β-catenin levels in cortical structures in βcat-GOF^{MM}. **A-C'**: Immunohistochemistry using anti-total β-catenin antibody. **A-C:** High magnification images focusing on regions of the cortex. **A'-C':** Oil immersion insets focusing on individual cells within the cortical structures. **A and A':** Dysplastic kidneys grown without quercetin show elevated β-

catenin levels in the nuclei (arrows, N) of uninduced mesenchyme cells (dotted line and arrow) found in the cortex. UB: ureteric bud epithelium. **B and B':** Compared to untreated dysplastic kidneys, dysplastic kidneys treated with 40 μM quercetin show decreased levels of β-catenin in the nuclei (arrows, N) of condensed mesenchyme cells (dotted line, CM) that form aggregates along the ureteric bud epithelium (UB). In addition, some of these mesenchyme cells show β-catenin expression at the cell membrane (arrows, M). This pattern of β-catenin expression in condensed mesenchyme cells is similar to that observed in a wild-type mouse embryonic kidney (**C and C'**). CM: condensed mesenchyme, UB: ureteric bud epithelium, RV: renal vesicle, SB: s-shaped body, N: nuclear β-catenin, M: membrane-bound β-catenin. **Scale bars:** 20 μm (**A-C**); 10 μm (**A'-C'**). **Note:** These images are representative examples of multiple independent experimental trials.

Figure 16: Quercetin treatment reduces nuclear β-catenin levels in medullary structures in βcat-GOF^{MM}

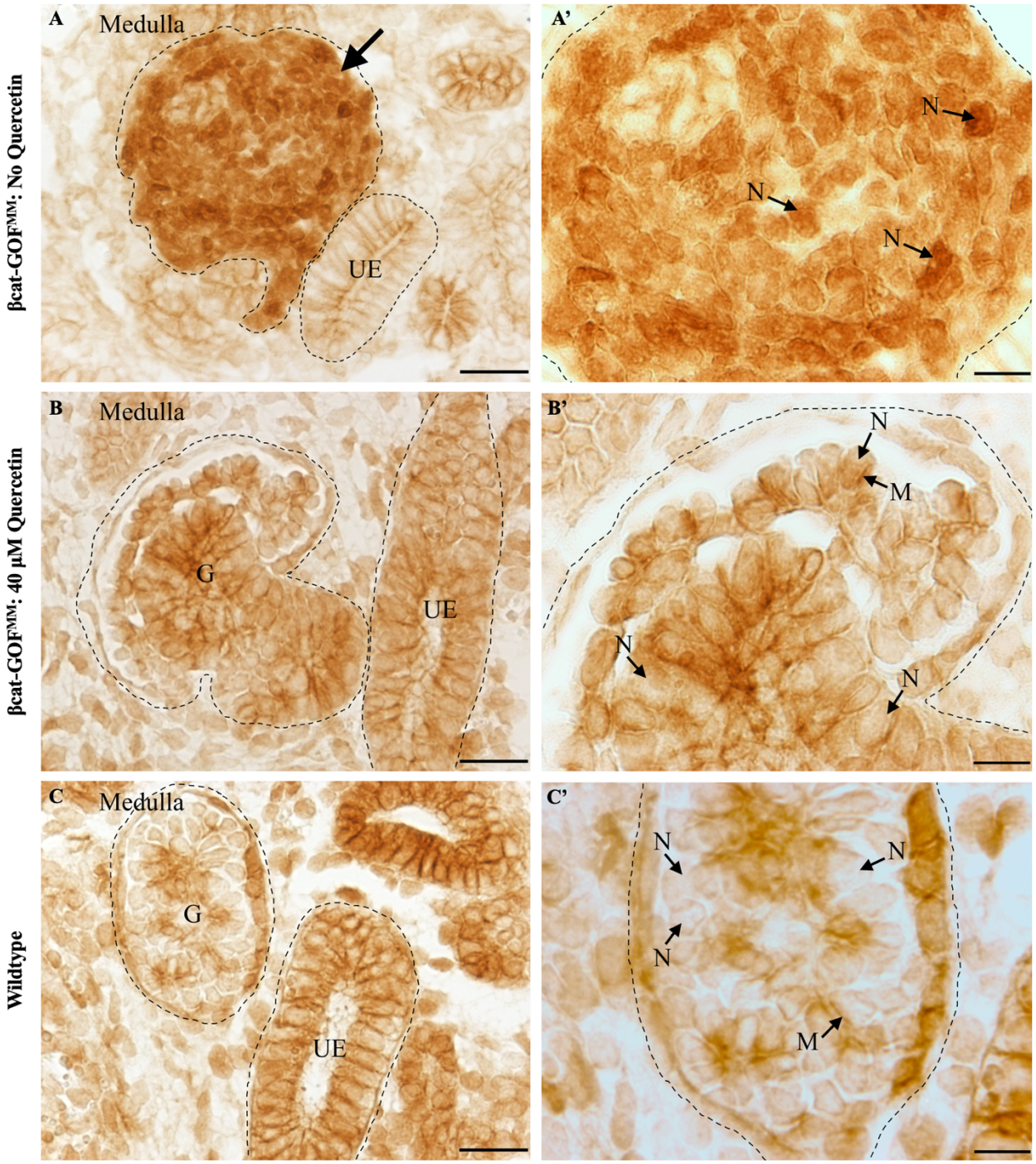

Quercetin treatment reduces nuclear β-catenin levels in medullary structures in βcat-GOF^{MM}. **A-C'**: Immunohistochemistry using anti-total β-catenin antibody. **A-C:** High magnification images focusing on regions of the medulla. **A'-C':** Oil immersion insets focusing on individual cells within the medullary structures. **A and A':** Dysplastic kidneys grown without quercetin show

elevated β-catenin levels in the nuclei (arrows, N) of stalled nephrogenic structures (dotted line and arrow) found in the medulla. UE: ureteric epithelium. **B and B':** Compared to untreated dysplastic kidneys, dysplastic kidneys treated with 40 μM quercetin show decreased levels of β-catenin in the nuclei (arrows, N) of developing glomeruli (G) in the medulla, and some of these cells also show β-catenin expression at the cell membrane (arrows, M). UE: ureteric epithelium. This pattern of β-catenin expression in developing glomeruli is similar to that observed in a wild-type mouse embryonic kidney (**C and C'**). G: glomerulus, UE: ureteric epithelium, N: nuclear β-catenin, M: membrane-bound β-catenin. **Scale bars:** 20 μm (**A-C**); 10 μm (**A'-C'**). **Note:** These images are representative examples of multiple independent experimental trials.

12. Quercetin treatment reduces β-catenin transcriptional activity in βcat-GOF^{MM}

In renal dysplasia, increased levels of β-catenin in the nuclei of cells in the developing kidney lead to an increase in its transcriptional activity, causing dysregulated gene expression (*Sarin et al., 2014; Bridgewater et al., 2011; Boivin et al., 2016*).

I next analyzed the expression of β-catenin target genes (*Pax2, Six2* and *GDNF*) in untreated and quercetin-treated dysplastic tissue. Quantitation of changes in mRNA expression levels using the $2^{\Delta\Delta Ct}$ method showed that βcat-GOF^{MM} dysplastic kidneys cultured in 40 μM quercetin demonstrated a reduced expression of *Pax2* relative to untreated dysplastic kidneys: 0.6853±0.06944, n=5, versus 1.00, n=5, p=0.0106 (**Figure 17A**). The quercetin treatment also resulted to a modest decrease in expression of *Six2*: 0.8562±0.1766, n=5, versus 1.00, n=5, p>0.05 (**Figure 17B**) and *GDNF*: 0.8443±0.1240, n=5 versus 1.00, n=5, p>0.05 (**Figure 17C**); however, these decreased expression levels are non-significant.

Taken together, these results demonstrated that quercetin treatment reduces the transcriptional activity of β-catenin on *Pax2* in βcat-GOF^{MM} dysplastic kidneys, but does not significantly reduce the expression of *Six2* and *GDNF*.

Figure 17: Quercetin treatment reduces β-catenin transcriptional activity in βcat-GOF^{MM}

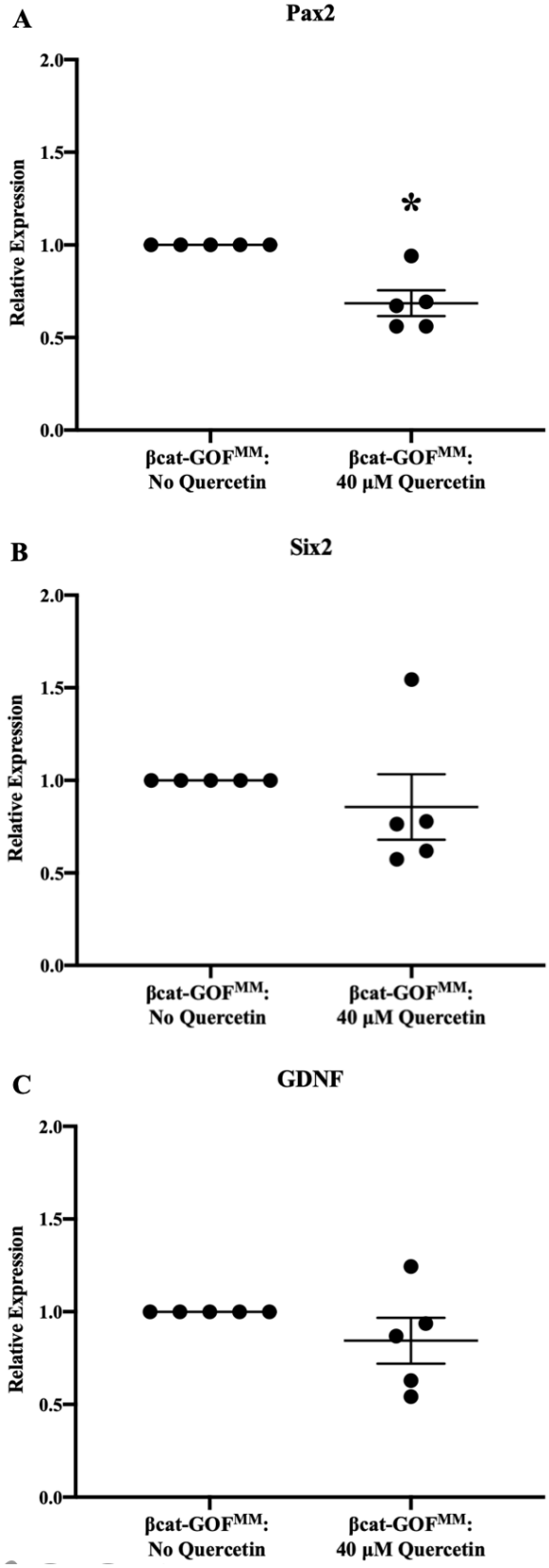

Quercetin treatment reduces β-catenin transcriptional activity in βcat-GOF^{MM}. **A-C:** Quantitative reverse-transcriptase PCR for β-catenin transcriptional targets: *Pax2*, *Six2* and *GDNF*. **A:** Compared to dysplastic kidneys without treatment, dysplastic kidneys treated with 40 µM quercetin show a reduced expression level of *Pax2*: 1.00, n=5, versus 0.6853±0.06944, n=5, p=0.0106 (*). **B:** Quercetin treatment resulted to a modest decrease in expression of *Six2*, but this decrease is not significant: 0.8562±0.1766, n=5, versus 1.00, n=5, p>0.05. **C:** Quercetin treatment resulted to a modest decrease in expression of *GDNF*, but this decrease is not significant: 0.8443±0.1240, n=5 versus 1.00, n=5, p>0.05.

13. Quercetin treatment results in a more organized E-cadherin expression in βcat-GOF^{MM}

I next investigated mechanisms by which quercetin exerts these rescue effects on this mouse model of renal dysplasia.

My previous findings demonstrated that quercetin treatment resulted in a redistribution of β-catenin to the membrane-bound compartment of cells (**Figure 7**, **Figure 15** and **Figure 16**). At the cell membrane, β-catenin plays a role in cell-cell adhesion (*Daugherty & Gottardi, 2007; Boivin et al., 2015a*) where it forms a complex with E-cadherin to mediate intercellular adhesion and interaction between the actin microfilaments of the cell and adherens junction proteins. This process is important in maintaining cell-cell contact and regulating tissue morphogenesis and organogenesis of the kidney (*Daugherty & Gottardi, 2007; Boivin et al., 2015a*). I predict that βcat-GOF^{MM} dysplastic kidneys without treatment will have a disorganized pattern of E-cadherin expression in the renal parenchyma, since the mesenchymal cells that overexpress β-catenin fail to properly epithelialize and form normally-developing nephrogenic structures. Furthermore, βcat-GOF^{MM} dysplastic kidneys treated with 40 μM quercetin will result in a more organized pattern of E-cadherin expression because the reduction in β-catenin levels in mesenchymal cells resulted in an improvement in the formation of nephrogenic structures.

To test this, I performed immunofluorescence staining for E-cadherin on formalin-fixed, paraffin-embedded kidney explants. I observed that without treatment, dysplastic kidneys reveal an irregular and sporadic distribution of E-cadherin in the stalled nephrogenic structures (**Figures 18A and 18A'**). Compared to untreated dysplastic kidneys, dysplastic kidneys cultured in 40 μM quercetin showed a more organized pattern of E-cadherin expression in the renal parenchyma, with E-cadherin detected at adherens junctions between adjacent cells in nephrogenic structures (**Figures 18B and 18B'**). The pattern of E-cadherin expression observed in dysplastic kidneys

treated with 40 μM quercetin is more similar to that observed in age-matched wild-type embryonic kidneys (**Figures 18C and 18C'**).

These results showed that quercetin treatment improves the cellular expression pattern of E-cadherin in βcat-GOF^{MM} dysplastic kidneys. As a result, the interaction between membrane-bound β-catenin and E-cadherin facilitates the proper epithelialization of mesenchymal cells that were initially unable to undergo the proper nephrogenic program.

Figure 18: Quercetin treatment results in a more organized E-cadherin expression in βcat-GOF^{MM}

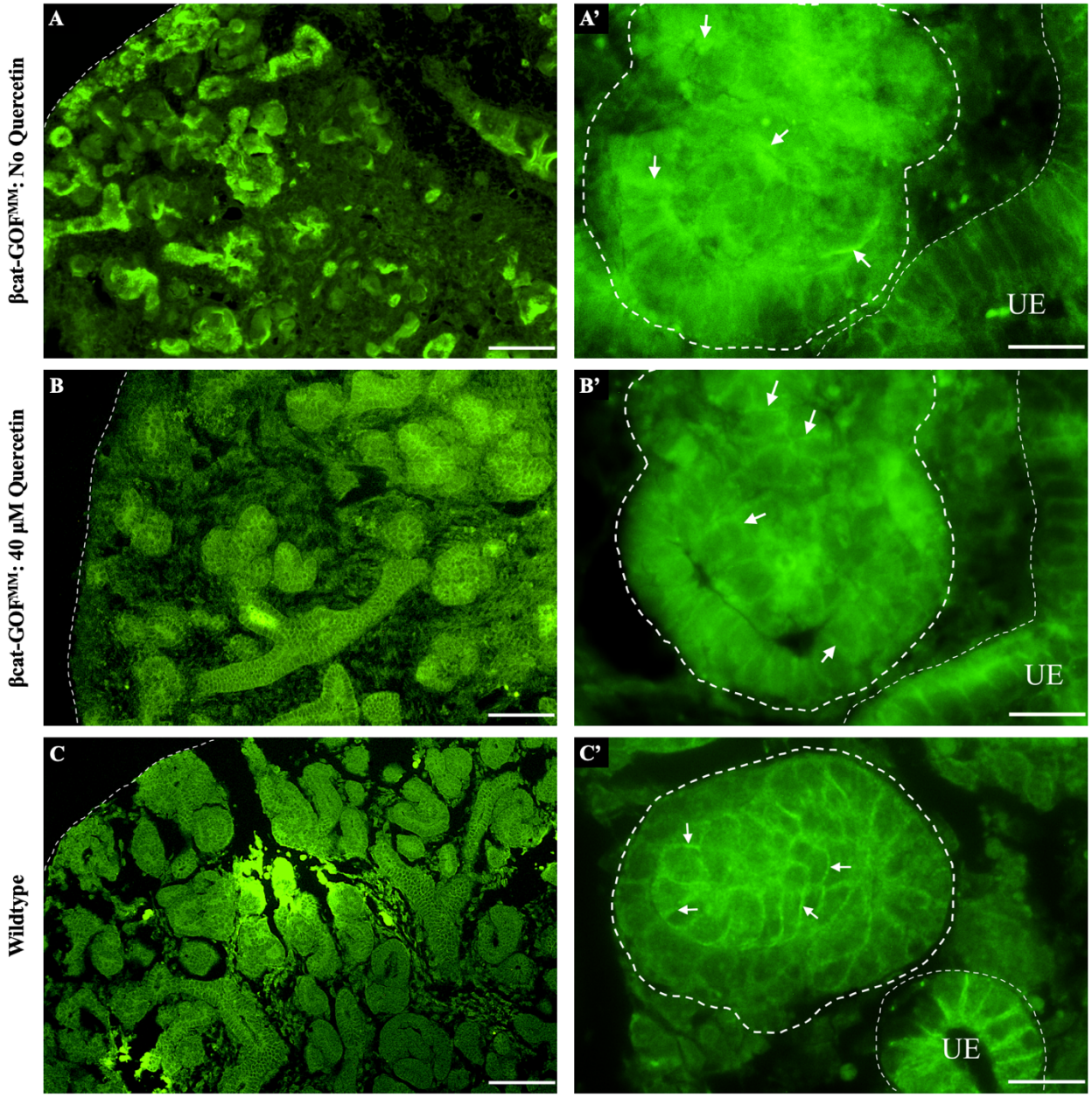

Quercetin treatment results to a more organized E-cadherin expression in βcat-GOF^{MM}. **A-C':** Immunofluorescence using anti-E-cadherin antibody. **A-C:** Low magnification images showing the renal parenchyma. **A'-C':** High magnification images focusing on developing nephrogenic structures found in the medullary area of the kidney tissue. **A and A':** Dysplastic kidneys grown without quercetin show a highly disorganized pattern of E-cadherin expression throughout the renal parenchyma, and a closer look reveals an irregular distribution of E-cadherin (arrows) in cells that make up a stalled nephrogenic structure (dotted line) in the medulla. UE: Ureteric epithelium. **B and B':** Compared to untreated dysplastic kidneys, dysplastic kidneys cultured in

40 μM quercetin show a more organized pattern of E-cadherin expression in the renal parenchyma, with E-cadherin detected at adherens junctions (arrows) between adjacent cells in nephrogenic structures (dotted line). UE: Ureteric epithelium. **C and C':** Age-matched wild-type embryonic kidneys showing the normal pattern of E-cadherin expression in the renal parenchyma; E-cadherin is expressed in adjacent epithelial cells (arrows) that make up the nephrogenic structures (dotted line). UE: Ureteric epithelium. **Scale bars:** 100 μm (**A-C**); 10 μm (**A'-C'**). **Note:** These images are representative examples of multiple independent experimental trials.

14. βcat-GOF^{RS} mutants demonstrate renal dysplasia

My results have shown that quercetin reduces the severity of renal dysplasia in a mouse model where β-catenin is overexpressed in the metanephric mesenchyme. I next utilized another mouse model of renal dysplasia to determine whether quercetin can also rescue the abnormalities in this model.

Our laboratory generated another mouse model of renal dysplasia in which β-catenin is specifically overexpressed in the renal stroma of the embryonic kidney, termed βcat-GOF^{RS} (β-catenin gain-of-function in the renal stroma). Mutant embryos were generated by crossing male Foxd1-Cre mice with female mice that contain LoxP sites flanking exon 3 of *β-catenin* (*Boivin et al., 2016*). Progeny of this cross have a mutated form of β-catenin that lacks a phosphorylation site required for degradation, resulting in the accumulation of β-catenin in the stromal cells of the developing kidney (*Boivin et al., 2016*).

In comparison to the organization of the renal parenchyma observed in wild-type mouse embryonic kidneys (**Figure 19A**), dysplastic kidneys from βcat-GOF^{RS} mutants reveal focal zones of abnormally-expanded renal stroma and several poorly-developed and immature tubules (Figure 19B). Compared to wild-type kidneys (**Figure 19A**), the dysplastic kidneys also have a smaller size and demonstrate a marked reduction in the number of early nephrogenic structures in the cortex and an absence of maturing nephrons in the medulla (**Figure 19B**).

Figure 19: βcat-GOF^{RS} mutants demonstrate renal dysplasia

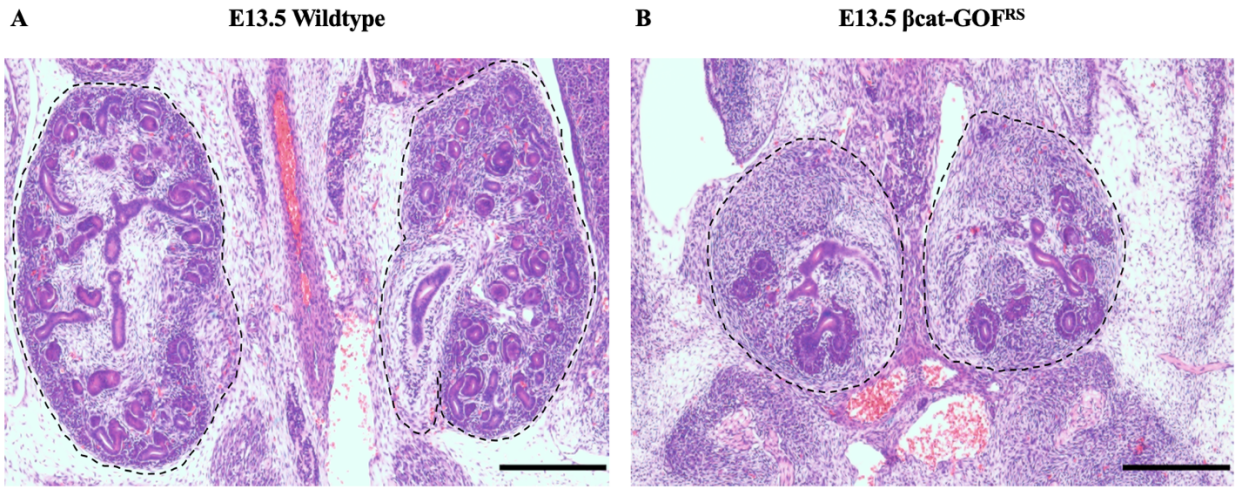

βcat-GOF^{RS} mutants demonstrate renal dysplasia. **A:** Histological analysis of E13.5 wild-type mouse embryonic kidneys show normal kidney structure, including proper corticomedullary patterning of the renal parenchyma, and normally-developing nephrogenic and ductal structures. **B:** Compared to wild-type kidneys, E13.5 βcat-GOF^{RS} mutant kidneys reveal an abnormal kidney structure, including smaller kidney size, fewer nephrogenic structures in the cortex and an absence of maturing nephrons in the medulla, several poorly-developed and immature tubules, and focal zones of abnormally-expanded renal stroma cells throughout the renal parenchyma. **Scale bars:** 200 μm.

15. Quercetin treatment rescues abnormal branching morphogenesis in βcat-GOF^{RS}

The renal stroma secretes β-catenin-mediated signals to the ureteric epithelium in order to regulate proper branching morphogenesis (*Boivin et al., 2015b*). Our previous work has established that an overexpression of nuclear β-catenin in the renal stroma in the developing kidney (β-cat^{GOF-RS}) causes renal dysplasia that is characterized by disrupted branching morphogenesis *(Boivin et al., 2016)*. I hypothesize that quercetin can also reduce the elevated nuclear β-catenin levels in this mouse model of renal dysplasia and can rescue abnormal branching morphogenesis in these dysplastic kidneys.

To test this, I resected E13.5 kidneys from β-cat^{GOF-RS} mutant embryos and the kidneys were cultured either in the presence or absence of 40 μM quercetin for 48 hours. Whole-mount immunofluorescence staining for cytokeratin was performed to visualize ureteric branching. We further characterized the branch patterns by manually tracing and mapping out the branching generations of each kidney. As expected in this mouse model, I found that mutant kidneys grown without quercetin display an abnormal overall kidney shape (**Figure 20A**), several abnormally-elongating branch tips and a highly disorganized ureteric branching involving a lack of proper bifurcation pattern (**Figures 20A' and 20A''**). In contrast, mutant kidneys grown with 40 μM quercetin show an improvement in branching pattern as observed in an overall improved kidney shape (**Figure 20B**) and a more distinct bifurcation pattern of the ureteric epithelium, involving up to six branching generations (**Figures 20B' and 20B''**). The quercetin-treated mutant kidneys display a branching pattern and overall structure that is more comparable to age-matched wild-type kidneys (**Figures 20C, 20C' and 20C''**).

Taken together, these findings demonstrated that quercetin treatment partially rescues disrupted branching morphogenesis in this mouse model of renal dysplasia, resulting to a ureteric branching pattern that more closely resembles that of normal kidney development.

Figure 20: Quercetin treatment rescues abnormal branching morphogenesis in βcat-GOF^{RS}

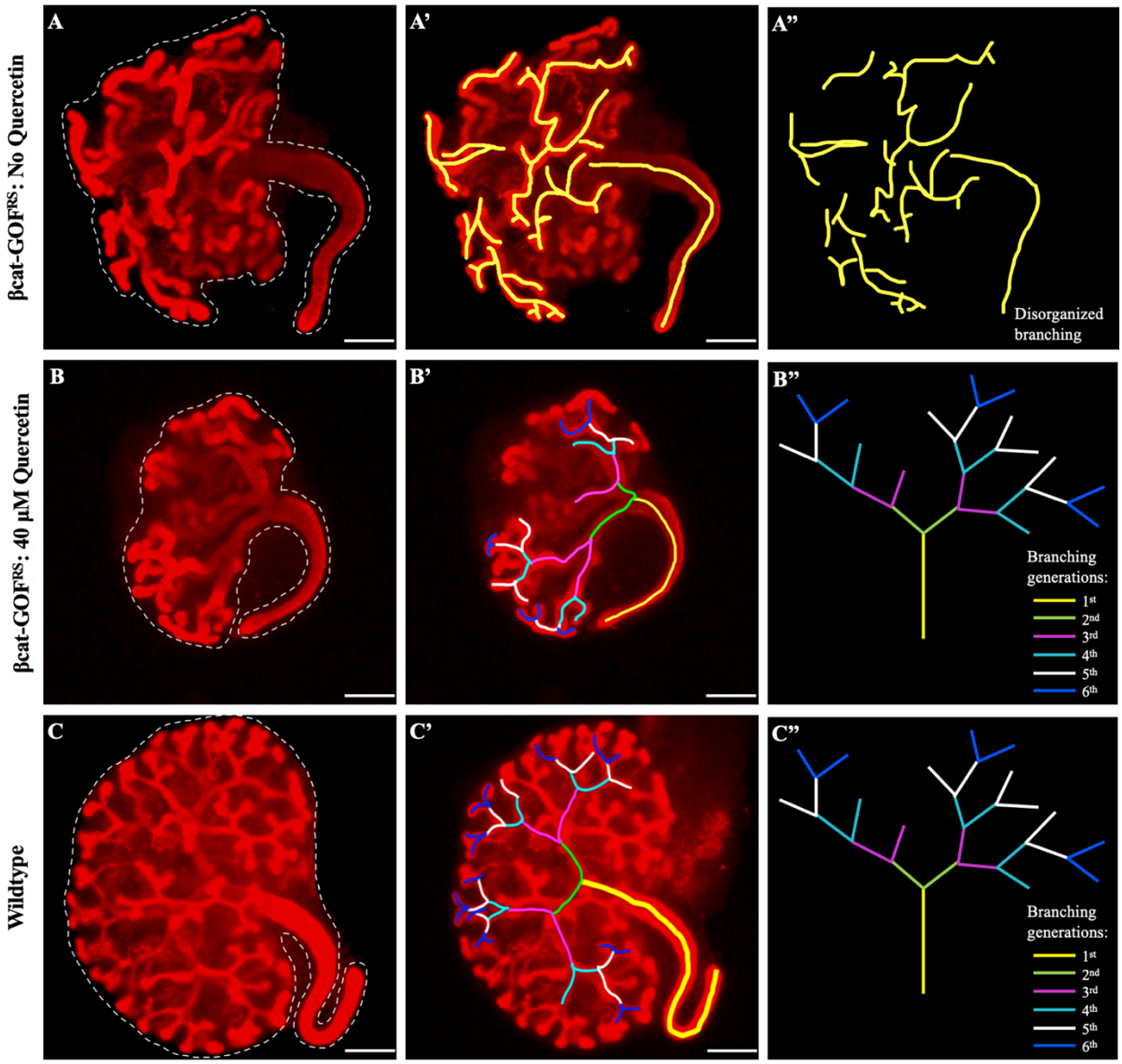

Quercetin treatment rescues abnormal branching morphogenesis in βcat-GOF^{RS}. **A-C':** Whole-mount immunofluorescence using anti-cytokeratin antibody. **A-C:** 4X magnification showing the whole kidney. **A'-C':** Analysis of the branching pattern of the kidney explants. **A''-C'':** Mapping out the branching generations of the kidney explants. **A:** Untreated dysplastic kidneys show an abnormal kidney shape. **B:** Compared to untreated controls, dysplastic kidneys grown in quercetin treatment show an improved kidney shape, more closely resembling the bean-shape seen in wild-type kidneys (**C**). **A' and A'':** Dysplastic kidneys grown without quercetin treatment demonstrate abnormal branching morphogenesis, indicated by the highly disorganized branching pattern and a

lack of proper ureteric branch bifurcation. **B' and B'':** Dysplastic kidneys treated with quercetin show an improved branching pattern, as demonstrated by a more organized ureteric branch bifurcation generating up to 6 branch generations, similar to that observed in wild-type kidneys (**C' and C''**). **Scale bars:** 200 μm (**A-C'**). **Note:** These images are representative examples of multiple independent experimental trials.

DISCUSSION

1. Overall findings

Renal dysplasia is the defective development and formation of the kidney resulting from abnormalities in the fundamental processes that underlie kidney development (*Schedl, 2007*). While renal dysplasia is the leading cause of end-stage kidney disease in children *(Chen & Chang, 2015*), there is no cure to this congenital defect. Our previous work demonstrated that cases of human renal dysplasia have elevated cellular levels of β-catenin, primarily in the nuclei of kidney cells (*Sarin et al., 2014*). In our mouse models of renal dysplasia, the overexpression of β-catenin in select cells of the developing kidney confirmed its pathogenic role in renal dysplasia. In fact, the mouse model of renal dysplasia was almost identical to the histopathology that is observed in human renal dysplasia (*Sarin et al., 2014; Bridgewater et al., 2011; Boivin et al., 2015b*). Previous work from our laboratory demonstrated that the overexpression of β-catenin resulted in the dysregulation of genes essential for kidney development (i.e. *Pax2, GDNF* and *Six2*) (*Sarin et al., 2014; Bridgewater et al., 2011; Boivin et al., 2015b*). Therefore, our previous work identified β-catenin as a potential therapeutic target for renal dysplasia. In this study, I demonstrated that in wild-type kidneys, quercetin caused alterations in normal kidney development and these alterations were associated with reductions in nuclear β-catenin and in the transcription of genes involved in kidney development (i.e. *Pax2, Six2* and *GDNF)*. I also showed that quercetin treatment reduces the severity of renal dysplasia in dysplastic kidneys by reducing the elevated levels of nuclear β-catenin to levels similar to wild-type kidneys and reduced the expression of genes important in kidney development (i.e. *Pax2, Six2* and *GDNF*). Consistent with these reductions in abnormal β-catenin activity, I observed that quercetin treatment of dysplastic kidneys

resolves disorganized ureteric branching and abnormal nephron formation, rescues abnormal corticomedullary patterning, and increases the number of properly-forming nephrons in the parenchyma. To better understand the mechanism of the improved histopathology, I noted that quercetin treatment resolves a disorganized and abnormal pattern of E-cadherin expression in the abnormally-developing kidney structures. Altogether, these studies demonstrate, for the first time, that quercetin is effective in modulating β-catenin expression during kidney development and can be used to reduce abnormally-elevated β-catenin levels in dysplastic kidneys, resulting in reduced severity of renal dysplasia.

2. Quercetin mechanism of action on β-catenin signaling

My data showed that quercetin treatment of embryonic kidneys resulted in reduced nuclear β-catenin and increased cytoplasmic and membrane-bound expression. These findings suggest that the mechanism of quercetin action is by reducing nuclear β-catenin levels and therefore decreasing its transcriptional activation. In support of this, other studies have demonstrated that quercetin mitigates abnormal Wnt/β-catenin signaling in specific diseases by decreasing β-catenin nuclear accumulation. In triple-negative breast cancer cells grown *in vitro*, quercetin decreased nuclear β-catenin levels and increased cytoplasmic localization of β-catenin (*Srinivasan et al., 2016*). This resulted in decreased mRNA expression levels of *cyclin D1* and *c-myc*, transcriptional targets involved in tumourigenesis. Further, the treatment of breast cancer cells with quercetin showed a dose-dependent decrease in cancer cell proliferation and migration (*Srinivasan et al., 2016).* Studies on pancreatic cancer cells (*Cao et al., 2015*) and colon cancer cells (*Park et al., 2005*) have also demonstrated a quercetin-induced decrease in nuclear β-catenin, resulting in decreased transcriptional activity and reduced tumourigenesis. Finally, a study in a mouse model of kidney

fibrosis found that mice with acute kidney fibrosis with subsequent quercetin treatment showed a reduction in elevated β-catenin levels in renal interstitial cells. This resulted in decreased intensity of the fibrotic response (i.e. TGFβ1-mediated fibroblast activation) and attenuating the progression of kidney fibrosis (*Ren et al., 2016*). Combined, these studies provide evidence that quercetin can decrease nuclear β-catenin levels in tissues and decrease the transcriptional activation of its targets, resulting in phenotypic outcomes that show decreased severity of the disease. Therefore, these studies support my conclusion that quercetin decreases nuclear β-catenin levels and transcriptional activity in dysplastic kidneys, resulting in improvements to nephron formation and branching morphogenesis.

3. Quercetin treatment alters β-catenin cellular localization

My data demonstrated that quercetin treatment of wild-type and dysplastic developing kidneys resulted in decreased nuclear β-catenin expression and increased cytoplasmic and membrane-bound expression. These findings are consistent with previous studies that showed quercetin changes the cellular distribution of β-catenin in cancer cells, where untreated cells show β-catenin expression predominantly in the nucleus while quercetin-treated cells show decreased nuclear β-catenin levels and higher cytoplasmic expression (*Srinivasan et al., 2016*). It is possible that with quercetin treatment, β-catenin is prevented from entering the nucleus and is sequestered at the cytoplasm and membrane-bound compartments. Another possibility is that quercetin activates a mechanism by which non-phosphorylated β-catenin is being shuttled out of the nucleus and being redistributed back to the cytoplasm. My data supports both possibilities since β-catenin is not in the nucleus, suggesting it may be shuttled out of the nucleus, and cytoplasmic β-catenin cannot enter the nuclear compartment.

Quercetin might cause a redistribution of β-catenin by preventing it from entering the nucleus and sequestering β-catenin in the cytoplasm and cell membrane. A study by Orsulic *et al.* (1999) demonstrated that: 1) Lef-1 only binds to β-catenin that is not already complexed with either APC or E-cadherin, and 2) E-cadherin expression prevents excessive nuclear localization of β-catenin. E-cadherin binds to cytoplasmic β-catenin that has not been targeted by the degradation complex and stabilizes β-catenin at the cell membrane. Wnt signaling blocks the degradation machinery and leads to an excess of cytosolic β-catenin and this saturates the binding capacity of E-cadherin, therefore excess β-catenin enters the nucleus and activates gene expression (*Orsulic et al., 1999*). Interestingly, this study found that deletion of E-cadherin resulted in elevated nuclear β-catenin levels and increased β-catenin/Lef-1 binding. In contrast, E-cadherin overexpression led to a substantial decrease in β-catenin levels in the nuclei; E-cadherin overexpression can prevent β-catenin from entering the nucleus and instead being redistributed at the cell membrane (*Orsulic et al.,* 1999). Taken together, Orsulic *et al.* showed that cellular localization of β-catenin is primarily determined by E-cadherin levels. Furthermore, studies on human cancer cell lines have shown that quercetin was effective in increasing E-cadherin expression and inducing proper cell adhesion, resulting to reduced β-catenin-driven activation of genes involved in metastasis (*Srinivasan et al., 2016*; *Kee et al., 2016*; *Feng et al., 2018*). The findings from this study support my data showing lack of proper E-cadherin expression and elevated nuclear β-catenin levels in dysplastic kidneys grown without quercetin, whereas there is normal E-cadherin expression in adherens junctions and increased membrane-bound β-catenin and decreased nuclear β-catenin in quercetin-treated dysplastic kidneys. Based from these studies and my observations, quercetin resolves proper E-cadherin expression in dysplastic kidneys, which sequesters β-catenin in the membrane and prevents its nuclear translocation. Further studies will confirm whether there is an

increase in β-catenin/E-cadherin binding and decreased β-catenin/Lef-1 binding in quercetin-treated kidneys compared to untreated controls.

Quercetin might also remove β-catenin from the nucleus and shuttle it to the cytoplasm. There have been several proposed mechanisms by which β-catenin is trafficked in and out of the nuclear compartment in response to homeostatic and physiological signals. In addition to its role in the destruction complex, APC has been proposed to be a β-catenin chaperone (*Henderson & Fagotto, 2002*). In non-stimulated cells, APC actively removes β-catenin from the nucleus to the cytoplasm where its levels are mediated by kinase-driven phosphorylation and degradation. In contrast, cancerous cells or a constitutively active Wnt signaling have high levels of stabilized β-catenin that can move β-catenin in and out of the nucleus independently of APC (*Henderson & Fagotto, 2002*). However, more studies are still needed to elucidate the exact mechanisms by which β-catenin nuclear entry and exit is regulated in cells. Future experiments can be performed to determine whether quercetin treatment of embryonic kidneys causes any changes in APC/β-catenin complex formation and cellular distribution.

4. Quercetin treatment resolves abnormal mesenchyme-to-epithelial transition dysplastic kidneys

A hallmark histopathological characteristic of renal dysplasia in both mice and humans is sporadic clusters of undifferentiated mesenchyme and stalled nephrogenesis. This results in poorly-differentiated nephrogenic and ductal structures, leading to a decrease in nephron number in the renal parenchyma (*Chen & Chang, 2015; Kakkar et al., 2006*). In normal cases, properly-developing nephrons undergo mesenchymal-to-epithelial transition to form polarized epithelial cells, which is critical in the formation of the nephron (*Davies, 1996*). During normal kidney development, cell-cell adhesion mediated by E-cadherin and β-catenin facilitates mesenchymal-

to-epithelial transition in nephron formation (*Schmidt-Ott & Barasch, 2008*). In renal dysplasia, however, stalled nephrogenic structures demonstrate a lack of a proper mesenchymal-to-epithelial transition. In my study, I observed that untreated dysplastic kidneys had numerous stalled and disorganized nephrogenic structures. I also demonstrated a highly disorganized pattern of E-cadherin expression in these stalled nephrogenic structures. In contrast, quercetin treatment of dysplastic kidneys showed a significant reduction in the number of abnormally-developed nephrons. I found that quercetin treatment resulted in a normal pattern of E-cadherin expression in these developing nephrons, with E-cadherin detected at adherens junctions between adjacent cells in nephrogenic structures. My observations suggest that quercetin possibly plays a role in altering E-cadherin expression to facilitate the transition of the undifferentiated and disorganized mesenchymal cells in dysplastic kidneys into polarized epithelial cells that will develop into mature nephrons. Similar to my findings, a study observed that treatment of isolated metanephric mesenchyme cells with lithium chloride and bromoindirubin-3'-oxime induced the formation of nephron-like epithelial structures that started expressing cell polarity markers including E-cadherin (*Schmidt-Ott & Barasch, 2008*). In addition, breast cancer cells treated with quercetin showed increased expression levels of E-cadherin compared to untreated controls and demonstrated a reversal of epithelial-to-mesenchyme-transition into mesenchyme-to-epithelial transition, resulting to decreased metastatic activity (*Srinivasan et al., 2016*). Combined, these studies provide insights into a potential mechanism by which quercetin is able to rescue abnormal nephron formation in our mouse models of renal dysplasia. In support of my findings, these studies demonstrate that it is possible to induce the epithelialization of mesenchymal cells *in vitro* and that quercetin can trigger epithelial transition in mesenchymal cells. Furthermore, quercetin can restore the normal pattern of E-cadherin expression, possibly allowing for mesenchymal-to-epithelial

transition to proceed. Further experiments will elucidate whether the quercetin-mediated increase in cytoplasmic and membrane-bound β-catenin, consequently enhancing β-catenin/E-cadherin interaction in adjacent epithelial cells in the nephron, is an underlying mechanism that resolved proper E-cadherin expression and promoted epithelial transition in dysplastic kidneys.

5. Quercetin treatment alters β-catenin activity during nephron formation

β-catenin regulates the expression of *Pax2* in the metanephric mesenchyme during the formation of nephrons (*Carroll et al., 2005*). My findings on both wild-type and dysplastic mouse kidneys showed decreased nuclear β-catenin levels in mesenchymal cells undergoing epithelial transition and decreased expression levels of *Pax2* in quercetin-treated samples. Pax2 is a transcription factor that plays a role in the conversion of mesenchymal cells into the tubular epithelium of the nephron (*Torban et al.,* 2006). Interestingly, in both mice and humans, Pax2 deficiency causes defective growth of the fetal kidney while overexpression is associated with epithelial overgrowth and dysplastic kidney formation (*Dressler & Woolf, 2003*). Consistent with this, I found that quercetin treatment of wild-type kidneys led to reduced nephron formation. Here, the decrease in nuclear β-catenin resulted to a reduction in *Pax2* expression, preventing the further maturation and development of early nephron progenitors. As a result, I observed fewer nephrogenic structures in the renal parenchyma of quercetin-treated kidneys, similar to findings in human hypoplastic kidneys (*Schedl, 2007*). In contrast, elevated β-catenin levels resulting to increased Pax2 levels in the mesenchyme led to a dysregulated formation of nephrogenic structures. I observed sporadic regions of uninduced mesenchyme and disorganized nephron formation in untreated dysplastic kidneys, consistent with our previous histological findings in this mouse model of the disease (*Sarin et al., 2014*). Consequently, treating dysplastic kidneys with

quercetin decreases nuclear β-catenin levels and *Pax2* expression towards more steady-state levels, resulting to a rescue in nephron formation. My findings highlight the importance of tightly regulating cellular levels of β-catenin and its transcriptional activation of targets during nephrogenesis.

Pax2 induces the differentiation of mesenchymal cells into renal epithelium (*Dressler & Woolf, 2003*). During normal kidney development, *Pax2* expression is activated in mesenchyme cells with high levels detected in the condensing mesenchyme. As the induced mesenchyme undergoes epithelialization, forming the renal vesicles, comma-shaped and S-shaped structures, *Pax2* expression becomes gradually downregulated, and expression becomes restricted to some parts of the developing glomeruli and low levels detected in postnatal collecting ducts (*Dressler & Woolf, 2003*). This is consistent with my findings on untreated wild-type kidneys, where the induced mesenchymal cells in the nephrogenic zone and early nephrogenic structures (renal vesicles, comma-shaped and S-shaped structures) in the cortex have high levels of Pax2, whereas maturing nephron segments deep in the medulla have reduced expression and Pax2 is only present in some parts of the glomeruli (particularly in the podocytes). In human renal dysplasia, however, analysis of postnatal dysplastic tissue revealed persistent patterns of Pax2 expression resulting to sustained proliferation of cells, whereas normal postnatal kidneys showed downregulated expression in mature renal epithelia (*Dressler & Woolf, 2003*). This is consistent with my findings on untreated dysplastic kidneys which revealed high expression of Pax2 particularly in clusters of undifferentiated mesenchyme and immature nephrogenic structures in the renal parenchyma. Sustained *Pax2* expression in these abnormal nephrogenic structures prevent proper epithelial transition, accounting for a marked decrease in the number of maturing nephrons compared to wild-type embryonic kidneys. Quercetin treatment of dysplastic kidneys decreased the expression

levels of *Pax2* and resulted in a resolved nephrogenic pattern similar to wild-type kidneys, with Pax2 detected in self-renewing progenitors and early nephrons in the cortex, and maturing glomeruli in the medulla are now starting to downregulate Pax2 expression. Based on these findings, quercetin resolves abnormal nephron formation in dysplastic kidneys by reducing elevated β-catenin levels resulting in a decrease to Pax2 expression, consequently allowing the disrupted nephrogenic structures in the mesenchyme to undergo epithelialization and form maturing nephrons.

6. Quercetin treatment alters β-catenin activity during nephron progenitor self-renewal

β-catenin is also involved in regulating the expression of *Six2* in the metanephric mesenchyme during nephrogenesis (*Karner et al., 2011*). My findings on both wild-type and dysplastic mouse kidneys showed decreased nuclear β-catenin levels in condensed mesenchymal cells undergoing progenitor self-renewal. In wild-type kidneys, I also showed a decrease in *Six2* expression levels as a result of quercetin treatment. Although this decrease did not show a dose-dependent pattern, further analysis by immunofluorescence revealed a gradual disorganization in the spatial distribution of Six2-expressing cells in the nephrogenic zone: with each increase in the dose of quercetin, there is an increasing gap between the Six2-positive cells and the adjacent ureteric bud. I also observed that kidneys grown in the higher quercetin doses have several sporadic regions of uninduced Six2-expressing cells found in the nephrogenic zone. These indicate that quercetin disrupts proper ureteric bud induction of the condensed mesenchyme cells. The Six2-expressing cells in the condensed mesenchyme form tight aggregates and respond to signals from the adjacent ureteric bud epithelium to maintain an undifferentiated progenitor state (*Karner et al., 2011*). These mesenchymal progenitor cells must be continually induced by the ureteric bud and

constantly renewed in order for the kidney to continue to grow and induce additional generations of nephrons (*Self et al., 2006*). Consistent with this, my findings demonstrate quercetin disrupts nephron progenitor self-renewal in wild-type kidneys, possibly by decreasing *Six2* levels, thereby preventing the Six2-positive mesenchymal cells from properly responding to inductive signals originating from the ureteric bud. This lack of induction can prevent the progenitor cells from undergoing further self-renewal and progenitor expansion and may contribute to the stalled growth of the kidney.

There is also a modest decrease in *Six2* expression levels in quercetin-treated dysplastic kidneys, and this is correlated with the improved pattern of nephron progenitor self-renewal in treated dysplastic kidneys in comparison to untreated controls. I observed that untreated dysplastic kidneys have an abnormal expansion of Six2-positive progenitor cells deep in the medulla, similar to findings previously observed in this mouse model (*Sarin et al., 2014*). This can account for the stalled nephrogenic structures found in the medullary area; β-catenin overexpression in the mesenchyme, consequently leading to abnormal increase in *Six2* transcription, may cause these cells to retain their progenitor status and unable to undergo differentiation. This is not observed in wild-type kidneys where only maturing nephron segments are found in the medulla. On the other hand, quercetin treatment on dysplastic kidneys show a moderate decrease in *Six2* expression levels compared to untreated controls. Consistent with this, quercetin-treated kidneys show a normal pattern of Six2-expressing cells that are found only within the nephrogenic zone of the cortex and have no ectopic Six2-positive cells in the medulla. The quercetin-mediated decrease in *Six2* expression may contribute to allowing the uninduced mesenchymal cells in the medulla to switch from their progenitor state and start undergoing differentiation. As a result, there are no ectopic Six2-positive cells in the medulla the remaining Six2-expressing cells are re-established

in the cortex where successive waves of nephrogenesis will occur, similar to the pattern observed in wild-type kidneys. These findings demonstrate that quercetin resolves the abnormal pattern of nephron progenitor self-renewal in renal dysplasia.

7. Quercetin treatment alters β-catenin activity during branching morphogenesis

Due to the reciprocal nature of the inductive signaling between the ureteric epithelium and metanephric mesenchyme, a reduction in ureteric bud branching occurs as an indirect effect of a loss of nephrogenic zone (*Park et al., 2007*). Here, loss of β-catenin within the nephron progenitor pool not only leads to a reduction in the Six2-expressing cell population but also results to a cessation of ureteric branching, characterized by a decrease in branch tips found at the peripheral regions of the kidney (*Park et al., 2007*). This is consistent with my observations in wild-type kidneys showing a dose-dependent decrease in the number of ureteric branch tips found on the outer kidney surface, as a result of quercetin treatment. This also ties in with my observations showing quercetin treatment of wild-type kidneys resulted in an increased gap between the Six2-expressing mesenchymal cells in the cortex and the ureteric bud epithelium. This demonstrates that disruptions in the Six2-expressing cell populations in the nephrogenic zone due to quercetin treatment also disrupts ureteric branching at the outer cortex of the kidney, possibly resulting in a reduced number of successive branching events and an overall reduction in ureteric branching. Interestingly, I also observed that in dysplastic kidneys where quercetin treatment resolved the normal spatial pattern of Six2-positive cells in the nephrogenic zone, the abnormally-elongating ureteric branches are now starting to bifurcate at their branch tips where the Six2-expressing cells are now found aggregated on the surface of these branch tips. This indicates that as quercetin rescues nephron progenitor self-renewal in dysplastic kidneys, this also causes a resolution of

proper ureteric branch tip bifurcation at the nephrogenic zone. It is interesting to note that because of the reciprocal signaling between the metanephric mesenchyme and ureteric epithelium, a quercetin-induced improvement in the developing mesenchyme also leads to a rescue in the formation of the epithelium.

β-catenin also activates the expression of *GDNF* in the metanephric mesenchyme, and GDNF diffuses and binds to Ret receptors found on the surface of the ureteric bud tips; this GDNF/Ret interaction at the tips of the ureteric epithelium gives rise to the successive rounds of ureteric branching (*Sarin et al., 2014*). I observed that quercetin treatment of wild-type kidneys resulted in a decrease to *GDNF* expression, although this decrease did not follow a dose-dependent pattern. Nonetheless, I observed that the quercetin-treated kidneys show abnormally-elongating branch tips found at the outer cortex, which is not observed in wild-type kidneys. This indicates that quercetin decreases nuclear β-catenin in the mesenchyme, leading to the observed decrease in *GDNF* expression levels and consequently less GDNF available to bind to Ret receptors. This can account for the lack of bifid branching of the ureteric branch tips; since the lack of GDNF/Ret binding at the tip regions fails to trigger the morphological processes that drive ureteric bifurcation, these branches do not receive sufficient signals to undergo branching and instead continue to elongate towards the periphery of the kidney. I also observed that quercetin treatment of dysplastic kidneys resulted in a modest decrease to *GDNF* expression. In our mouse models of renal dysplasia, elevated β-catenin levels in the mesenchyme results to increased *GDNF* expression, leading to increased binding to Ret receptors in the ureteric epithelium (*Sarin et al., 2014*). This in turn results to dysregulated expression of target genes involved in proper ureteric branching and causes disrupted and ectopic ureteric branching (*Sarin et al., 2014*). Consistent with these findings from this model, I observed abnormally-elongating ureteric branches and the formation of ectopic

branch-like structures in untreated dysplastic kidneys. In contrast, quercetin treatment resulted to a resolved branching pattern in dysplastic kidneys, with proper ureteric bifurcation observed at the branch tips on the outer cortex. These findings indicate that the quercetin-mediated decrease in abnormally-elevated *GDNF* levels in dysplastic kidneys reduced the ectopic GDNF/Ret interactions, thereby resolving the normal pattern of GDNF/Ret binding at the ureteric branch tips, allowing for the proper bifurcation pattern to proceed.

In our other renal dysplasia mouse model where β-catenin is elevated in the renal stroma, I also observed a highly disorganized pattern of branching morphogenesis that demonstrates a lack of proper bifid branching pattern, which is expected in this mouse model (*Boivin et al., 2016*). Treatment with quercetin, however, rescued this abnormal branching pattern, resulting to a pattern that follows a proper bifid branching and giving rise to several branching generations. The exact mechanisms by which the renal stroma regulates branching morphogenesis during kidney development still needs to be further investigated. However, based from my observations, it is likely possible that β-catenin overexpression in the stroma leads to a consequent overexpression of targets in the ureteric epithelium that prevents proper branching to take place, and that quercetin facilitates a decrease in this overexpression and as a result restores the normal pattern of branching morphogenesis.

8. Quercetin treatment increases the number of nephrogenic structures in dysplastic kidneys

The nephrons are the functional units of the kidney, performing essential homeostatic functions such as waste filtration, water and pH regulation. Therefore, proper development and formation of the nephrons is critical for normal renal function. Consequently, renal dysplasia

associated with reduced nephron number at birth is a risk factor for developing progressive renal disease and hypertension in children and adults (*Hoy et al., 2005*). In severe forms of renal dysplasia, with an 80% reduction in nephron number at birth, there is a rapid development of proteinuria, hypertension, and renal failure in children (*McGraw et al., 1984; Drukker, 2002*). Therefore, a major cause of renal failure in children born with renal dysplasia is the associated reduction in nephron number (*Chen & Chang, 2015*). This concept is further supported by animal studies where an experimentally-induced loss of nephron mass during embryonic development or shortly after birth is strongly correlated to the progression of hypertension and kidney damage (*Woods, 1999; Moritz, 2002*). I demonstrated that treatment of dysplastic kidneys with quercetin resulted in a 44.45% increase in the number of properly-developing nephrogenic structures compared to untreated dysplastic kidneys. Based on previous studies, this increase in the number of nephrogenic structures likely would translate into improved renal function after birth and therefore reducing the severity of adverse renal outcomes that result from decreased nephron numbers. This may also delay or avoid the need for invasive renal replacement procedures in patients with kidney disease. While our studies are promising, future *in vivo* experiments involving treatment of pregnant mice at an appropriate gestational time point will address whether the quercetin rescues renal dysplasia *in vivo* and also results in increased nephron number and improved kidney function.

9. Future directions and implications

Overall, my data shows for the first time that *in vitro* quercetin treatment affects β-catenin activity during kidney development and can rescue dysplastic kidneys that have elevated β-catenin levels. Future studies using our mouse models of the disease can determine whether quercetin

treatment delivered *in vivo* can also attenuate the progression of renal dysplasia in the developing mouse embryo. If improvements are observed *in* vivo, further studies are also needed to demonstrate whether rescuing defective nephron formation and abnormal branching morphogenesis in the developing kidney will translate to improvements in kidney function (for instance, as determined by improvements in glomerular filtration rate and creatinine output). To date, the roles of β-catenin in the kidney have not been completely described. Therefore, my model of dose-dependent changes induced by quercetin in branching morphogenesis and nephrogenesis can address gaps in knowledge by identifying novel molecular mechanisms and genetic targets that are controlled by β-catenin. Lastly, it is clear from my data that quercetin modulates the nuclear versus cytoplasmic and membrane-bound distribution of β-catenin, however, there has been no consensus on how β-catenin subcellular levels are regulated. Therefore, my model system can also be valuable in further understanding the mechanisms and signaling pathways that regulate β-catenin entry into the nucleus and its transport back to the cytoplasm and cell membrane.

CONCLUSION

In summary, quercetin decreases nuclear β-catenin levels and increases its cytoplasmic and membrane-bound expression during normal kidney development. This results in decreased transcriptional activation of genes that regulate branching morphogenesis and nephron formation, consequently resulting in alterations to kidney development. In our mouse models of renal dysplasia where β-catenin levels are elevated in specific cells of the embryonic kidney, quercetin decreases nuclear β-catenin levels, leading to a decrease in abnormal expression levels of transcriptional targets, resulting to a rescue in branching morphogenesis and nephron formation. The rescue in nephron formation resulted in an increase in the number of properly-forming nephrons in the renal parenchyma and this can have further implications in terms of improved renal function in the fetus after birth. Quercetin also increases the cytoplasmic and membrane-bound expression of β-catenin in dysplastic kidneys; this is correlated with a resolved E-cadherin expression pattern in these diseased kidneys, therefore providing a possible mechanism of action for quercetin in mediating changes in subcellular localization of β-catenin.

My novel findings show for the first time that quercetin affects developmental processes in the kidney that are driven by β-catenin. More importantly, I demonstrated that it is possible to inhibit abnormal β-catenin levels and transcriptional activity during kidney development and this translates to a significant reduction in the severity of abnormal kidney development, resulting in a kidney phenotype that is more similar to normal kidney development. Overall, by demonstrating that altering β-catenin levels results to phenotypic changes in the embryonic kidney, my data provide support to previous studies demonstrating the critical role of β-catenin during kidney development. Furthermore, my experiments using quercetin as an inhibitor of β-catenin activity emphasize the importance of proper regulation of normal β-catenin levels and activity during the

formation of the kidney and shows the therapeutic potential of targeting defects in β-catenin signaling during development and disease.

My findings can have important implications in terms of management and treatment of patients with renal dysplasia. To date, renal dysplasia has no cure and treatment only involves symptom management such as dialysis and kidney transplants. Patients born with renal dysplasia account for a majority of children suffering from chronic kidney failure and in need of renal replacement therapies. Rescuing abnormal kidney development at an appropriate developmental time point can resolve the defective development and potentially avert or reduce the need for invasive renal replacement procedures.

REFERENCES

Amado, N. G., Fonseca, B. F., Cerqueira, D. M., Neto, V. M., & Abreu, J. G. (2011). Flavonoids: potential Wnt/beta-catenin signaling modulators in cancer. *Life Sciences*, *89*(15-16), 545-554.

Amri, K., Freund, N., Vilar, J., Merlet-Benichou, C., & Lelievre-Pegorier, M. (1999). Adverse effects of hyperglycemia on kidney development in rats: in vivo and in vitro studies. *Diabetes*, *48*(11), 2240-2245.

Basson, M. A., Watson-Johnson, J., Shakya, R., Akbulut, S., Hyink, D., Costantini, F. D., ... & Licht, J. D. (2006). Branching morphogenesis of the ureteric epithelium during kidney development is coordinated by the opposing functions of GDNF and Sprouty1. *Developmental biology*, *299*(2), 466-477.

Boivin, F. J., Sarin, S., Evans, J. C., & Bridgewater, D. (2015a). The Good and Bad of β-Catenin in Kidney Development and Renal Dysplasia. *Frontiers in Cell and Developmental Biology*, *3*.

Boivin, F. J., Sarin, S., Lim, J., Javidan, A., Svajger, B., Khalili, H., & Bridgewater, D. (2015b). Stromally expressed β-catenin modulates Wnt9b signaling in the ureteric epithelium. *PLoS One*, *10*(3), e0120347.

Boivin, F. J., Sarin, S., Dabas, P., Karolak, M., Oxburgh, L., & Bridgewater, D. (2016). Stromal β-catenin overexpression contributes to the pathogenesis of renal dysplasia. *The Journal of Pathology*, *239*(2), 174-185.

Bonomini, V., Mioli, V., Albertazzi, A., & Scolari, P. (1972). Daily-dialysis programme: Indications and results. *Proceedings of the European Dialysis and Transplant Association* (Vol. 9, pp. 44-52).

Brembeck, F. H., Rosário, M., & Birchmeier, W. (2006). Balancing cell adhesion and Wnt signaling, the key role of β-catenin. *Current Opinion in Genetics & Development*, *16*(1), 51-59.

Bridgewater, D., Cox, B., Cain, J., Lau, A., Athaide, V., Gill, P. S., ... & Rosenblum, N. D. (2008). Canonical WNT/β-catenin signaling is required for ureteric branching. *Developmental Biology*, *317*(1), 83-94.

Bridgewater, D., & Rosenblum, N. D. (2009). Stimulatory and inhibitory signaling molecules that regulate renal branching morphogenesis. *Pediatric Nephrology*, *24*(9), 1611-1619.

Bridgewater, D., Di Giovanni, V., Cain, J. E., Cox, B., Jakobson, M., Sainio, K., & Rosenblum, N. D. (2011). β-catenin causes renal dysplasia via upregulation of Tgfβ2 and Dkk1. *Journal of the American Society of Nephrology*, *22*(4), 718-731.

Cao, C., Sun, L., Mo, W., Sun, L., Luo, J., Yang, Z., & Ran, Y. (2015). Quercetin mediates β-catenin in pancreatic cancer stem-like cells. *Pancreas*, *44*(8), 1334-1339.

Carroll, T. J., Park, J. S., Hayashi, S., Majumdar, A., & McMahon, A. P. (2005). Wnt9b plays a central role in the regulation of mesenchymal to epithelial transitions underlying organogenesis of the mammalian urogenital system. *Developmental Cell*, *9*(2), 283-292.

Chen, R. Y., & Chang, H. (2015). Renal dysplasia. *Archives of Pathology and Laboratory Medicine*, *139*(4), 547-551.

Clevers, H. (2006). Wnt/β-catenin signaling in development and disease. *Cell*, *127*(3), 469-480.

Combes, A. N., Phipson, B., Zappia, L., Lawlor, K., Er, P. X., Oshlack, A., & Little, M. (2017). High throughput single cell RNA-seq of developing mouse kidney and human kidney organoids reveals a roadmap for recreating the kidney. *bioRxiv*, 235499.

Costantini, F., & Kopan, R. (2010). Patterning a complex organ: branching morphogenesis and nephron segmentation in kidney development. *Developmental Cell*, *18*(5), 698-712.

Costantini, F., & Shakya, R. (2006). GDNF/Ret signaling and the development of the kidney. *Bioessays*, *28*(2), 117-127.

D'Andrea, G. (2015). Quercetin: a flavonol with multifaceted therapeutic applications? *Fitoterapia*, *106*, 256-271.

Dart, A. B., Ruth, C. A., Sellers, E. A., Au, W., & Dean, H. J. (2015). Maternal diabetes mellitus and congenital anomalies of the kidney and urinary tract (CAKUT) in the child. *American Journal of Kidney Diseases*, *65*(5), 684-691.

Daugherty, R. L., & Gottardi, C. J. (2007). Phospho-regulation of β-catenin adhesion and signaling functions. *Physiology*, *22*(5), 303-309.

Davies, J. A. (1996). Mesenchyme to epithelium transition during development of the mammalian kidney tubule. *Cells Tissues Organs*, *156*(3), 187-201.

Dressler, G. R. (2006). The cellular basis of kidney development. *Annual Review of Cell and Developmental Biology*, *22*, 509-529.

Dressler, G. R., & Woolf, A. S. (2003). Pax2 in development and renal disease. *International Journal of Developmental Biology*, *43*(5), 463-468.

Drukker, A. (2002). Oligonephropathy: from a rare childhood disorder to a possible health problem in the adult. *The Israel Medicine Association Journal*, *4*(3), 191-195.

Feng, J., Song, D., Jiang, S., Yang, X., Ding, T., Zhang, H., ... & Yin, Q. (2018). Quercetin restrains TGF-β1-induced epithelial–mesenchymal transition by inhibiting Twist1 and regulating E-cadherin expression. *Biochemical and Biophysical Research Communications*, *498*(1), 132-138.

Henderson, B. R., & Fagotto, F. (2002). The ins and outs of APC and β-catenin nuclear transport. *EMBO Reports*, *3*(9), 834-839.

Hoppe, C. C., Evans, R. G., Bertram, J. F., & Moritz, K. M. (2007). Effects of dietary protein restriction on nephron number in the mouse. *American Journal of Physiology-Regulatory, Integrative and Comparative Physiology*, *292*(5), R1768-R1774.

Hoy, W. E., Hughson, M. D., Bertram, J. F., Douglas-Denton, R., & Amann, K. (2005). Nephron number, hypertension, renal disease, and renal failure. *Journal of the American Society of Nephrology*, *16*(9), 2557-2564.

Huh, K. H., Kim, M. S., Ju, M. K., Chang, H. K., Ahn, H. J., Lee, S. H., ... & Park, K. (2008). Exchange living-donor kidney transplantation: merits and limitations. *Transplantation*, *86*(3), 430-435.

Kakkar, N., Menon, S., & Radotra, B. D. (2006). Histomorphology of renal dysplasia—an autopsy study. *Fetal and Pediatric Pathology*, *25*(2), 73-86.

Karner, C. M., Das, A., Ma, Z., Self, M., Chen, C., Lum, L., ... & Carroll, T. J. (2011). Canonical Wnt9b signaling balances progenitor cell expansion and differentiation during kidney development. *Development*, *138*(7), 1247-1257.

Kee, J. Y., Han, Y. H., Kim, D. S., Mun, J. G., Park, J., Jeong, M. Y., ... & Hong, S. H. (2016). Inhibitory effect of quercetin on colorectal lung metastasis through inducing apoptosis, and suppression of metastatic ability. *Phytomedicine*, *23*(13), 1680-1690.

Kerecuk, L., Schreuder, M. F., & Woolf, A. S. (2008). Renal tract malformations: perspectives for nephrologists. *Nature Reviews Nephrology*, *4*(6), 312.

Kobayashi, A., Valerius, M. T., Mugford, J. W., Carroll, T. J., Self, M., Oliver, G., & McMahon, A. P. (2008). Six2 defines and regulates a multipotent self-renewing nephron progenitor population throughout mammalian kidney development. *Cell Stem Cell*, *3*(2), 169-181.

Lelièvre-Pégorier, M., & Merlet-Bénichou, C. (2000). The number of nephrons in the mammalian kidney: environmental influences play a determining role. *Nephron Experimental Nephrology*, *8*(2), 63-65.

Li, Y., Yao, J., Han, C., Yang, J., Chaudhry, M., Wang, S., ... & Yin, Y. (2016). Quercetin, inflammation and immunity. *Nutrients*, *8*(3), 167.

McGraw, M., Poucell, S., Sweet, J., & Baumal, R. (1984). The significance of focal segmental glomerulosclerosis in oligomeganephronia. *The International Journal of Pediatric Nephrology*, *5*(2), 67-72.

Merlet-Benichou, C. L. (2003). Influence of fetal environment on kidney development. *International Journal of Developmental Biology*, *43*(5), 453-456.

Moore, K. L., Persaud, T. V. N., & Torchia, M. G. (2015). *Before we are born: essentials of embryology and birth defects*. Elsevier Health Sciences.

Moritz, K. M., Wintour, E. M., & Dodic, M. (2002). Fetal uninephrectomy leads to postnatal hypertension and compromised renal function. *Hypertension*, *39*(6), 1071-1076.

Narlis, M., Grote, D., Gaitan, Y., Boualia, S. K., & Bouchard, M. (2007). Pax2 and pax8 regulate branching morphogenesis and nephron differentiation in the developing kidney. *Journal of the American Society of Nephrology*, *18*(4), 1121-1129.

Nusse, R., & Clevers, H. (2017). Wnt/β-catenin signaling, disease, and emerging therapeutic modalities. *Cell*, *169*(6), 985-999.

Orsulic, S., Huber, O., Aberle, H., Arnold, S., & Kemler, R. (1999). E-cadherin binding prevents beta-catenin nuclear localization and beta-catenin/LEF-1-mediated transactivation. *Journal of Cell Science*, *112*(8), 1237-1245.

Parikh, C. R., McCall, D., Engelman, C., & Schrier, R. W. (2002). Congenital renal agenesis: case-control analysis of birth characteristics. *American Journal of Kidney Diseases*, *39*(4), 689-694.

Park, C. H., Chang, J. Y., Hahm, E. R., Park, S., Kim, H. K., & Yang, C. H. (2005). Quercetin, a potent inhibitor against β-catenin/Tcf signaling in SW480 colon cancer cells. *Biochemical and Biophysical Research Communications*, *328*(1), 227-234.

Park, J. S., Valerius, M. T., & McMahon, A. P. (2007). Wnt/β-catenin signaling regulates nephron induction during mice kidney development. *Development*, *134*(13), 2533-2539.

Park, J. S., Ma, W., O'Brien, L. L., Chung, E., Guo, J. J., Cheng, J. G., ... & McMahon, A. P. (2012). Six2 and Wnt regulate self-renewal and commitment of nephron progenitors through shared gene regulatory networks. *Developmental Cell*, *23*(3), 637-651.

Park, S., & Choi, J. (2010). Inhibition of β-catenin/Tcf signaling by flavonoids. *Journal of Cellular Biochemistry*, *110*(6), 1376-1385.

Pietta, P. G. (2000). Flavonoids as antioxidants. *Journal of Natural Products*, *63*(7), 1035-1042.

Pohl, M., Bhatnagar, V., Mendoza, S. A., & Nigam, S. K. (2002). Toward an etiological classification of developmental disorders of the kidney and upper urinary tract. *Kidney International*, *61*(1), 10-19.

Preuss, H. G. (1993). Basics of renal anatomy and physiology. *Clinics in Laboratory Medicine*, *13*(1), 1-11.

Ren, J., Li, J., Liu, X., Feng, Y., Gui, Y., Yang, J., ... & Dai, C. (2016). Quercetin Inhibits fibroblast activation and kidney fibrosis involving the suppression of mammalian target of rapamycin and β-catenin Signaling. *Scientific Reports*, *6*, 23968.

Renkema, K. Y., Winyard, P. J., Skovorodkin, I. N., Levtchenko, E., Hindryckx, A., Jeanpierre, C., ... & Schedl, A. (2011). Novel perspectives for investigating congenital anomalies of the kidney and urinary tract (CAKUT). *Nephrology Dialysis Transplantation, 26*(12), 3843-3851

Ritchey, M. L., Kelalis, P. P., Breslow, N., Etzioni, R., Evans, I., Haase, G. M., & D'angio, G. J. (1992). Surgical complications after nephrectomy for Wilms' tumor. *Surgery, Gynecology & Obstetrics*, *175*(6), 507-514.

Saxén, L., & Sariola, H. (1987). Early organogenesis of the kidney. *Pediatric Nephrology*, *1*(3), 385-392.

Schedl, A. (2007). Renal abnormalities and their developmental origin. *Nature Reviews Genetics*, *8*(10), 791.

Schmidt-Ott, K. M., & Barasch, J. (2008). WNT/β-catenin signaling in nephron progenitors and their epithelial progeny. *Kidney International*, *74*(8), 1004-1008.

Self, M., Lagutin, O. V., Bowling, B., Hendrix, J., Cai, Y., Dressler, G. R., & Oliver, G. (2006). Six2 is required for suppression of nephrogenesis and progenitor renewal in the developing kidney. *The EMBO Journal*, *25*(21), 5214-5228.

Selvaraj, S., Krishnaswamy, S., Devashya, V., Sethuraman, S., & Krishnan, U. M. (2014). Flavonoid–metal ion complexes: a novel class of therapeutic agents. *Medicinal Research Reviews*, *34*(4), 677-702.

Srinivasan, A., Thangavel, C., Liu, Y., Shoyele, S., Den, R. B., Selvakumar, P., & Lakshmikuttyamma, A. (2016). Quercetin regulates β-catenin signaling and reduces the migration of triple negative breast cancer. *Molecular Carcinogenesis*, *55*(5), 743-756.

Stark, K., Vainio, S., Vassileva, G., & McMahon, A. P. (1994). Epithelial transformation of metanephric mesenchyme in the developing kidney regulated by Wnt-4. *Nature*, *372*(6507), 679.

Torban, E., Dziarmaga, A., Iglesias, D., Chu, L. L., Vassilieva, T., Little, M., ... & Goodyer, P. (2006). PAX2 activates WNT4 expression during mammalian kidney development. *Journal of Biological Chemistry*, *281*(18), 12705-12712.

Vize, P. D., Woolf, A. S., & Bard, J. B. (Eds.). (2003). *The kidney: from normal development to congenital disease*. Elsevier.

Winyard, P., & Chitty, L. S. (2008). Dysplastic kidneys. In *Seminars in Fetal and Neonatal Medicine* (Vol. 13, No. 3, pp. 142-151). Elsevier.

Woolf, A. S., Price, K. L., Scambler, P. J., & Winyard, P. J. (2004). Evolving concepts in human renal dysplasia. *Journal of the American Society of Nephrology*, *15*(4), 998-1007.

Woods, L. L. (1999). Neonatal uninephrectomy causes hypertension in adult rats. *American Journal of Physiology-Regulatory, Integrative and Comparative Physiology*, *276*(4), R974-R978.